

1-1-2003

Protein matrices engineered for control of cell and tissue behavior.

Kathleen A. DiZio

University of Massachusetts Amherst

Follow this and additional works at: https://scholarworks.umass.edu/dissertations_1

Recommended Citation

DiZio, Kathleen A., "Protein matrices engineered for control of cell and tissue behavior." (2003). *Doctoral Dissertations 1896 - February 2014*. 1047.

https://scholarworks.umass.edu/dissertations_1/1047

This Open Access Dissertation is brought to you for free and open access by ScholarWorks@UMass Amherst. It has been accepted for inclusion in Doctoral Dissertations 1896 - February 2014 by an authorized administrator of ScholarWorks@UMass Amherst. For more information, please contact scholarworks@library.umass.edu.



312066 0288 1169 8



DATE DUE			

UNIVERSITY LIBRARY

UNIVERSITY OF MASSACHUSETTS
AMHERST

SCIENCE
LD
3234
M267
D6255

PROTEIN MATRICES ENGINEERED
FOR CONTROL OF CELL AND TISSUE BEHAVIOR

A Dissertation Presented

by

KATHLEEN A. DI ZIO

Submitted to the Graduate School of the
University of Massachusetts Amherst in partial fulfillment
of the requirements for the degree of

DOCTOR OF PHILOSOPHY

February 2003

Polymer Science and Engineering

© Copyright by Kathleen A. Di Zio 2003

All Rights Reserved

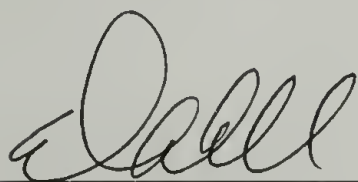
PROTEIN MATRICES ENGINEERED FOR CONTROL OF CELL AND TISSUE
BEHAVIOR

A Dissertation Presented

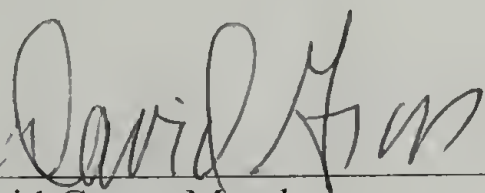
by

KATHLEEN A. DI ZIO

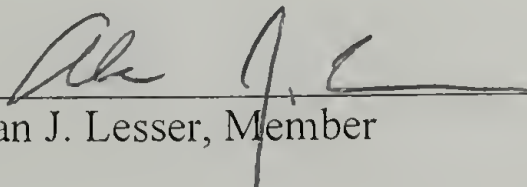
Approved as to style and content by:



David A. Tirrell, Chair



David Gross, Member



Alan J. Lesser, Member



Thomas J. McCarthy, Department Head
Polymer Science and Engineering

ACKNOWLEDGEMENTS

I will begin by thanking my advisor David Tirrell for providing me with the opportunity to achieve this goal. His gentle guidance and unrelenting support have served as a foundation for my scientific and personal development. He has instilled a strong independence and unwavering integrity that will serve me well in future endeavors.

I would also like to thank my committee Alan Lesser and David Gross for their valuable advice, perspectives, and understanding.

The many group members in the Tirrell Laboratory, past and present, have provided much influential personal and scientific advice. Their friendships, opinions, and conversations have been mind broadening and fulfilling. Friends from both within and outside of the laboratory have helped me maintain a healthy perspective and balance. Their belief in me has often granted me well-timed encouragement.

My family has remained the backbone of my support over these years. Their undying confidence and faith in me have served as a necessary reassurance.

Most of all I would like to thank my husband, Mark Brongersma, for being the person he is.

ABSTRACT

PROTEIN MATRICES ENGINEERED FOR CONTROL OF CELL AND TISSUE BEHAVIOR

FEBRUARY 2003

KATHLEEN A. DI ZIO, B.S., UNIVERSITY OF CALIFORNIA SANTA BARBARA

M.S. UNIVERSITY OF MASSACHUSETTS AMHERST

Ph.D., UNIVERSITY OF MASSACHUSETTS AMHERST

Directed by: Professor David A. Tirrell

Genetic engineering of artificial extracellular matrix (ECM) proteins represents an exciting avenue for the preservation and control of the specificity of natural polymers on a molecular level. This work focuses on controlling the mechanical and cell adhesion properties of artificial extracellular matrices intended for vascular graft applications.

Genetic engineering methods were used for the design and preparation of artificial proteins containing sequences chosen to mimic elements of the ECM. The cell-binding domains (CBDs) of fibronectin impart biologic function, while an elastin-like repeat, $[(VPGIG)_2(VPGKG)(VPGIG)_2]$ provides mechanical properties and sites for covalent crosslinking.

Three proteins were constructed using this design that differ only by the CBD. The CBDs chosen for the proteins were the CS5 domain, the scrambled CS5 (SC5) domain, and the CS1 domain and are denoted by the respective CBDs. The SC5 protein was prepared as a negative control for the CS5 protein to assure cell adhesion was

mediated by the CS5 domain. The CS1 domain binds the same integrin as the CS5 with a 20 – 100 fold higher affinity.

Bis(sulfosuccinimidyl)suberate and disuccinimidyl suberate were used to crosslink protein films for mechanical testing. By varying the amount of crosslinker and protein weight fraction, films were prepared with Young's moduli ranging from 0.06 MPa to 0.97 MPa. The molecular weight between crosslinks (M_c) was calculated to lie between 3,000 and 38,000. The moduli and M_c of the proteins span the range reported for natural elastin. Thiolyating the lysines in CS5 with N-succinimidyl S-acetylthioacetate allowed investigation of the effect of disulfide crosslinking on the mechanical properties. The modulus of the disulfide crosslinked films was 0.48 MPa corresponding to a M_c of 6000.

Adhesion studies of human umbilical vein endothelial cells (HUVEC) showed increased and stronger adhesion to the CS5 protein over the SC5 protein. HUVEC adhesion to the SC5 was similar to the negative control (BSA) with very low or no adhesion. HUVEC adhesion to the CS5 ranged from the same as fibronectin to lower than fibronectin as the detachment force was increased. These studies indicated adhesion was mediated by the CBD since the proteins were otherwise identical.

TABLE OF CONTENTS

	Page
ACKNOWLEDGMENTS	iv
ABSTRACT	v
LIST OF TABLES.....	xii
LIST OF FIGURES.....	xiii
CHAPTER	
1. INTRODUCTION: VASCULAR GRAFTS	1
1.1 Motivation	1
1.2 History	2
1.3 Current Graft Materials	2
1.4 Background.....	5
1.5 Artificial Extracellular Matrix Proteins.....	9
1.6 Reference.....	15
2. PREPARATION OF ARTIFICIAL EXTRACELLULAR MATRIX PROTEINS	22
2.1 Introduction and Objectives	22
2.2 Experimental Section.....	22
2.2.1 Genetic Manipulation	22
2.2.1.1 Design of Artificial Gene El-IK	23
2.2.1.2 Preparation of Synthetic DNA	23
2.2.1.3 Cloning and Amplification of Synthetic DNA	24
2.2.1.4 Polymerization of El-IK Monomer and Cloning of El-IK Multimers	24
2.2.1.5 Construction of the Bacterial Expression Vectors	25
2.2.2 Protein Expression and Purification	26
2.2.2.1 10 L Fermentation	26
2.2.2.2 Protein Purification	26
2.3 Results and Discussion	28

2.3.1	Protein Expression and Purification	28
2.3.1.1	Expression and Yield of Protein	28
2.3.1.2	Purification by the LCST	28
2.3.1.3	Measures of Purity	29
2.4	Summary and Conclusions	29
2.5	References	41
3.	MECHANICAL PROPERTIES OF CS5 AND SC5 PROTEINS	42
3.1	Introduction and Objectives	42
3.2	Experimental Section.....	42
3.2.1	Measuring the LCST	42
3.2.2	Crosslinking Chemistry	43
3.2.3	Film Casting	43
3.2.3.1	Method I	43
3.2.3.2	Method II	44
3.2.4	Film Characterization	44
3.2.4.1	Weight Fraction Protein	44
3.2.4.2	Residual Lysine Content	45
3.2.5	Tensile Testing	46
3.3	Results and Discussion	46
3.3.1	LCST Behavior.....	46
3.3.2	NHS-ester Crosslinking.....	47
3.3.3	Film Characterization	47
3.3.3.1	Weight Fraction Protein	47
3.3.3.2	Residual Lysine Content	48
3.3.4	Mechanical Properties of Films.....	49
3.3.4.1	Treatment of Mechanical Testing Data.....	49
3.3.4.2	Mechanical Properties of Method I Films.....	50

3.3.4.2.1	Variation of NHS to Lysine Stoichiometry.....	50
3.3.4.2.2	Variation of Crosslinking Time.....	50
3.3.4.2.3	Variation of Protein Concentration.....	51
3.3.4.2.4	Variation of Crosslinking Temperature...	51
3.3.4.2.5	Variation of Testing Temperature	52
3.3.4.3	Mechanical Properties of Method II Films	53
3.3.5	Theoretical Mc.....	53
3.4	Summary and Conclusions	54
3.5	References.....	80
4.	MECHANICAL PROPERTIES OF CS1 PROTEIN	82
4.1	Introduction and Objectives	82
4.2	Experimental Section.....	82
4.2.1	Measuring the LCST	82
4.2.2	Film Casting	83
4.2.2.1	Method I.....	83
4.2.2.2	Method III	83
4.2.3	Film Characterization.....	83
4.2.3.1	Weight Fraction Protein	83
4.2.3.2	Residual Lysine Content	83
4.2.4	Tensile Testing	84
4.3	Results and Discussion	84
4.3.1	LCST Behavior.....	84
4.3.2	Film Characterization	84
4.3.2.1	Weight Fraction Protein	84
4.3.2.2	Residual Lysine Content	85
4.3.3	Mechanical Properties of Films.....	86
4.3.3.1	Treatment of Mechanical Testing Data.....	86

4.3.3.2	Mechanical Properties of Method I Films	86
4.3.3.2.1	Variation of NHS to Lysine Stoichiometry.....	86
4.3.3.2.2	Variation of Crosslinking Time.....	87
4.3.3.2.3	Variation of Protein Concentration.....	87
4.3.3.2.4	Variation of Crosslinking Temperature...	88
4.3.3.3	Mechanical Properties of Method III Films.....	88
4.3.4	Theoretical Mc.....	89
4.4	Summary and Conclusions	90
4.5	References.....	102
5.	THIOLATION OF CS5 PROTEIN FOR DISULFIDE CROSSLINKING	103
5.1	Introduction and Objectives.....	103
5.2	Experimental Section.....	104
5.2.1	Protein Thiolation.....	104
5.2.2	NMR Analysis of Thiolated Protein.....	104
5.2.3	Measuring the LCST.....	105
5.2.4	Film Casting.....	105
5.2.5	Film Characterization	105
5.2.5.1	Reduction of Disulfides	105
5.2.5.2	Weight Fraction Protein.....	105
5.2.5.3	Residual Lysine Content	106
5.2.6	Mechanical Testing.....	106
5.3	Results and Discussion	106
5.3.1	Protein Thiolation.....	106
5.3.2	NMR Analysis of Thiolated Protein.....	106
5.3.3	LCST Behavior.....	107
5.3.4	Film Casting.....	107
5.3.5	Film Characterization	108
5.3.5.1	Reduction of Disulfides	108
5.3.5.2	Weight Fraction Protein.....	108
5.3.5.3	Residual Lysine Content	108
5.3.6	Mechanical Properties and Theoretical Mc	109

5.4	Summary and Conclusions	110
5.5	References.....	122
6.	HUVEC ADHESION TO CS5 AND SC5 PROTEINS	123
6.1	Introduction and Objectives.....	123
6.2	Experimental Section.....	123
6.2.1	Substrate Preparation.....	123
6.2.2	Culturing HUVEC	124
6.2.2	Fluorescent Labeling of HUVEC	124
6.2.3	Plating of HUVEC.....	125
6.2.4	Detachment by Centrifugation.....	125
6.2.5	Crystal Violet Staining of Adhered HUVEC.....	126
6.3	Results and Discussion	126
6.3.1	Substrate Preparation.....	126
6.3.2	Fluorescent Labeling of HUVEC	127
6.3.3	Detachment by Centrifugation.....	127
6.3.4	HUVEC Adhesion to CS5 and SC5 Proteins	128
6.4	Summary and Conclusions	129
6.5	References.....	136
7.	FUTURE RESEARCH DIRECTIONS	137
7.1	Mechanical and Biological Considerations	137
7.2	References.....	139
	APPENDIX: LIST OF AMINO ACIDS	140
	BIBLIOGRAPHY.....	141

LIST OF TABLES

Table	Page
2.1 Amino acid analysis of CS5 and SC5 proteins showing amino acid compositions within 1 mole % of expected.....	30
2.2 Amino acid analysis of CS1 protein showing amino acid compositions within 1 mol % of expected with the exception of valine that is within 1.5 mol %.....	31
3.1 Physical properties of crosslinked CS5 and SC5 protein films.....	56
3.2 Mechanical properties of crosslinked CS5 and SC5 protein films.....	57
4.1 Physical properties of crosslinked CS1 protein films.....	91
4.2 Mechanical properties of crosslinked CS1 protein films.....	92
5.1 Physical properties of disulfide crosslinked CS5-SATA protein films.....	111
5.2 Mechanical properties of disulfide crosslinked CS5-SATA protein films.....	112
6.1 HUVEC adhesion to substrates relative to fibronectin.....	131

LIST OF FIGURES

Figure	Page
1.1	Number of HUVEC attached to artificial ECM proteins indicating better adhesion to the protein with a higher cell-binding domain density.....14
2.1	Construction of pUC El-IK plasmid by insertion of the El-IK fragment into the pUC 19 plasmid at the Eco RI/Bam HI restriction sites32
2.2	Construction of the pEC CBD(El-IK) ₄ plasmids by insertion of the tetramer (El-IK) ₄ into the pEC CBD plasmids at the Ban I restriction site (where CBD = CS5, SC5, and CS1).....33
2.3	Construction of the bacterial expression vector pET CBD(El-IK) ₄34
2.4	Purification flowchart showing a simple, batch purification to obtain multi-gram quantities of target proteins35
2.5	Three proteins were made by genetic engineering and are denoted by the cell-binding domain CS5, SC5, and CS136
2.6	SDS-PAGE gel and western blot of the CS5 and SC5 proteins37
2.7	SDS-PAGE gel and western blot of the CS1 protein38
2.8	Mass spectrometry of the CS5 protein, showing a peak at 37150, within experimental error of the expected mass of 3712039
2.9	Mass spectrometry of SC5 protein, showing a mass peak at 37174, within experimental error of the expected mass of 3712040
3.1	Reaction scheme for crosslinking the lysine residues of the protein with bifunctional NHS esters. R' is (CH ₂) ₆ , for DSS, R=H; for BS3, R=SO ₃ ⁻ Na ⁺ ...58
3.2	Film casting by Method I.....59
3.3	Film casting by Method II.....60
3.4	Reaction of Sulfo-SDTB for detection of residual lysines in crosslinked films by measuring absorbance at 498 nm of the dimethoxytrityl cation product.....61
3.5	Tensile testing apparatus allowing uniaxial tensile tests under simulated physiological conditions (37 °C, PBS pH 7.4)..... 62

3.6	LCST behavior of CS5 protein at 10, 20, and 30 mg/ml concentrations.....	63
3.7	LCST behavior of SC5 protein at 10, 20, and 30 mg/ml concentrations.....	64
3.8	Stress-strain behavior of CS5 protein films crosslinked by Method I at 0.5:1, 1:1, and 1.5:1 NHS to lysine stoichiometries	65
3.9	Stress-strain behavior of SC5 protein films crosslinked by Method I at 0.5:1, 1:1, and 1.5:1 NHS to lysine stoichiometries	66
3.10	Determination of shear modulus, G , of CS5 protein films by measuring the slope of the line formed by plotting stress vs. $\lambda - 1/\lambda^2$	67
3.11	Determination of tensile or Young's modulus, E , of CS5 protein films by measuring the slope of the line formed by plotting stress vs. strain for the first 5 % strain.....	68
3.12	Stress-strain behavior of CS5 protein films crosslinked by Method I for 12, 24, and 48 hr	69
3.13	Stress-strain behavior of CS5 protein films crosslinked by Method I at 0.2 w/v and 0.4 w/v concentrations	70
3.14	Stress-strain behavior of SC5 protein films crosslinked by Method I at 0.2 w/v and 0.4 w/v concentrations	71
3.15	Two films clamped in an Instron testing grip, exhibiting difference in appearance between (a) films crosslinked above the LCST (25 °C) and (b) films crosslinked below the LCST (4 °C).....	72
3.16	SEM micrographs of a CS5 film crosslinked by Method I above the LCST (25 °C).....	73
3.17	SEM micrographs of CS5 protein films crosslinked by Method I below the LCST (4 °C).....	74
3.18	Stress-strain behavior of CS5 protein films crosslinked by Method I at 4 °C and 25 °C	75
3.19	Stress-strain behavior of SC5 protein films crosslinked by Method I at 4 °C and 25 °C	76
3.20	Stress-strain behavior of a 0.2 w/v crosslinked CS5 protein film tested at 15, 25, 37, and 45 °C	77

3.21	Stress-strain behavior of a 0.4 w/v crosslinked CS5 protein film tested at 15, 25, 37, and 45 °C	78
3.22	Stress-strain behavior of films crosslinked by Method II in solutions with 100:1, 10:1 and 5:1 NHS to lysine stoichiometries	79
4.1	Film casting by Method III	93
4.2	LCST behavior of the CS1 protein at 10, 20, and 30 mg/ml concentrations.....	94
4.3	Stress-strain behavior of CS1 protein films crosslinked by Method I at 0.5:1, 1:1, and 1.5:1 NHS to lysine stoichiometries	95
4.4	Determination of shear modulus, G, of crosslinked CS1 protein films.....	96
4.5	Determination of tensile or Young's modulus, E, of crosslinked CS1 films	97
4.6	Stress-strain behavior of CS1 protein films crosslinked by Method I for 12, 24, and 48 hr	98
4.7	Stress-strain behavior of CS1 protein films crosslinked by Method I at 0.2 w/v and 0.4 w/v concentrations	99
4.8	Stress-strain behavior of CS1 protein films crosslinked by Method I at 4 °C and 37 °C.....	100
4.9	Stress-strain behavior of CS1 protein films crosslinked by Method III at 0.1, 0.2, and 0.3 w/v protein concentrations.....	101
5.1	SATA-modification reaction scheme for the thiolation of CS5 protein.....	113
5.2	Film casting by Method IV	114
5.3	NMR spectrum of SATA	115
5.4	NMR spectrum of CS5	116
5.5	NMR spectrum of CS5-SATA. SATA-derived signals are labeled with asterisks.....	117
5.6	LCST behavior of CS5-SATA protein at 10, 20, and 30 mg/ml concentrations.....	118
5.7	Stress-strain behavior of disulfide crosslinked CS5-SATA protein films.....	119

5.8	Determination of the shear modulus, G , of disulfide crosslinked CS5-SATA protein films.....	120
5.9	Determination of the tensile or Young's modulus, E , of CS5-SATA protein films.....	121
6.1	The fluorescent label BCECF-AM is a mixture of the above three molecule...	132
6.2	Standard curve for the labeled HUVEC showing linear dependence of fluorescence emission at 535 nm with number of cells.....	133
6.3	HUVEC adhesion, measured in fluorescence, to CS5 and SC5 relative to fibronectin and BSA.....	134
6.4	HUVEC adhesion, measured by crystal violet staining, to CS5 and SC5 relative to fibronectin and BSA.....	135

CHAPTER 1

INTRODUCTION: VASCULAR GRAFTS

1.1 Motivation

Degenerative diseases of the arteries, arterioles, and capillaries are responsible for 2% of all deaths annually [1]. In an effort to treat these diseases, there are more than 500,000 vascular grafts implanted yearly in the United States [2, 3]. Large diameter vascular grafts introduced to areas of high blood flow remain patent for many years. Conversely, grafts with diameters less than 6 mm have been plagued by failure through thrombosis and intimal hyperplasia [4]. Despite the large demand and over forty years of research, an acceptable synthetic material for small diameter grafts does not exist.

Most grafting success has been realized through the use of the autologous saphenous vein. Although this is currently the most desired material, the demand severely exceeds the availability [4, 5]. Recent studies show that 28 % of patients have an unusable or absent saphenous vein [6]. The lack of adequate saphenous vein and its potential, preferential use are motivation enough for the development of an adequate alternative. In addition, 30 % of saphenous vein grafts stenose within five years [7]. This unsatisfactory patency rate combined with the unavailability of the saphenous vein has driven the focus of much research toward finding a new graft material.

1.2 History

The first successful application of a synthetic vascular graft was reported in 1952. Vinyon N was used to replace a section of the artery that was believed to be a simple conduit through which blood passed [8]. Research has since focused on developing materials that were biologically inert, when it was believed that biocompatible meant minimizing interactions with the body. Currently, researchers have concentrated on the design of a biointeractive material, which provides the appropriate biological signals, subsequently redefining the term “biocompatible.” Nonetheless, biomaterials that have predominated in the last decade are dated and far behind the revolution that has evolved in the basic sciences. It seems the rate-limiting step in the clinical application of new and effective biomaterials is the discovery of truly biocompatible implants and prostheses [9].

1.3 Current Graft Materials

Application of current synthetic vascular graft technologies yields high failure rates. Despite the many materials that have been explored, expanded polytetrafluoroethylene (ePTFE) and Dacron have remained dominant [4]. Although these materials prove suitable for large diameter grafts, they are inadequate in small diameter (< 6 mm) applications, leading to thrombosis and intimal hyperplasia. For reasons that are currently unknown, migratory activity of the native endothelium ceases after the cells have migrated approximately one centimeter into the graft; a phenomenon observed in all animal species including man [10]. The surface spanning this centimeter

remains antithrombogenic at both the proximal and distal ends of the graft, leaving the thrombogenicity of the intermediate portion unaffected [10]. Depending on the study, and animal used, untreated ePTFE grafts show 100 % failure rates at 12 weeks in dogs [11] to six and a half years in humans [12].

In an effort to reduce failure rates, attempts have been made to endothelialize or promote endothelialization of the graft. Initial strategies concentrated on graft pacification, using various protein coatings to minimize blood/biomaterial interactions. The surfaces of existing grafts were modified by impregnation with albumin [13], gelatin [14], and collagen [15], clotting with whole blood [16], or treatment with fibrin glue [17]. More recently, preseeding grafts with endothelial cells in the operating room [18] or establishing a confluent layer of endothelial cells prior to implantation [19] has been demonstrated in humans. The establishment of the confluent monolayer of endothelial cells has produced patency results comparable to that of saphenous vein [12]. Although these results are promising, a five-year failure rate of 30 % remains unsatisfactory.

Although the creation of a confluent monolayer improves long-term patency of grafts, it is evident that the existence of this monolayer alone is not sufficient. Several factors can induce a procoagulant state in the endothelium. Such stimuli include mechanical trauma, bacterial endotoxins, and inflammatory mediators [20, 21]. Endothelial cells are capable of releasing smooth muscle cell mitogens that can cause elevated mitotic activity [22-25].

In addition to biological considerations, the mechanical properties of a small diameter synthetic graft are a primary concern. The graft must withstand physical demands of its environment, requiring crush strength and flexibility for cross-joint

applications, and maintaining mechanical integrity during long-term pulsatile stress and the load imposed by lumen pressure. Another important matter is the hemodynamic trauma imposed on the endothelium by a compliance mismatch between the graft and native vessel, leading to thrombus formation and intimal hyperplasia [26-30]. This indicates the dependence of the cell physiology on the mechanics of the material and the significance of incorporating both bioactive and biomechanical properties into the design of small diameter vascular grafts.

Polyurethanes have been the subject of recent studies in an effort to reduce the compliance mismatch between native vascular materials and biomaterials. Polyurethanes are used in a variety of blood-contacting biomaterials, including catheters, blood filters, and blood tubing [31, 32]. These materials provide strength, moldability, and elasticity but are known to activate platelets. The platelet reactivity has been decreased by blending polyurethane with poly(tetramethylene oxide) [31]. This material appropriately addresses the compliance mismatch issue, but does not possess the necessary biologic signals to maintain a healthy endothelium.

Another route to address the biological and biomechanical considerations for a synthetic vascular graft is the use of completely biological materials. Endothelial cells and smooth muscle cells will grow their own extracellular matrix in culture [33]. Layered, tubular structures have been created, producing well-defined tissues including the intima, media, and adventitia [34]. Some of the drawbacks of this structure for use as a vascular graft are a three-month preparation time and compliance mismatch from that of native vessels. Although this approach seems promising, the research is still in the

very early stages, and the time required for regeneration of a vessel by entirely autologous or cell-derived components makes the technique impractical.

It seems reasonable that an effective vascular graft might first serve as a simple scaffold to provide the appropriate biological signals and the necessary mechanical integrity for the vessel to eventually rebuild itself into a natural organ. In addition to biological signals, biocompatibility and biodegradability must be built into the material. For use in clinical applications this material must be available at the time of demand. Success will likely rely on the incorporation of synthetic as well as biological aspects. Progress is rapidly being achieved in the search for factors that control thrombus formation, intimal hyperplasia, and angiogenesis; this will undoubtedly lead to the production of a more acceptable material for vascular grafts.

1.4 Background

In an effort to create the environment for a healthy endothelium, researchers have looked more closely at specific cell-extracellular matrix (ECM) interactions. An understanding of the molecular basis of cell adhesion should provide some insight into the role of these interactions during normal development and growth, as well as in disease states. Integrins are a group of sequence-related proteins that are involved in cell-ECM and cell-cell adhesion. The ECM-receptor integrins are heterodimers composed of a number of different α and β subunits [35]. The composition of the ECM determines which integrins are included in focal contact formation during cell adhesion. Integrins, a word formulated to represent the integration of the ECM and the cytoskeleton, affect the

cell's activities with respect to their extracellular environment. Integrins are an important component in cellular signal transduction and are involved in remodeling associated with wound healing and angiogenesis [36]. The attachment of human umbilical endothelial cells (HUVEC) on fibronectin through integrins causes the cells to set up "micro-compartments" for protein synthesis in the region of the integrin receptor [37]. This indicates integrins play an important role in the formation of proteins and ensuing regeneration of the ECM by the cell. It would seem necessary to involve integrins in the biological signals provided by a scaffold that allowed the regeneration of a natural ECM.

Recently there has been appreciable progress toward elucidating the biochemical nature of the interaction of cells with purified ECM components. Fibronectin, a multifunctional protein found in the ECM and blood serum contains many cell-adhesion domains [38]. REDV is the minimal active sequence in the CS5 domain of fibronectin known to bind the $\alpha_4\beta_1$ integrin [39-42]. This peptide is of particular interest because in culturing studies it has been shown to adhere HUVEC but not smooth muscle cells (SMC), platelets, or fibroblasts [43, 44]. In fact, immobilization of GREDVY on glycophasic glass has produced surfaces that selectively attach HUVEC and not fibroblasts, smooth muscle cells (SMC) or platelets [44]. In order to explore the role of receptor-ligand affinity, another cell-adhesion domain of interest is the CS1 segment of fibronectin. The CS1 domain is also known to bind the $\alpha_4\beta_1$ integrin, but with a 20-100 fold higher affinity than the CS5 domain [42]. It is possible that a material incorporating CS5 or CS1 domains would support selective attachment of HUVEC and bypass thrombus formation or intimal hyperplasia.

RGD is another sequence found in the central cell-binding domain of fibronectin, which can adhere a variety of cell types, including endothelial cells, through $\alpha_5\beta_1$ and $\alpha_v\beta_3$ integrins [40, 45]. Grafting RGD peptides to ePTFE surfaces improves endothelial cell adhesion in vitro [46].

Due to the limited time available for endothelial cells to attach and spread to graft surfaces in a clinical environment, factors that promote rapid and strong adhesion need to be examined. Altering the receptor-ligand affinity is one approach to increase the adhesion strength. The conformation of the peptide seems to play an integral role in cell attachment. When Hubbell et al. grafted the GRGDY peptide on glass through the C-terminus rather than the N-terminus, it showed a higher affinity to attach platelets [47]. Xiao and Truskey showed the immobilization of RGD on glass illustrated a higher affinity of the surface for bovine endothelial cell adhesion when attached in a cyclic form instead of a linear one [48]. This indicates that the presentation of the sequence is important for receptor recognition. It is possible that the looped presentation is more analogous to the native conformation, which is within the backbone of the fibronectin molecule. This suggests integration of a bioactive sequence into the backbone of a material may result in higher cell adhesion than for a material with the grafted peptide.

In addition to the integrin-binding domains, many naturally occurring ECM proteins contain heparin-binding domains [49-52]. It has been shown that heparin not only exhibits anticoagulant activity, but also serves as a potent and specific inhibitor of SMC proliferation [53, 54]. Specifically, the peptide sequence RYVVLPRPVCFEKGMNYTVR has been identified in murine laminin to bind heparin and aid adhesion of cells when immobilized on polystyrene [55]. It is believed heparin-

sulfate proteoglycans present on the cell surfaces bind to the heparin-binding domains and promote the formation of cellular, focal-adhesion contacts [56].

Coincident to the biological features of ECM proteins, structural features have also been examined. A natural blood vessel consists of an intima with an endothelial cell layer, a media that is primarily elastin and smooth muscle cells, and an adventitia that is mainly collagen and fibroblasts. Elastin is a major component of the elastic lamina of small muscular arteries found directly adjacent to the endothelium. It is a fibrous protein found within arterial walls, ligaments, and other connective tissue with its principal function to provide elasticity and resilience [57]. The high content of hydrophobic residues makes elastin one of the most chemically and proteinase-resistant proteins in the body. In a natural artery the mechanical strength to withstand the load imposed by the lumen pressure is provided by the vessel's elastin structure and the contractile force of the smooth muscle cells [58]. In contrast to the modulus of ePTFE (600 MPa), naturally occurring elastin has a modulus of 0.3 MPa – 0.6 MPa [59].

The sequence VPGVG has been shown to repeat up to eleven times consecutively in native elastin [60]. The exploration of elastin-like sequences has produced materials with a large span of mechanical properties. Reported elastic moduli for crosslinked samples encompass a range of values from 10^4 to 10^8 dynes/cm² depending on sequence and water content [61]; a range encompassing moduli recorded for that of the arterial wall [62]. The water solubility of these materials allows facile processing for evaluation of materials properties, films, and device formation [63]. Poly(VPGVG) has been extensively studied with regard to mutagenicity, toxicity, antigenicity, pyrogenicity, and thrombogenicity with promising performance [60].

Elastin-like materials may be favorable for vascular graft applications because of their mechanical characteristics and ability to build in cell-specific interactions. Whereas poly(VPGVG) is non-adhesive towards HUVEC, variants that contain periodic GRGDS inserts exhibit adhesion [64]. The non-adhesive behavior of elastin-like materials could allow the insertion of only the desired function of the cell-adhesion protein, permitting cell-type selectivity that is otherwise unattainable. Similar insertion of the REDV sequence did not produce adhesive substrates [65]. This may be a result of the inability of the short insert to adopt the proper conformation since analogous sequences incorporating the entire region of the CS5 domain show adhesive behavior toward HUVEC [66].

Even though the individual cell types of the arterial wall may be easily cultured and the protein components isolated, the production of a cohesive, three-dimensional structure with mature extracellular-matrix (ECM) elastic tissue layers has been a major technological obstacle [67]. This may in part be a result of the tendency to use existing materials where the original design intent of these materials is usually unrelated to the biomedical application. It should be possible to engineer a material that incorporates the necessary biological and mechanical characteristics for a small diameter vascular graft.

1.5 Artificial Extracellular Matrix Proteins

Natural polymers possess properties inherently difficult to reproduce in synthetic macromolecules. However, natural biosynthetic machinery can be harnessed and manipulated to synthesize protein polymers with specific sequences, molecular weights

and functionalities [68]. Here we have designed artificial ECM proteins to produce a material with both biologic and mechanical functionality. To impart these characteristics, two naturally occurring ECM proteins, fibronectin and elastin were used to derive the artificial ECM sequence.

The design presented here is based on the material prepared by Alyssa Panitch. Panitch's design incorporated CS5 domains from fibronectin interspersed at controlled intervals in a VPGIG elastin-like matrix material. Varying the VPGVG pentapeptide repeat found in elastin by changing the fourth amino acid does not disrupt the elastin-like behavior such as a lower critical solution temperature (LCST) [69]. A distinctive characteristic of elastin-like polymers in aqueous solvents is the existence of an LCST above which a polymer-rich coacervate forms and below which, the polymer is soluble. The LCST is believed to be responsible for a significant aspect of the elasticity of the protein [70]. The CS5 domain, LDGEEIQIGHIPREDVDYLHPLKN, was chosen for its selectivity to bind the $\alpha_4\beta_1$ integrin and because the minimal active sequence, REDV was found to adhere HUVEC, not SMC or platelets. The design utilized bacterial synthesis to maintain exact control of the peptide sequence. Two materials were studied: $(\text{CS5}(\text{VPGIG})_x)_y$, $x = 20, 40$; $y = 5, 3$, respectively. These proteins demonstrated promising adhesion behavior towards HUVEC. Both the number of cells attached and the corresponding spreading of the adherent cells were evaluated. The $(\text{CS5}(\text{VPGIG})_{20})_5$ which contains twice the number of CS5 domains as the $(\text{CS5}(\text{VPGIG})_{40})_3$ showed an increase in the number of attached cells compared to the $(\text{CS5}(\text{VPGIG})_{40})_3$ when coated on glass (Figure 1.1) [66].

Panitch's material maintained the LCST characteristic of elastin-like materials [66]. The LCST can be shifted depending on the hydrophobicity of the fourth residue [61]. Isoleucine was chosen in the VPGIG repeat because it was predicted to yield a material with an LCST of 10°C, which is below room temperature and ensured reduction of water-solubility at physiological temperatures. The measured LCST for the materials was 12°C for the higher CS5 density and 13.4°C for the lower CS5 density material. It was hypothesized that the LCST below physiological temperature would stabilize surface coatings of the protein at these conditions. Panitch showed the majority of protein cast in films dissolved from the surface of glass cover slips even when formed above the LCST [66]. Essentially, all but the amount that was adsorbed onto the surface was washed away. Assuming a uniform coating, the surface layer would be approximately ten nanometers in thickness, however, the low amounts of protein made it difficult to evaluate film continuity. Field emission scanning electron microscopy (FESEM) and energy dispersive x-ray spectrometry (EDX) were performed on CS5 VPGIG₂₀ coated glass cover slips of with a JEOL 6320-FX field emission scanning electron microscope. The FESEM micrographs illustrated that the surface of the films was rough and inconsistent within the film. EDX analysis indicated that the amount of protein present on the cover slip was not sufficient to produce a signal intensity that could be resolved over that of the Si and O from the glass.

The desire to produce stable films and a material with appropriate mechanical properties motivated the development of a crosslinking mechanism for the CS5 VPGIG constructs. The available methods for crosslinking these elastin-like materials are limited. Physical crosslinking methods such as γ -irradiation have been used to crosslink

VPGVG constructs [63]. Although this produces three-dimensional networks with promising mechanical properties for vascular graft applications, it results in a low crosslink density and is nonspecific [71]. It was shown that γ -irradiation crosslinked VPGVG constructs required incorporation of a higher RGD density to attain the same cell-adhesion behavior as with the uncrosslinked materials [65].

Eosin Y has been used to crosslink BSA and collagen [72]. Attempts to photochemically crosslink the CS5 (VPGIG)_x constructs with Eosin Y as a photosensitizer and triethanol amine as an electron donor failed to produce an insoluble material.

Glutaraldehyde (GTA) and carbodiimide (CDI) with hexamethylene diamine (HMDA) have been used extensively to crosslink collagen [73]. Although crosslinking with GTA provides a convenient and effective means of crosslinking, degradation of the protein during implantation releases monomeric GTA into the tissue, resulting in cytotoxicity and inflammation [73]. Efforts to crosslink the CS5(VPGIG)_x constructs using GTA and CDI/HMDA techniques also failed to produce crosslinked materials.

Welsh introduced lysines into the N- and C-terminal regions of the (CS5(VPGIG)₂₀)_x proteins of varying lengths and crosslinked with glutaraldehyde yielding films with tensile moduli analogous to natural elastin [74]. An elastin-like motif was used by Conticello and coworkers where lysines were incorporated within a VPGVG repeat and crosslinked to create elastin-mimetic hydrogels where the extent of crosslinking with bifunctional N-hydroxysuccinimidyl (NHS) esters and swelling behavior were characterized [75]. Urry and coworkers explored the swelling and

mechanical behavior of various elastin-like proteins crosslinked by γ -irradiation, dicumyl peroxide and carbodiimide [76-78].

In an effort to make a material with the desired mechanical properties and further explore the biologic effects of the cell-binding domains (CBD), the proposed design introduces a crosslinking residue within the elastin-like region. The replacement of a lysine for every fifth isoleucine residue allows a mechanism for crosslinking the protein and yields a repeated protein sequence as follows:



Incorporation of the lysine in this position would permit crosslinking within the elastin-like sequence and potentially not affect the cell-binding behavior. The following CBD will be incorporated into the above elastin-like motif: CS5, SC5, and CS1. The SC5 domain will serve as a negative control for the CS5, where the REDV part of the CS5 is scrambled to REVD in the SC5. In order to explore the role of ligand affinity, another cell-binding domain of interest is the CS1 domain of fibronectin. The CS1 domain is also known to bind the $\alpha 4 \beta 1$ integrin, but with a 20-100 fold higher affinity [42].

The crosslinkable elastin-like structure will provide the mechanical integrity and compliance while the CBD domain will impart the biological activity of the material. The precisely controllable molecular architecture offers the ability to systematically alter the material properties and further understand the requirements for a vascular graft.

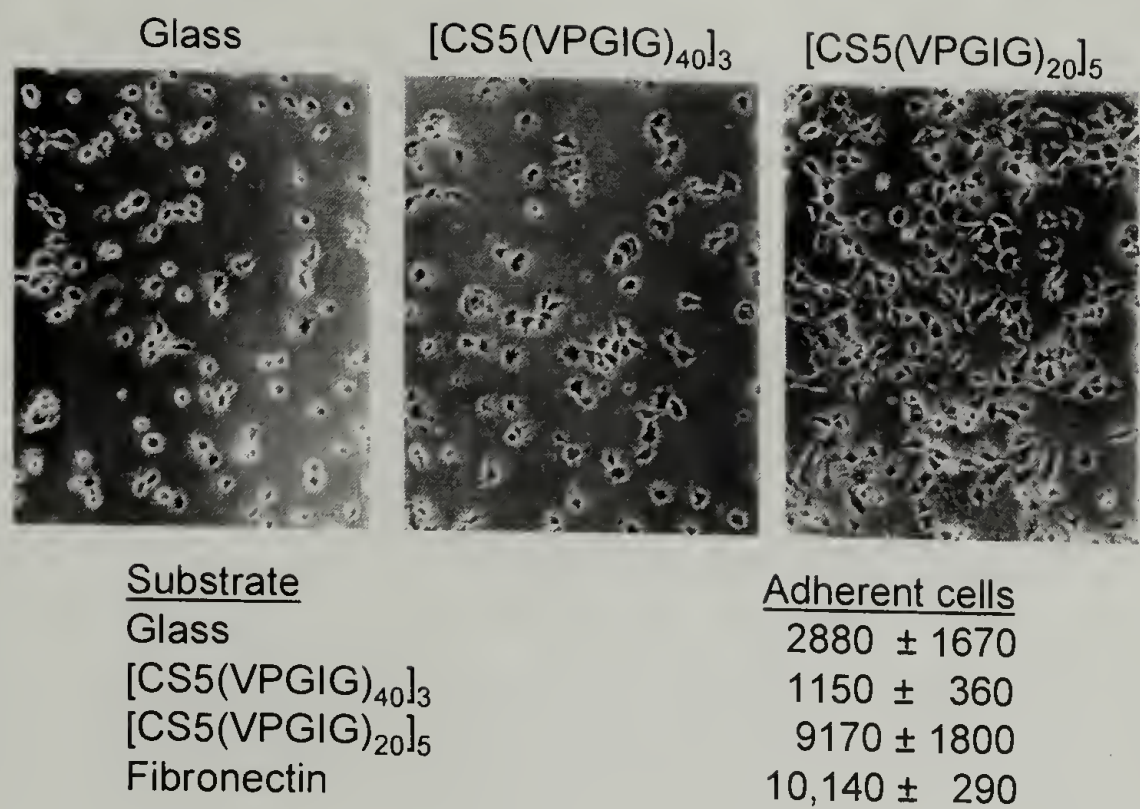


Figure 1.1 Number of HUVEC attached to artificial ECM proteins indicating better adhesion to the protein with a higher cell-binding domain density [66].

1.6 References

1. Statistics, N.C.f.H., *Vital Statistics of the United States*. 1992, Center for Disease Control. p. 1-757.
2. Greisler, H. *Angiogenic Mechanisms in Healing of Synthetic Grafts*. in *How to Build a Blood Vessel*. 1997. Bethesda, MD.
3. Langer, R.W. and J. Vacanti, *Tissue Engineering*. Science, 1993. **260**: p. 920-926.
4. Greisler, H.P., *New Biologic and Synthetic Vascular Prostheses*. 1991, Austin, TX: R.G. Landes Company.
5. Musella, R.A. and E.N. Willey, *Evaluation of Patency of Synthetic and Autogenous Venous and Arterial Micrografts in Rats*. Microsurgery, 1985. **6**: p. 85-91.
6. Abbott, W.M. and J.J. Vignati, *Prosthetic Grafts: When are They a Reasonable Alternative?* Seminars in Vascular Surgery, 1995. **8**(3): p. 236-245.
7. Kohler, T.R., et al., *Mechanisms of Long-Term Degradation of Arterialized Vein Grafts*. Am. J. Surg., 1990. **160**: p. 257.
8. Voorhees, A.B., A. Jaretzki, and A.H. Blakemore, *The Use of Tubes Constructed from Vinyon N Cloth in Bridging Arterial Defects*. Ann. Surg., 1952. **135**: p. 332.
9. Greco, R.S., *Implantation Biology: The Host Response and Biomedical Devices*. 1994: CRC Press, Inc. 417.
10. Williams, S.K., et al., *Formation of a Functional Endothelium on Vascular Grafts*. Electron Microscopy Technique, 1991. **19**: p. 439-451.
11. Williams, S.T., D.C. Rose, and B.E. Jarrell, *Microvascular Endothelial Cell Seeding of ePTFE Vascular Grafts: Improved Patency and Stability of the Cellular Lining*. J. Biomed. Mat. Res., 1994. **28**: p. 203-212.
12. Zilla, P., et al., *Long-term Effects of Clinical In-vitro Endothelialization on Grafts*, in *How to Build a Blood Vessel*, L.F.R.I.i.V.D. Conference, Editor. 1997: Bethesda, MD.
13. Rumisek, J.D., et al., *Heat-denatured Albumin-Coated Dacron Vascular Grafts: Physical Characteristics and In-vivo Performance*. J. Vasc. Surg., 1986. **4**: p. 136-143.

14. Drury, J.K., et al., *Experimental and Clinical Experience with a Gelatin Impregnated Dacron Prosthesis*. Ann. Vasc. Surg., 1987. **1**: p. 542-547.
15. Freishlag, J.A. and W.S. Moore, *Clinical Experience with a Collagen-Impregnated Knitted Dacron Vascular Graft*. Ann. Vasc. Surg, 1990. **4**: p. 449-454.
16. Yates, S.G., et al., *The Preclotting of Porous Arterial Prostheses*. Ann. Surg., 1978. **188**: p. 612-622.
17. Gray, L.J., et al., *FGF-1 Affixation Stimulates ePTFE Endothelialization without Intimal Hyperplasia*. J. Surg. Res., 1994. **57**: p. 596-612.
18. Williams, S.K., *Endothelial Cell Transplantation*. Cell Transplantation, 1995. **4**: p. 401-410.
19. Zilla, P., et al., *Clinical In-vitro Endothelialization of Femoropopliteal Bypass Graft: An Actuarial Follow-up over Three Years*. J. Cardiovasc. Surg., 1994. **19**: p. 540-548.
20. Bevilacqua, M.P., et al., *Recombinant Tumor Necrosis Factor Induces Procoagulant Activity in Cultured Human Vascular Endothelium: Characterization and comparison with the Actions of Interleukin I*. Proc. Natl. Acad. Sci. USA, 1986. **83**: p. 4533.
21. Colucci, M., G.I. Balcon, and R. Lorenzet, *Cultured Human Endothelial Cells Generate Tissue Factor in Response to Endotoxin*. J. Clin. Invest., 1983. **71**: p. 1893.
22. Dicoletto, P.E. and D. Bowen-Pope, *Cultured Endothelial Cells Produce a Platelet-Derived Growth Factor-like Protein*. Proc. Natl. Acad. Sci. USA, 1983. **80**: p. 1919-1923.
23. Fox, P.L. and P.E. DiCorleto, *Regulation of Production of a Platelet-Derived Growth Factors-like Protein in Cultured Bovine Aortic Endothelial Cells*. J. Cell Physiol., 1984. **121**: p. 298-308.
24. Ross, R., E. Raines, and D. Bowen-Pope, *Growth Factors from Platelets, Monocytes, and Endothelium: Their Role in Cell Proliferation*. Ann. NY. Acad. Sci., 1982. **397**: p. 18-24.
25. Clowes, A.W., R.D. Kirkman, and M.A. Reidy, *Mechanism of Arterial Graft Healing: Rapid Transmural Capillary Ingrowth Provides a Source of Intimal Endothelium and Smooth Muscle in Porous PTFE Prostheses*. Am. J. Path., 1986. **123**: p. 220-230.

26. Abbott, W.M. and R.P. Cambria, *Control of Physical Characteristics (Elasticity and Compliance) of Vascular Grafts, in Biologic and Synthetic Vascular Prostheses*, ed. J.C. Stanley. 1982, New York: Gurne and Stratton. 189-220.
27. Greisler, H.P., et al., *Spatial and Temporal Changes in Compliance Following Implantation of Bioresorbable Vascular Grafts*. J. Biomed. Mat. Res., 1992. **26**: p. 1449-1461.
28. Kinley, C.E. and A.E. Marble, *Compliance: A Continuing Problem with Vascular Grafts*. J. Cardiovasc. Surg., 1980. **21**: p. 163-170.
29. Zwolak, R.M., M.C. Adams, and A.W. Clowes, *Kinetics of Vein Graft Hyperplasia: Association with Tangential Stress*. J. Vasc. Surg., 1987. **5**: p. 126-136.
30. Clowes, A.W., M.A. Reidy, and M.M. Clowes, *Kinetics of Cellular Proliferation After Arterial Injury: Smooth Muscle Cell Growth in Absence of Endothelium*. Lab. Invest., 1983. **49**(3): p. 327-333.
31. Herbert, C.B., A.M. Hernandez, and J.A. Hubbell, *Platelet Adhesion to Polyurethane Blended with Polytetramethylene Oxide*. Biotech. Bioeng., 1996. **52**: p. 81-88.
32. Kajiyama, T. and A. Takahara, *Surface Properties and Platelet Reactivity of Segmented Poly(etherurethanes) and Poly(etherurethaneureas)*. J. Biomat. Appl., 1991. **6**: p. 42-71.
33. Jones, P.A., *Construction of an Artificial Blood Vessel Wall from Cultured Endothelial and Smooth Muscle Cells*. Proc. Natl. Acad. Sci. USA, 1979. **76**(4): p. 1882-1886.
34. L'Heureux, N., et al., *A Completely Biological Tissue-Engineered Human Blood Vessel*. FASEB, 1998. **12**: p. 47-56.
35. Carey, D.J., *Control of Growth and Differentiation of Vascular Cells by Extracellular Matrix Proteins*. Ann. Rev. Physiol., 1991. **53**: p. 161-177.
36. Luscinskas, F.W. and J. Lawler, *Integrins as Dynamic Regulators of Vascular Function*. FASEB, 1994. **8**: p. 929-938.
37. Ingber, D., *Prodding Cells to Make Proteins*. Science, 1998. **279**(27): p. 1308.
38. McGrath, K.P. and D. Kaplan, *Protein-Based Materials*. Bioengineering of Materials, ed. D. Kaplan. 1996, Medford, MA: Birkhauser. 429.

39. Humphries, J.J., et al., *Identification of an Alternatively Spliced Site in Human Plasma Fibronectin that Mediates Cell Type-specific Adhesion*. J. Cell Biol., 1986. **103**: p. 2637-2647.
40. Mould, A.P. and M.J. Humphries, *Identification of a Novel Recognition Sequence for the Integrin $\alpha_4\beta_1$ in the COOH-terminal Heparin-Binding Domain of Fibronectin*. EMBO J., 1991. **10**(13): p. 4089-4095.
41. Mould, A.P., et al., *The CS5 Peptide is a Second Site in the IIICS Region of Fibronectin Recognized by the Integrin $\alpha_4\beta_1$: Inhibition of $\alpha_4\beta_1$ Function by RGD Peptide Homologues*. J. Biol. Chem., 1991. **266**(6): p. 3579-3585.
42. Mould, A.P., et al., *Affinity Chromatographic Isolation of the Melanoma Adhesion Receptor for the IIICS Region of Fibronectin and Its Identification as the Integrin $\alpha_4\beta_1$* . J. Biol. Chem., 1990. **265**(7): p. 4020-4024.
43. Hubbell, J.A., et al., *Endothelial Cell-Selective Materials for Tissue Engineering in the Vascular Graft Via a New Receptor*. Biotechnology, 1991. **9**: p. 568-572.
44. Massia, S.P. and J.P. Hubbell, *Vascular Endothelial Cell Adhesion and Spreading Promoted by the Peptide REDV of the IIICS Region of Plasma Fibronectin is Mediated by Integrin $\alpha_4\beta_1$* . J. Biol. Chem., 1992. **267**(20): p. 14019-14026.
45. Hynes, R.O., *Integrins: Versatility, Modulation, and Signaling in Cell Adhesion*. Cell, 1992. **69**: p. 11.
46. Waluscheck, K.P., et al., *Improved endothelial cell attachment on ePTFE vascular grafts pretreated with synthetic RGD-containing peptides*. A. Eur. J. Endovasc. Surg, 1996. **12**: p. 321-330.
47. Hubbell, J.A., S.P. Massia, and P.D. Drumheller, *Surface-grafted Cell-binding Peptides in Tissue Engineering of the Vascular Graft*. Ann. N Y Acad. Sci., 1992: p. 253-258.
48. Xiao, Y. and A. Truskey, *Effect of Receptor-Ligand Affinity on the Strength of Endothelial Cell Adhesion*. Biophys. J., 1996. **71**: p. 2869-2884.
49. Hynes, R.O., *Molecular Biology of Fibronectin*. Ann. Rev. Cell Dev. Biol., 1985. **1**: p. 67.
50. Kornblihtt, A.R., et al., *Primary Structure of Human Fibronectin: Differential Splicing May Generate at least 10 Polypeptides from a Single Gene*. EMBO J., 1985. **4**: p. 1755.
51. Kleinman, H.k., et al., *Biological Activities of Laminin*. Vitamins and Hormones, 1993. **47**: p. 161-196.

52. Mecham, R., *Laminin Receptors*. Ann. Rev. Cell. Dev. Biol., 1991. 7: p. 71-91.
53. Clowes, A.W. and M.A. Reidy, *Prevention of Stenosis After Vascular Reconstruction: Pharmacological Control of Intimal Hyperplasia- A Review*. J. Vasc. Surg., 1991. 13(6): p. 885-891.
54. Lindner, V., et al., *Inhibition of Smooth Muscle Cell Proliferation in Injured Rat Arteries: Interaction of Heparin with Basic Fibroblast Growth Factor*. J. Clin. Invest., 1992. 90: p. 2044-2049.
55. Charonis, A.S., et al., *A Novel Synthetic Peptide from the B1 Chain of Laminin with Heparin-Binding and Cell Adhesion-promoting Activities*. J. Cell Biol., 1988. 107: p. 1253-1260.
56. Woods, A., et al., *Adhesion and Cytoskeletal Organization of Fibroblasts in Response to Fibronectin Fragments*. EMBO J., 1986. 5(4): p. 665-670.
57. Ayad, S., et al., *The Extracellular Matrix Factsbook*. FactsBook Series. 1994, San Diego: Academic Press Inc.
58. Ziegler, T. and R.M. Nerem, *Tissue Engineering a Blood Vessel: Regulation of Vascular Biology by Mechanical Stresses*. J. Cell. Biochem., 1994. 56: p. 204-209.
59. Fung, Y.C., *Biomechanics: Mechanical Properties of Living Tissues*. Second ed. 1993, New York, NY: Springer-Verlag New York, Inc.
60. Urry, D.W., et al., *Biocompatibility of the Bioelastic Materials, poly (GVGVP) and its γ -irradiation Cross-Linked Matrix: Summary of Generic Biological Test Results*. J. Bioact. Comp. Polym., 1991. 6: p. 263-282.
61. Urry, D.W., et al., *Protein Based Materials with a Profound Range of Properties and Applications: The Elastin ΔT Hydrophobic Paradigm*, in *Protein-Based Materials*, K. McGrath and D. Kaplan, Editors. 1997, Birkhauser: Boston, MA.
62. Chandran, K.B., *Cardiovascular Biomechanics*. New York University Biomedical Engineering Series, ed. W. Welkowitz. 1992, New York: University Press. 539.
63. Urry, D.W., et al., *Properties, Preparations and Applications of Bioelastic Materials*, in *Handbook of Biomaterials and Applications*. 1995, Marcel Dekker: New York.
64. Nicol, A., D.C. Gowda, and D.W. Urry, *Cell Adhesion and Growth on Synthetic Elastomeric Matrices Containing ARG-GLY-ASP-SER*. J. Biomed. Mat. Res., 1992. 26: p. 393.

65. Nicol, A., et al., *Cell Adhesive Properties of Bioelastic Materials Containing Cell Attachment Sequences*, ed. C. Carraher and C. Gebelein. 1994, New York: Plenum Press.
66. Panitch, A., *Design, Synthesis, and Characterization of Artificial Extracellular Matrix Proteins for Tissue Engineering*, in *Polymer Science and Engineering*. 1997, University of Massachusetts, Amherst: Amherst.
67. Conte, M.S., *The Ideal Small Arterial Substitute: A Search for the Holy Grail?* FASEB J., 1998. **12**: p. 43-45.
68. Ferrari, F.A. and J. Capello, *Protein-Based Materials*, ed. K. McGrath and D. Kaplan. 1997, Boston, MA: Birkhauser. 37.
69. Urry, D.W., et al., *Hydrophobicity Scale for Proteins Based on Inverse Temperature Transitions*. Biopolymers, 1992. **32**: p. 1243-1250.
70. Urry, D.W., et al., *Synthetic, Cross-linked Polypentapeptide of Tropoelastin: an Anisotropic, Fibrillar Elastomer*. Biochemistry, 1976. **15**(18): p. 4083-4089.
71. Nicholas, F.L. and C.H. Gagnieu, *Denatured Thiolated Collagen: Crosslinking by Oxidation*. Biomaterials, 1997. **18**(11): p. 815-821.
72. Uhlich, T. and J.A. Hubbell. *Hydrogel Formation by Photochemical Crosslinking of Proteins Using Eosin Y as Photosensitizer*. in *Society for Biomaterials*. 1997. New Orleans, Louisiana.
73. McPherson, J.M., S. Sawamura, and R. Armstrong, *An examination of the biologic response to injectable, glutaraldehyde crosslinked collagen implants*. J. Biomed. Mater. Res., 1986. **20**: p. 93-107.
74. Welsh, E.R. and D.A. Tirrell, *Engineering the Extracellular Matrix: A Novel Approach to Polymeric Biomaterials. I. Control of the Physical Properties of Artificial Protein Matrices Designed to Support Adhesion of Vascular Endothelial Cells*. Biomacromolecules, 2000. **1**(1): p. 23-30.
75. McMillan, R.A. and V.P. Conticello, *Synthesis and Characterization of Elastin-Mimetic Protein Gels Derived from a Well-Defined Polypeptide Precursor*. Macromolecules, 2000. **33**(13): p. 4809-4821.
76. Lee, J., C.W. Macosko, and D.W. Urry, *Mechanical Properties of Cross-Linked Synthetic Elastomeric Polypentapeptides*. Macromolecules, 2001. **34**: p. 5968-5974.
77. Lee, J., C.W. Macosko, and D.W. Urry, *Elastomeric Polypentapeptides Cross-linked into Matrixes and Fibers*. Biomacromolecules, 2001. **2**: p. 170-179.

78. Lee, J., C. Mocosko, and D. Urry, *Swelling Behavior of γ -Irradiation Cross-Linked Elastomeric Polypentapeptide-Based Hydrogels*. *Macromolecules*, 2001. **34**: p. 4114-4123.

CHAPTER 2

PREPARATION OF ARTIFICIAL EXTRACELLULAR MATRIX PROTEINS

2.1 Introduction and Objectives

Genetic engineering methods were used for the design and preparation of artificial proteins containing sequences chosen to mimic elements of the naturally extracellular matrix (ECM). The CS5 and CS1 domains of fibronectin impart biologic function, while an elastin-like repeat $[(VPGIG)_2(VPGKG)(VPGIG)_2]$ provides mechanical properties and covalent sites for crosslinking. These proteins were then expressed and purified on a multi-gram batch scale. Bis(sulfosuccinimidyl)suberate and disuccinimidyl suberate are described for crosslinking the proteins specifically through the lysines.

2.2 Experimental Section

2.2.1 Genetic Manipulation

Standardized protocols were used in DNA manipulations, bacterial growth, protein expression, SDS-PAGE and Western blotting [1].

2.2.1.1 Design of Artificial Gene El-IK

The following DNA sequence and corresponding amino acids were designed to produce the (VPGIG)₂VPGKG(VPGIG)₂ monomer designated El-IK with Ban I/EcoRI and BanI/BamHI flanking regions for insertion into the cloning vector and multimerization:

Eco RI Ban I

F Z G V P G I G V P G I G V P

AA TTC TAA GGG GTG CCG GGT ATC GGC GTT CCG GGC ATC GGT GTA CCG

Ban I

Bam HI

G K G V P G I G V P G I G V P

GGC AAA GGT GTT CCG GGC ATC GGT GTT CCG GGT ATC GGG GTG CCG G

2.2.1.2 Preparation of Synthetic DNA

Genosys Biotechnologies, Inc. (Woodlands, Tx.) synthesized the oligonucleotide El-IK by solid-state synthesis. The El-IK was annealed by heating to 95°C in annealing salts for several minutes and then cooled slowly in a Styrofoam cooler to room temperature. The DNA was then precipitated and phosphorylated with T4 polynucleotide kinase. Phenol/chloroform extraction and subsequent isolation followed this on a 2% agarose gel electrophoresis. The corresponding 93 bp fragment was excised and purified from the agarose by the QiaexII protocol (Qiagen, 1994).

2.2.1.3 Cloning and Amplification of Synthetic DNA

The purified El-IK was ligated into an Eco RI/Bam HI digested, dephosphorylated pUC19 cloning vector (Figure 2.1) and transformed into the *E. coli* strain DH5 α -f'. Cells were grown at 37°C overnight on 2XYT solid medium containing 200ug/ml ampicillin. The DNA was harvested from the transformants with Qiagen miniprep spin columns and digested with Bam HI/Eco RI. The fragments were separated by agarose gel electrophoresis on a 3% gel and a 93 bp fragment confirmed insertion. Three of these transformants were chosen and sequenced using the CalTech Sequencing Facility with a NEB M13/pUC sequencing primer #1212. One transformant was chosen which showed no ambiguities in the sequencing chromatogram. The plasmid was designated pUC El-IK.

2.2.1.4 Polymerization of El-IK Monomer and Cloning of El-IK Multimers

The pUC El-IK was digested with Ban I and the resulting 75 bp fragment was separated on a 3 % agarose gel by electrophoresis. The fragment was excised and purified with a QiaexII gel extraction kit and self-ligated to produce a population of multimers. The tetramer (El-IK)₄ was separated on a 1.5% agarose gel by electrophoresis, excised, and purified with a QiaexII gel extraction kit. The purified tetramer was ligated into Ban I digested, dephosphorylated pEC CS5, pEC SC5, and pEC CS1 cloning vectors (Figure 2.2). Recombinant plasmids were used to transform the *E. coli* strain DH5 α -f' and designated pEC CS5(El-IK)₄, pEC SC5(El-IK)₄, and pEC

CS1(El-IK)₄. The colonies were screened by digestion with Sal I/Xho I to produce CS5(El-IK)₄, SC5(El-IK)₄, and CS1(El-IK)₄ as visualized following separation on a 1 % gel.

2.2.1.5 Construction of the Bacterial Expression Vectors

The recombinant pEC CS5(El-IK)₄, pEC SC5(El-IK)₄, and pEC CS1(El-IK)₄ vectors were digested with Xho I/Sal I to obtain the CS5(EL-IK)₄, SC5(EL-IK)₄, and CS1(EL-IK)₄ cassettes. The cassettes were separated by agarose gel electrophoresis on a 1 % gel and recovered by extraction with QiaexII DNA extraction kit. The recovered DNA was ligated into an Xho I digested, dephosphorylated pET-28rw vector (Figure 2.3) and used to transform the *E. coli* strain DH5 α -f'. Transformants were screened for insertion and orientation of each cassette by digestion with Xho I/Xba I. Visualization of the insert on a 1 % agarose gel by gel electrophoresis confirmed the presence of the CS5(EL-IK)₄, SC5(EL-IK)₄, and CS1(EL-IK)₄ cassettes. This step was repeated twice more to create the pET28rw[CS5(EL-IK)₄]₃, pET28rw[SC5(EL-IK)₄]₃, and pET28rw[CS1(EL-IK)₄]₃ recombinant plasmids. These plasmids were used to transform the expression host *E. coli* strain BL21(DE3)pLysS.

2.2.2 Protein Expression and Purification

2.2.2.1 10 L Fermentation

Expression was carried out in a 10 L Bioflow 3000 (New Brunswick Scientific, Edison, NJ) fermentor with Terrific Broth (TB) as the expression medium supplemented with 25 mg/l kanamycin (Sigma, St. Louis, MO) and 34 mg/l chloramphenicol (Sigma, St. Louis, MO). A 400 ml overnight culture was used for inoculation of the fermentation culture. The pH was maintained at 7.2 and the temperature at 37 °C. The culture was induced at an OD₆₀₀ of 5-6 with 2.5 mM IPTG and the expression was allowed to continue 2-3 hours to reach an OD₆₀₀ of 13-18. The cells were harvested by centrifugation (15 min., 10,000 g, 4 °C) yielding an average of 200 g wet cell mass per fermentation. The protein expression for these constructs yields 13 mg/g wet cell mass.

2.2.2.3 Protein Purification

The protein purification flowchart is shown in Figure 2.4. The wet cell mass was redispersed in TEN buffer (10 mM Tris-HCl, pH 8.0, 1 mM EDTA, 0.1 M NaCl) at 0.5 g/ml, frozen, then thawed at 4 °C with addition of 10 µg/ml deoxyribonuclease 1 (Sigma, St. Louis, MO), 10 µg/ml ribonuclease A (Sigma, St. Louis, MO), and 50 µg/ml phenylmethylsulfonyl fluoride (Sigma, St. Louis, MO). The solution was centrifuged (2 hr, 35,000 g, 4 °C) to separate soluble and insoluble fractions. The supernatant was brought to pH 9 and 1 M NaCl at 4 °C, and then allowed to equilibrate to 37 °C before

another centrifugation (2 hr, 35,000 g, 37 °C). The pellet was redispersed in distilled water, brought to pH 9, 1 M NaCl at 4 °C and centrifuged (2 hr, 35,000 g, 4 °C). The supernatant was then warmed to 37 °C and centrifuged (2 hr, 35,000 g, 37 °C). This process was repeated twice with the pellet from this step. The resulting final pellet was redispersed in distilled water, dialyzed for three days at 4 °C and lyophilized to yield the purified product. SDS-PAGE, western blot, mass spectrometry, and amino acid analysis were used to assess the purity and molecular weight of the proteins. Western blots were detected with a horse radish peroxidase conjugated antibody for the T7 tag (Novagen, Madison, WI). Matrix Assisted Laser Desorption Ionization-Mass Spectrometry (MALDI-MS) was conducted with a 1:20 ratio of matrix solution (10 mg/ml sinapic acid in 0.07 % trifluoroacetic acid, 30 % acetonitrile) to analyte solution (30 mg/ml protein in 4 °C water) on a Voyager DE spectrometer (Applied Biosystems). The plate was spotted at 4 °C followed by crystallization at 4 °C for 1 hr and 25 °C for 2 hr prior to analysis. Amino acid analysis was conducted at University of California at Davis Amino Acid Analysis Facility.

2.3 Results and Discussion

2.3.1 Protein Expression and Purification

2.3.1.1 Expression and Yield of Protein

Three proteins were made by genetic engineering as described and are shown in Figure 2.5. Each protein is denoted by the cell-binding domain, i.e. CS5, SC5, and CS1, respectively. Protein expression for these constructs yields approximately 13 mg/g wet cell mass. This allows almost 3 grams of protein to be attained from one 10 L fermentation.

2.3.1.2 Purification by the LCST

A distinctive characteristic of elastin-like polymers in aqueous solvents is the existence of an LCST above which a polymer-rich coacervate forms and below which the polymer is soluble. Cycling protein solutions above and below the LCST provides a simple method of purification of elastin-like proteins [2-6]. Upon thawing the whole cell lysate at 4 °C (below the LCST), the protein remains in solution, allowing separation of insoluble contaminating proteins by centrifugation. Following pH adjustment and addition of salt, raising the temperature to 30 °C (above the LCST) causes the protein to precipitate, and soluble contaminating proteins can be removed by centrifugation.

2.3.1.3 Measures of Purity

The purified CS5 and SC5 proteins are shown on an SDS-PAGE gel and western blot in Figure 2.6. Figure 2.7 shows the SDS-PAGE gel and western blot of CS1. The PAGE mobility of the proteins causes them to run at a higher molecular weight than expected. This is consistent with previously prepared elastin-like proteins [7, 8]. Mass spectrometry shows the molecular mass of CS5 in Figure 2.8 and of SC5 in Figure 2.9, both within instrumental error of the expected mass of 37120 Da. The amino acid analysis of both CS5 and SC5 proteins is shown in Table 2.1 and the CS1 in Table 2.2. All mole %s are within 1 % of the expected result with the exception of valine in CS1. The SDS-PAGE and mass spectrometry results along with the amino acid analysis confirm the isolation of pure proteins of correct molecular weight and amino acid composition.

2.4 Summary and Conclusions

The high expression level and simple, batch purification process allows multi-gram quantities of pure proteins to be attained easily.

Amino Acid	Theoretical N%	CS5 N%	SC5 N%
D/N	2	2.9	3.2
E/Q	3.7	3.5	3.8
S	0.2	0.5	0.2
G	32.8	33.3	32.4
H	3.2	2.5	3
R	0.7	0.8	0.8
T	0.2	0.1	0.3
A	0.2	0.2	0.3
P	17.1	18	18.1
Y	1.5	1.5	1.5
V	16.4	16.8	16.4
M	1	0	0.5
C	0	0	0
I	14.1	14.6	14.1
L	1.7	1.8	1.9
F	0	0	0
W	0	0	0
K	3.2	3.4	3.5
TOTAL	98	100	100

Table 2.1 Amino acid analysis of CS5 and SC5 proteins showing amino acid compositions within 1 mole % of expected.

AMINO ACID	Theoretical N%	CS1 N%
ASP (D)	3.10	4.19
GLU (E)	1.70	3.14
ASN (N)	0.70	0.00
SER (S)	1.00	0.89
GLN (Q)	1.20	0.00
GLY (G)	31.00	30.70
HIS (H)	3.10	3.18
ARG (R)	0.00	0.00
THR (T)	1.70	1.64
ALA (A)	0.20	0.34
PRO (P)	18.80	19.50
TYR (Y)	0.00	0.00
VAL (V)	16.60	15.01
MET (M)	1.00	1.05
CYS (C)	0.00	0.01
ILE (I)	12.30	12.08
LEU (L)	4.60	4.92
PHE (F)	0.00	0.00
TRP (W)	0.00	0.00
LSY (K)	3.10	3.33
TOTAL	100.10	100.00

Table 2.2 Amino acid analysis of CS1 protein showing amino acid compositions within 1 mol % of expected with the exception of valine that is within 1.5 mol %.

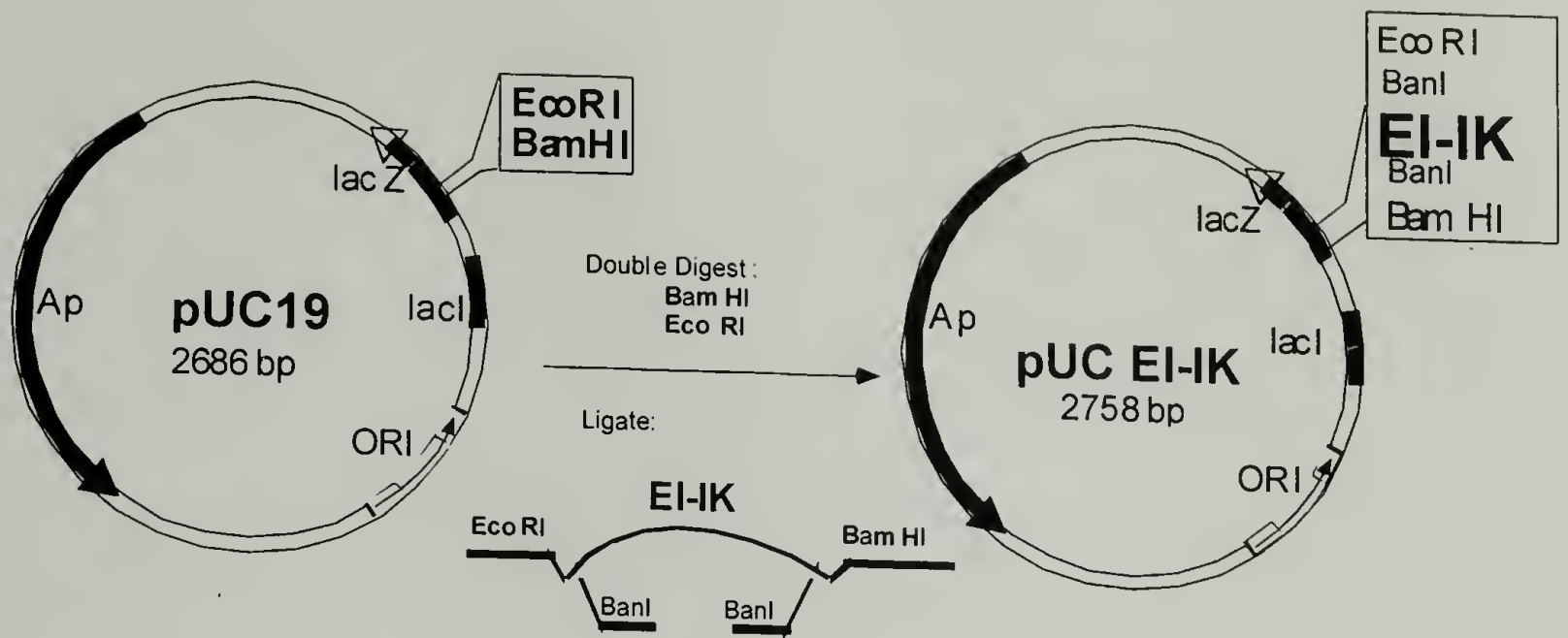


Figure 2.1 Construction of pUC EI-IK plasmid by insertion of the EI-IK fragment into the pUC 19 plasmid at the *EcoRI*/*BamHI* restriction sites.

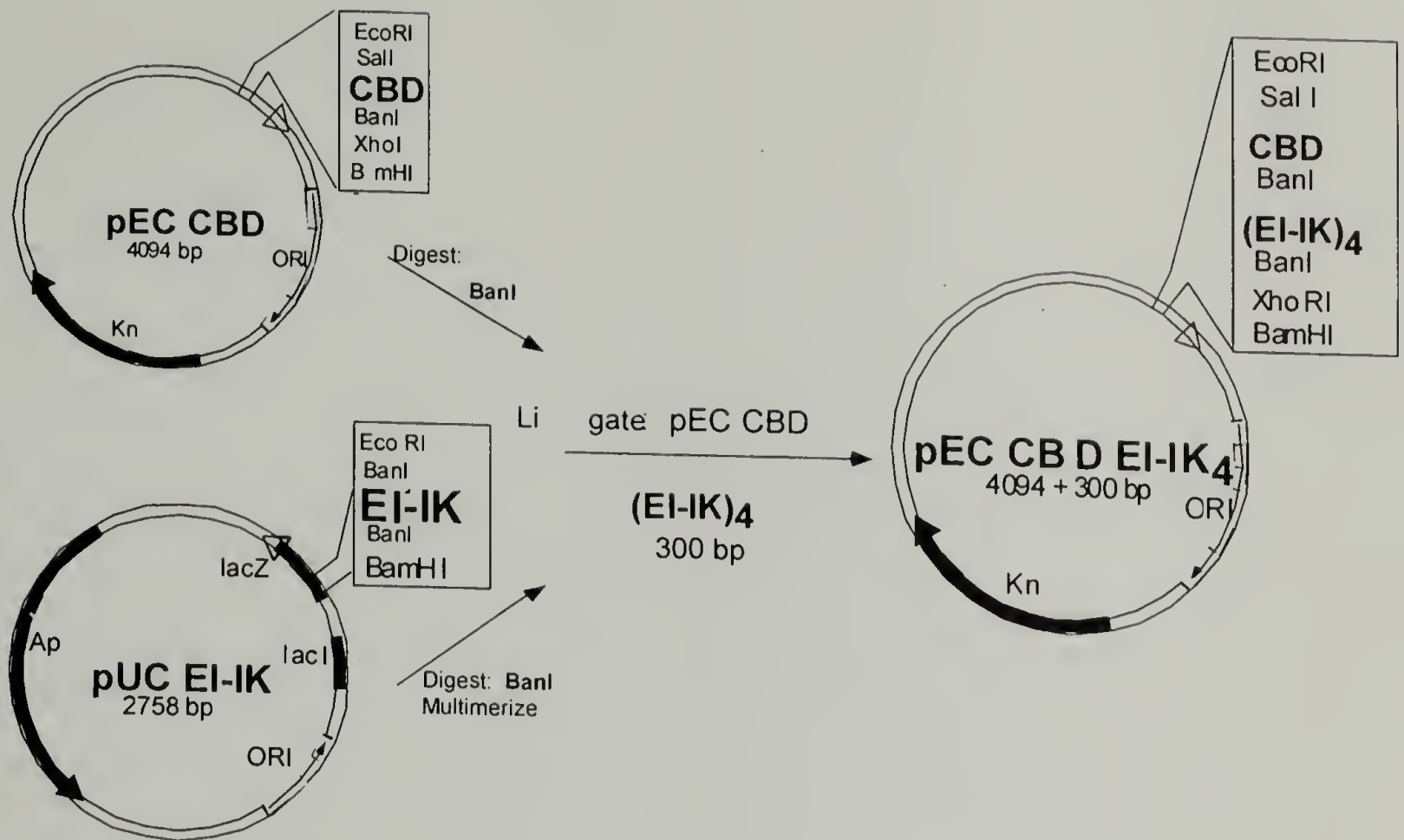


Figure 2.2 Construction of the pEC CBD(EI-IK)₄ plasmids by insertion of the tetramer (EI-IK)₄ into the pEC CBD plasmids at the Ban I restriction site (where CBD = CS5, SC5, and CS1).

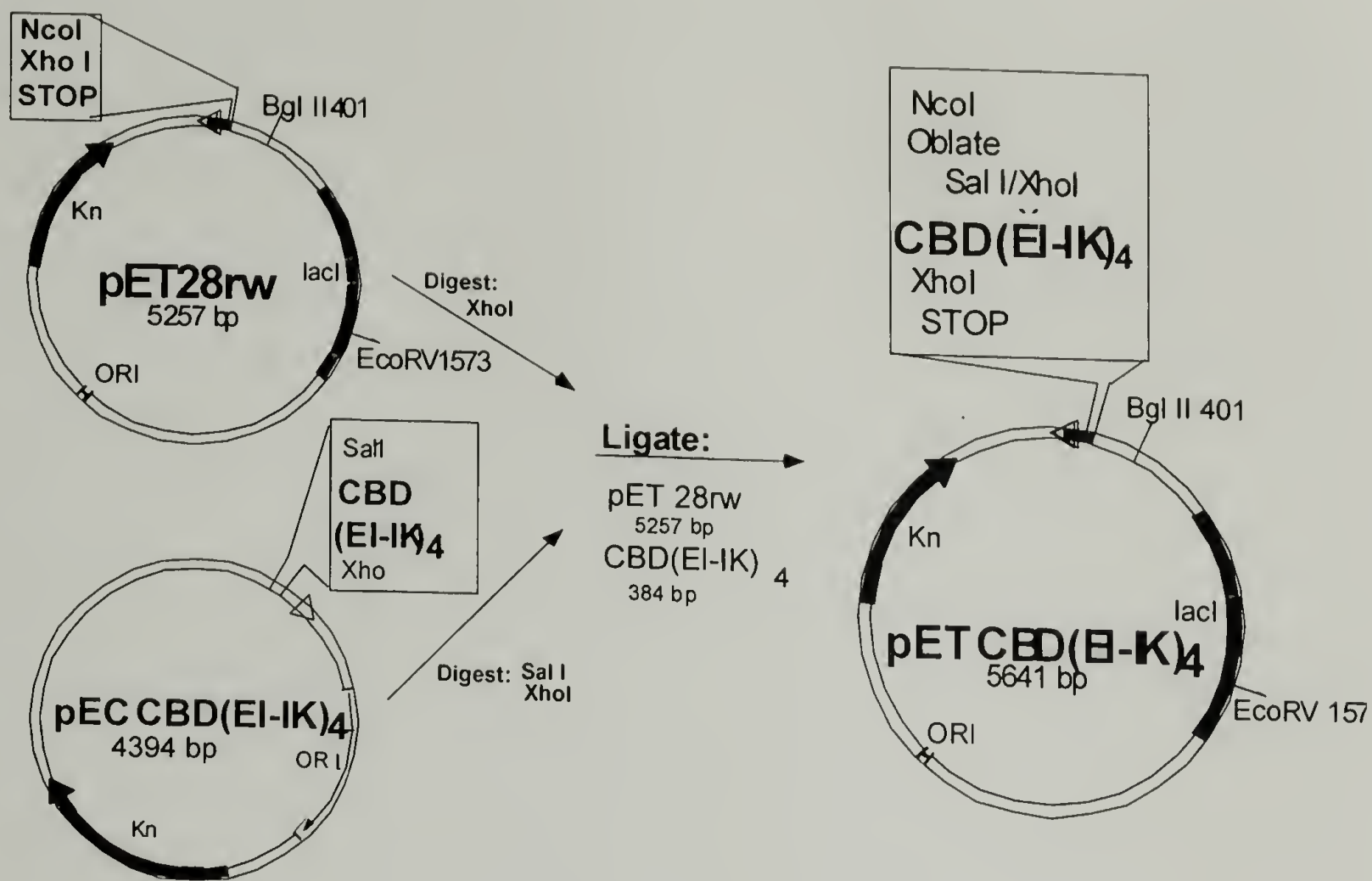


Figure 2.3 Construction of the bacterial expression vector pET CBD(EI-IK)₄.

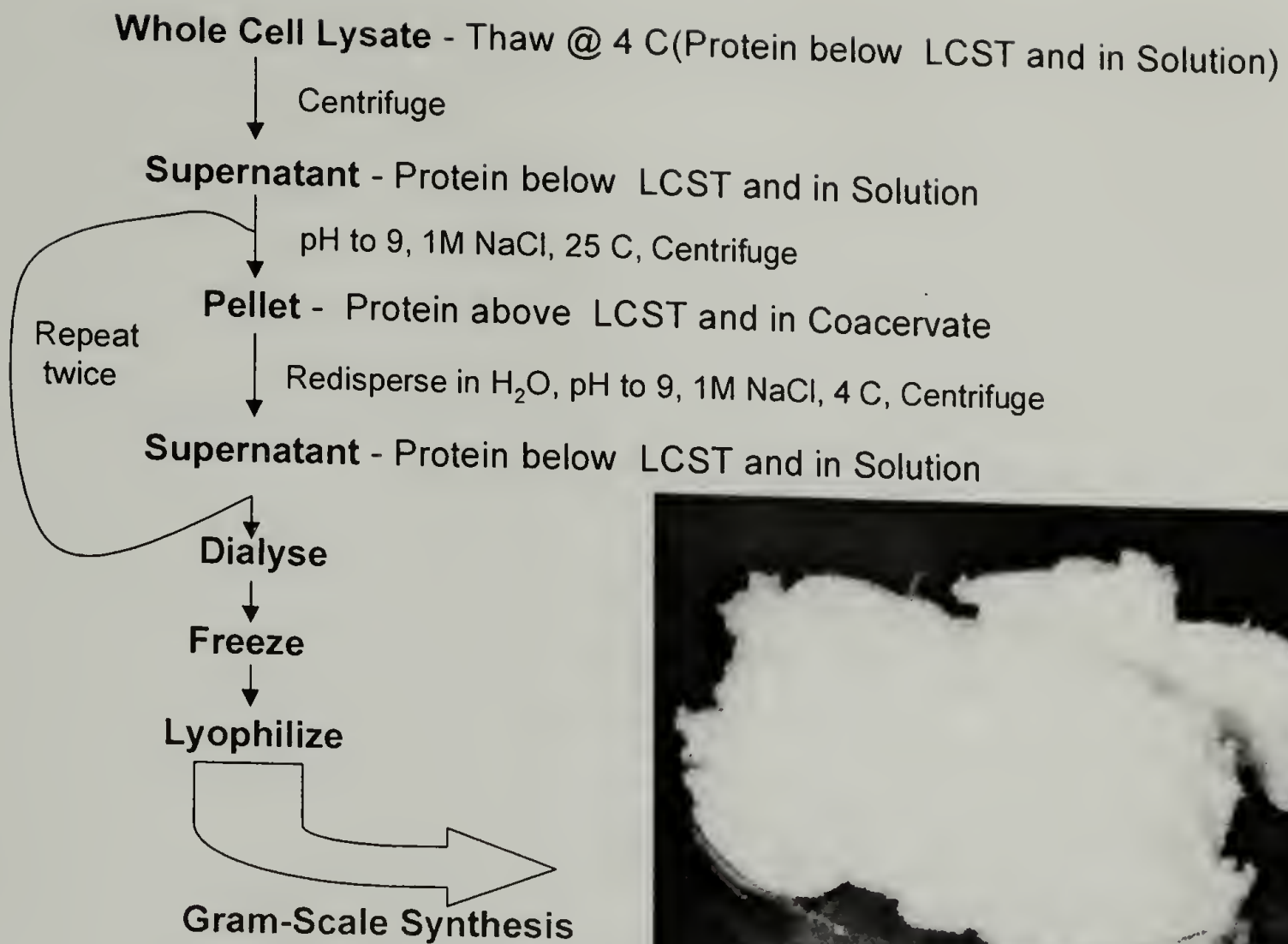


Figure 2.4 Purification flowchart showing a simple, batch purification to obtain multi-gram quantities of target proteins.

CS5:

M-MASMTGGQMGHHHHHHH-DDDDK-(GEEIQGHIPREDVYHLYR((VPGIG)₂VPGKG(VPGIG)₂)₄)₃-VPLE

T7 Tag His Tag Cleavage site CS5 Cell-binding Domain Elastin-like Repeat

SC5 :

M-MASMTGGQQMGHHHHHHH-DDDDK-(GEEIQGHIPREVDYHLYP(VPGIG)₂VPGKG(VPGIG)₂)₄)₃-VPLE

T7 Tag His Tag Cleavage site Scrambled CS5 Elastin-like Repeat
Cell-binding Domain

CS1 :

M-MASMTGGGQMG-~~HHHHHHHH~~-DDDDK-(LDDELPQLVTLPHPNLHGPEILDVPST-((VPGIG)₂VPGKG(VPGIG)₂)₄)₃-VPLE

T7 Tag His Tag Cleavage site CS1 Cell-binding Domain Elastin-like Repeat

Figure 2.5 Three proteins were made by genetic engineering and are denoted by the cell-binding domain CS5, SC5, and CS1.

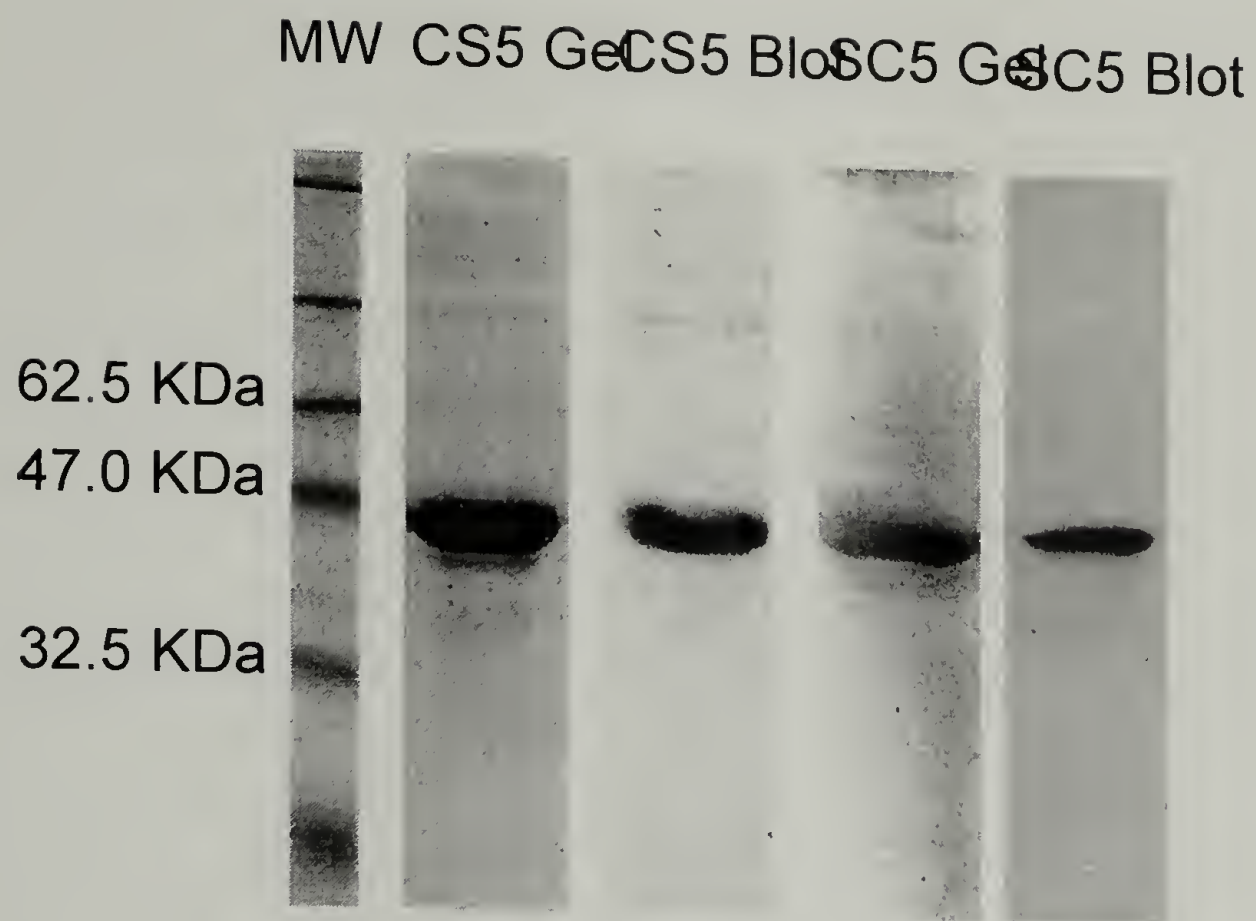


Figure 2.6 SDS-PAGE gel and western blot of the CS5 and SC5 proteins.

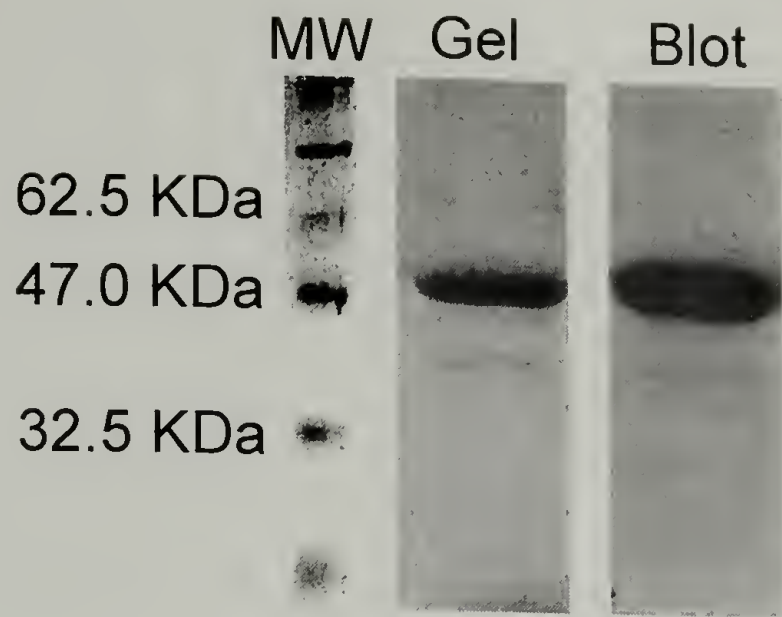


Figure 2.7 SDS-PAGE gel and western blot of the CS1 protein.

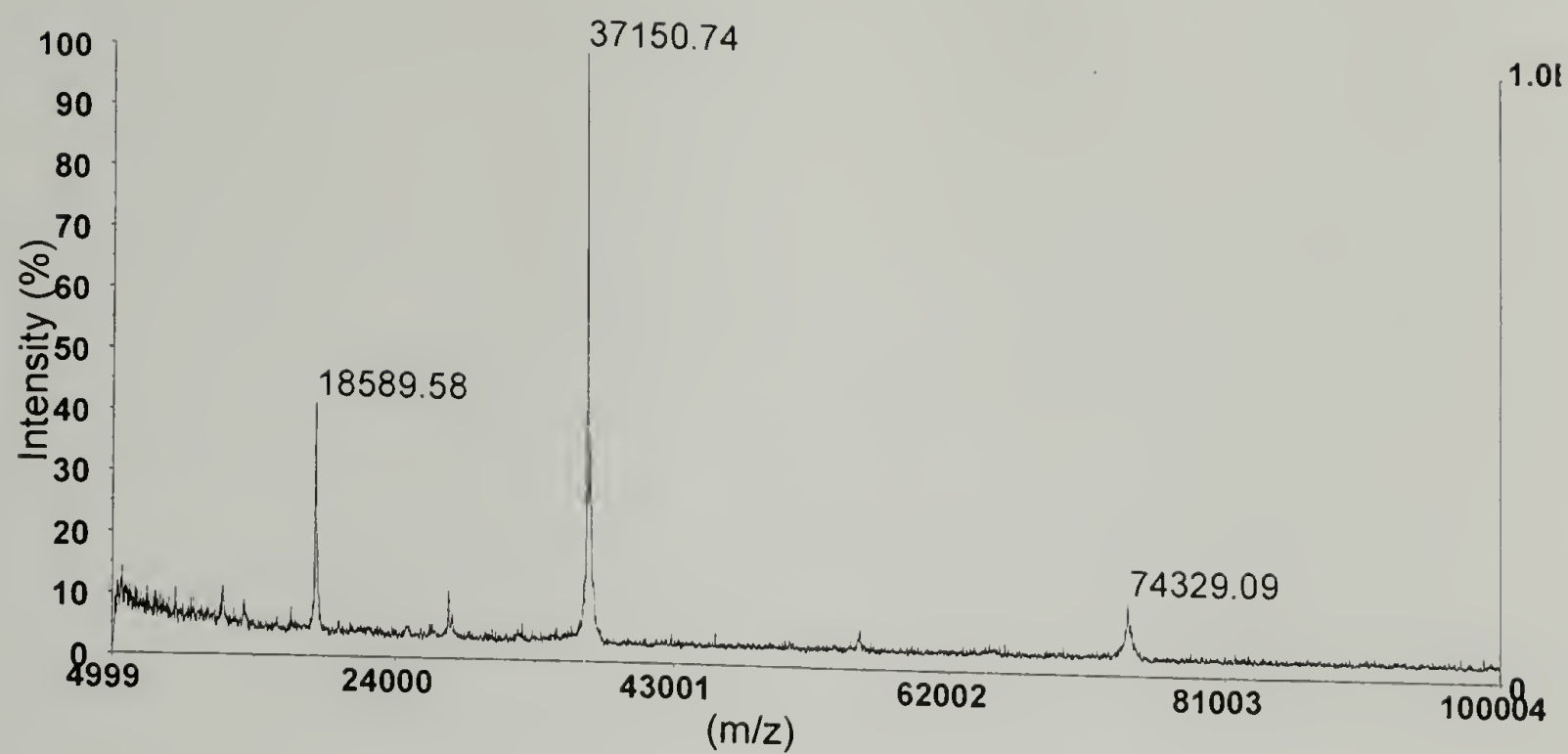


Figure 2.8 Mass spectrometry of the CS5 protein, showing a peak at 37150, within experimental error of the expected mass of 37120.

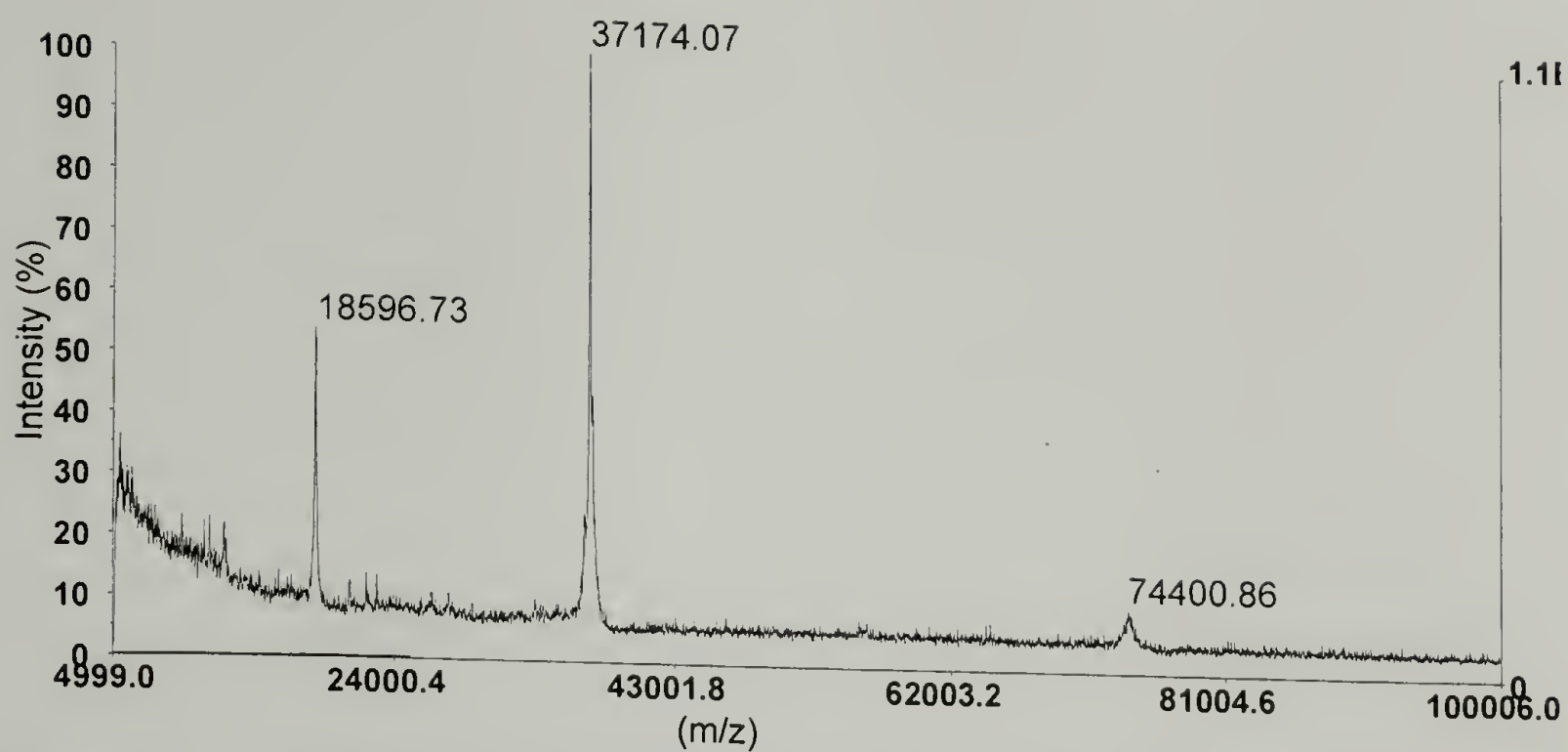


Figure 2.9 Mass spectrometry of SC5 protein, showing a mass peak at 37174, within experimental error of the expected mass of 37120.

2.5 References

1. Sambrook, J., E.F. Frisch, and T. Maniatis, *Molecular Cloning*. 2nd ed. 1989, Plainview, NY: Cold Spring Harbor Laboratory Press.
2. Urry, D.W., et al., *Properties, Preparations and Applications of Bioelastic Materials*, in *Handbook of Biomaterials and Applications*. 1995, Marcel Dekker: New York.
3. Urry, D.W., et al., *Protein Based Materials with a Profound Range of Properties and Applications: The Elastin ΔT Hydrophobic Paradigm*, in *Protein-Based Materials*, K. McGrath and D. Kaplan, Editors. 1997, Birkhauser: Boston, MA.
4. McMillan, R.A. and V.P. Conticello, *Synthesis and Characterization of Elastin-Mimetic Protein Gels Derived from a Well-Defined Polypeptide Precursor*. *Macromolecules*, 2000. **33**(13): p. 4809-4821.
5. Meyer, D. and A. Chilkoti, *Genetically encoded synthesis of protein-based polymers with precisely specified molecular weight and sequence by recursive directional ligation: examples from the elastin-like polypeptide system*. *Biomacromolecules*, 2002. **3**(2): p. 357-367.
6. Meyer, D. and A. Chilkoti, *Purification of recombinant proteins by fusion with thermally-responsive polypeptides*. *Nature Biotechnology*, 1999. **17**(11): p. 1112-1115.
7. Panitch, A., et al., *Design and Biosynthesis of Elastin-like Artificial Extracellular Matrix Proteins Containing Periodically Spaced Fibronectin CS5 Domains*. *Macromolecules*, 1999. **32**(5): p. 1701-1703.
8. Welsh, E.R. and D.A. Tirrell, *Engineering the Extracellular Matrix: A Novel Approach to Polymeric Biomaterials. I. Control of the Physical Properties of Artificial Protein Matrices Designed to Support Adhesion of Vascular Endothelial Cells*. *Biomacromolecules*, 2000. **1**(1): p. 23-30.

CHAPTER 3

MECHANICAL PROPERTIES OF CS5 AND SC5 PROTEINS

3.1 Introduction and Objectives

Bis(sulfosuccinimidyl)suberate and disuccinimidyl suberate were used to crosslink CS5 and SC5 into films for uniaxial tensile testing. The mechanical properties of the resultant films can be tuned by varying the amount of crosslinker and protein weight fraction during crosslinking. The residual lysine content was measured spectrophotometrically to quantify extent of crosslinking. The buffer content of the hydrated, crosslinked films was measured and the theoretical molecular weight between crosslinks (M_c) was determined. The modulus and M_c of the proteins were compared to data reported for natural elastin.

3.2 Experimental Section

3.2.1 Measuring the LCST

The LCST of the protein was measured at 10, 20, 30 mg/ml concentrations in phosphate buffered saline (PBS) pH 7.4 by increasing the temperature at a rate of 30 °C/hour and measuring the percent transmission at 300 nm on a CD spectrophotometer

Model 62DS (Aviv, Lakewood, NJ). This was repeated twice for each concentration of each protein with little or no variation in behavior.

3.2.2 Crosslinking Chemistry

The reaction scheme for crosslinking the protein is shown in Figure 3.1. Bis(sulfo-succinimidyl) suberate (BS3) and disuccinimidyl suberate (DSS) are commercially available bifunctional N-hydroxysuccinimidyl (NHS) esters (Pierce, Rockford, IL). Both reagents were used without purification.

3.2.3 Film Casting

3.2.3.1 Method I

Method I, shown in Figure 3.2, involved crosslinking a solution of protein, BS3, and PBS between two glass plates with 0.45 mm plastic spacers at the edges to set the gap height. Clamps held this assembly together until crosslinking was completed (see Table 3.1). Films were made varying the stoichiometric ratio of NHS to lysine at 0.5:1, 1:1, and 1.5:1. The protein was crosslinked at concentrations of 0.2 w/v and 0.4 w/v. The crosslinking was done both above the LCST (at 25 °C) and below the LCST (at 4 °C).

3.2.3.2 Method II

Method II is shown in Figure 3.3. A solution of protein (300 μ l of 100 mg/ml protein in dimethylsulfoxide (DMSO) (Sigma, St. Louis, MO)) was dried overnight at 50 °C in a teflon mold. The film was crosslinked by immersing it in a 5 ml solution of disuccinimidyl suberate (DSS) (Pierce, Rockford, IL) in anhydrous dimethylformamide (DMF) (Sigma, St. Louis, MO) at 5:1, 10:1, and 100:1 NHS to lysine stoichiometries.

3.2.4 Film Characterization

3.2.4.1 Weight Fraction Protein

Buffer content of the films was defined by the difference in weight between dry and wet samples. Wet samples were prepared by equilibration in PBS at 37 °C, followed by the wicking away of excess water with filter paper. The films were then placed at 50 °C overnight in a vacuum oven before the dry weights were measured. Film weight was measured again after 1 week at 50 °C under vacuum and showed no further weight reduction. The weight fraction protein was determined and the volume fraction subsequently calculated using a protein density of 1.3 g/cm³ (equivalent to that of collagen) [1] and a water density of 1.0 g/cm³.

3.2.4.2 Residual Lysine Content

Sulfo-succinimidyl-4-O-(4,4'-dimethoxytrityl)-butyrate (SDTB) (Pierce, Rockford, IL) was used to determine unreacted amines[2-5]. The reaction is shown in Figure 3.4. Crosslinked films (1-5 mg) were immersed in 0.4 ml 50 mM NaHCO₃ pH 8.5, 1 mM SDTB and agitated for at least two hours at room temperature. Films were removed from the solution, blotted with filter paper, immersed in 50 ml 50 mM NaHCO₃ pH 8.5 and allowed to remain at 4 °C overnight. Films were removed from the buffer, blotted with filter paper, and immersed in 1 ml 88 % formic acid. The films were agitated 1 hr at 25 °C and the resulting solution was diluted 1/100 in 88 % formic acid and the absorbance at 498 nm was determined with a SpectraMax Plus 384 UV spectrophotometer (Molecular Devices, Sunnyvale, CA).

A calibration curve was made using the uncrosslinked protein. The protein (3 mg) was dissolved in 0.4 ml 50 mM NaHCO₃ pH 8.5, 1 mM SDTB and agitated for at least two hours at room temperature. The excess SDTB was removed by precipitating the protein with 1 M NaCl, redispersing in 1 ml 50 mM NaHCO₃ and precipitating the protein with 1 M NaCl five times. The resultant precipitated protein was dispersed in 1 ml 88 % formic acid. These solutions were diluted 1/100 in 88 % formic acid and the absorbance at 498 nm was determined with a SpectraMax Plus 384 UV spectrophotometer (Molecular Devices, Sunnyvale, CA).

3.2.5 Tensile Testing

Protein films were measured with vernier calipers and a micrometer after equilibration in PBS at 37 °C to determine cross-sectional area. The samples were tensile tested under simulated physiological conditions (PBS, pH 7.4, 37 °C) on an Instron Universal Testing Machine Model 5564. A schematic of the test apparatus is shown in Figure 3.5. A uniform strain rate of 10 % gauge length per minute was used and the aspect ratio of the samples was at least five, based on the ASTM Standard D 882-00. The sample length was 12 ± 2 mm, width was 2 ± 1 mm and thickness 0.45 ± 0.1 mm.

3.3 Results and Discussion

3.3.1 LCST Behavior

Figure 3.6 and Figure 3.7 show the LCST behavior of the CS5 and SC5 proteins, respectively at 10, 20, and 30 mg/ml concentrations. Both CS5 and SC5 show similar LCST behavior. The onset of the transition occurs at 27 °C for the 10 mg/ml concentration and increases to 28.3 °C and 29 °C for the 20 mg/ml and 30 mg/ml solutions, respectively. The slope of the curve and maximum absorbance increases with increasing concentration. Similar proteins without the lysine residues within the elastin-like region have exhibited an LCST at 12 °C [6]. The addition of lysines at the N- and C-termini increased the LCST to 17 °C [7]. The introduction of twelve lysines within the protein for CS5 and SC5 raises the LCST to 27 °C. The increase in LCST is a result of

the substitution of a more hydrophilic amino acid (lysine) for isoleucine and is consistent with the prediction of Urry and coworkers [8].

3.3.2 NHS-ester Crosslinking

By taking advantage of the specificity of the reaction of NHS-esters with amines, the crosslinking should occur only in the films through the lysine residues [9, 10]. The most important competing reaction is likely to be hydrolysis of the ester by water, especially when crosslinking is done in PBS. Amines in the lysines react very quickly with the NHS-esters to produce insoluble films within minutes. The films are left to react for at least 12 hr to ensure full crosslinking.

3.3.3 Film Characterization

3.3.3.1 Weight Fraction Protein

Table 3.1 gives the weight fraction protein in the crosslinked films. Films prepared by Method I show a small increase in weight fraction protein with a decrease in crosslinker stoichiometry when crosslinked at the same concentration (cf. Samples 1-3). It is possible that the crosslinking restricts the film from excluding the water as it would in a less crosslinked film. The films crosslinked with 0.2 w/v protein concentration have a lower weight fraction protein (19.5 %) than those crosslinked at 0.4 w/v (28.7 % protein). The protein concentration during crosslinking is the most significant factor determining the final water content of the crosslinked film.

For films prepared by Method II, the higher the crosslinker concentration, the higher the weight fraction protein in the crosslinked film giving a range of 31.8 to 38.9 %. An increase in modulus is observed with an increase in weight fraction protein.

Purified, hydrated elastin is known to contain approximately 65 % protein [11].

Although this protein content is higher than the described films, the moduli of the films are in the same range.

3.3.3.2 Residual Lysine Content

Table 3.1 shows the percentage of reacted lysines in the films. Sample 1 shows 42 % of the lysines reacted which is approximately half of that of Sample 2. This change in the extent of reaction is consistent with the use of half the crosslinker needed to crosslink the sample. Adding 50 percent excess crosslinker as in Sample 3 does not significantly increase the number of reacted lysines. Sample 5 shows 61 % of the lysines reacted, lower than that of Sample 2 because at lower concentrations, hydrolysis would compete more strongly. The temperature of reaction does not affect the percentage of reacted lysines in the films (cf. Samples 4, 2). Samples 6 – 8 show 90 % reacted lysines as would be expected with the presence of excess crosslinker.

3.3.4 Mechanical Properties of Films

3.3.4.1 Treatment of Mechanical Testing Data

The mechanical properties of the different films are tabulated in Table 3.2. The statistical treatment of rubber elasticity provides a relationship between stress (σ) and elongation ratio (λ) of random network materials for strains below 50 %:

$$\sigma = G (\lambda - 1/\lambda^2), \quad (1)$$

where G is the shear modulus [11-13]. The Young's modulus (E) is related to the shear modulus by the formula

$$E = 2(1 + \nu)G, \quad (2)$$

where ν is Poisson's ratio. When the material is a volumetrically incompressible rubber $\nu = 1/2$ and Equation 2 becomes $E = 3G$ [13, 14]. E can be determined from the initial linear region of the stress-strain curve (strains $< 5\%$) and can be compared through the above relationship to G .

For rubbery materials, theory states that G is inversely proportional to the molecular weight between crosslinks (M_c) through the relationship

$$G = \rho RT/M_c, \quad (3)$$

where ρ is the protein concentration in g/cm^3 , R is the gas constant, and T , the temperature [11-14]. Equation 3 assumes the network is perfect, in that all chains are effective in giving rise to elastic stress and each crosslink connects four network chains. Equation 3 should hold for samples crosslinked in solution.

3.3.4.2 Mechanical Properties of Method I Films

3.3.4.2.1 Variation of NHS to Lysine Stoichiometry

Figure 3.8 and Figure 3.9 show the stress-strain behavior of CS5 and SC5 films crosslinked using Method I in PBS at 25 °C with NHS/lysine stoichiometries of 0.5:1, 1:1, and 1.5:1. Figure 3.10 shows the determination of G , and Figure 3.11 shows the determination of E . The tensile modulus is indeed one third of the shear modulus agreeing well with theory and yielding tensile moduli ranging from 0.07 to 0.19 MPa. As might be expected, the 0.5:1 stoichiometric amount of crosslinker yields a modulus less than half of the modulus for the 1.0:1.0 stoichiometry. Increasing the amount of crosslinker to 1.5:1 stoichiometry does not significantly change the modulus of the film from the 1:1 stoichiometry. Although this higher crosslinker concentration could be expected to decrease the modulus by increasing tethered ends and reducing the number of effective crosslinks in the sample, it remains unchanged. Competing hydrolysis and incomplete reaction could negate this effect.

3.3.4.2.2 Variation of Crosslinking Time

The effect of crosslinking time on the mechanical properties was explored by allowing the films to crosslink for 12, 24, and 48 hr. Figure 3.12 shows the stress-strain curves for CS5 protein films illustrating no difference in the mechanical properties with

an increase in reaction time. This ensures the reaction was complete for each of the studies since the films were allowed at least a 12 hr reaction time.

3.3.4.2.3 Variation of Protein Concentration

Figures 3.13 and 3.14 show the tensile properties of CS5 and SC5 protein films cast at both 0.2 and 0.4 w/v protein in PBS at 25 °C. For both proteins, the modulus for the 0.4 w/v sample is approximately twice that for the 0.2 w/v sample. From Equation 3, since the modulus is proportional to the chain density, a sample with twice the chain density and other properties remaining the same would have twice the modulus.

3.3.4.2.4 Variation of Crosslinking Temperature

In aqueous solution (PBS) the protein exhibits an LCST as mentioned previously. At the high concentration of 0.4 w/v the LCST is very close to 25 °C and as the lysines are neutralized by reaction, the LCST is lowered further. A film crosslinked at 25 °C is considered reacted above the LCST. All of the previously described films were crosslinked above the LCST (at 25 °C); as a result of this, the formation of the coacervate gives the film a completely opaque, white appearance. Conversely, protein films crosslinked below the LCST at 4 °C remain clear, and after crosslinking do not appear to go through the LCST even upon raising the temperature of the film. Figure 3.15 shows two films clamped in a testing grip, illustrating difference in appearance between films crosslinked above the LCST (25 °C) and films crosslinked below the LCST (4 °C).

Figure 3.16 and Figure 3.17 show SEM micrographs of films crosslinked above and below the LCST, respectively. The films crosslinked above the LCST show a very rough, inhomogeneous, aggregated morphology. In contrast, the sample reacted below the LCST has a smooth, homogeneous texture.

Figure 3.18 and Figure 3.19 show the tensile behavior of CS5 and SC5 protein films crosslinked above and below the LCST. Although the morphologies of the samples are very different, the modulus is unaffected when measured under these conditions. This might bring to question the role of secondary structure in affecting bulk mechanical behavior. It is possible, although the films remain clear, that the protein has undergone the conformational change, but appear the same since aggregation, which causes the opacity, is restricted by crosslinks. Although the films respond similarly when tested under simple uniaxial tension, there may be differences in other mechanical properties such as tear resistance and hysteresis that result from the morphological disparity.

3.3.4.2.5 Variation of Testing Temperature

Elastin swelling involves changes in hydrophobic interactions, and these swelling changes create a material whose mechanical properties are nearly temperature independent. While this temperature independence is not important in higher vertebrates that can maintain constant body temperature, in fishes where it evolved, elastin had to efficiently store elastic energy at temperatures as low as -2°C . It is therefore suggested that elastin evolved as a design feature to produce a temperature-independent rubber-like material [15].

The mechanical properties of the films were tested at temperatures varying from 4 °C to 45 °C. The stress-strain behavior of the 0.2 w/v and 0.4 w/v films at these temperatures is shown in Figure 3.20 and Figure 3.21, respectively. Similar to the response of natural elastin samples, the films do not show temperature dependent mechanical behavior.

3.3.4.3 Mechanical Properties of Method II Films

It is desired to mimic the properties of naturally occurring elastin which has a modulus in the range of 0.3-0.6 MPa [11, 14, 16]. Therefore the next set of films were made using Method II in an effort to increase the chain density and subsequently the modulus of the materials. The crosslinker concentrations were varied from 100:1 to 5:1 NHS/lysine stoichiometry. Figure 3.22 shows the mechanical behavior of these crosslinked films. As the concentration of crosslinker is increased, the modulus also increases, giving a range of 0.35 - 0.97 MPa, which lies close to or within the desired range of moduli.

3.3.5 Theoretical M_c

Using Equation 3, the theoretical M_c was determined. The M_c for the crosslinked films is shown in Table 3.1. For Method I, Sample 1 has a lower modulus than Sample 2 or 3, and a similar protein weight fraction. This would be expected from a lower amount of crosslinker and is indicative of an increase in M_c (as can be calculated from Equation

3). Although the moduli of Sample 1 and Sample 5 are similar, the values of M_c are 20,000 g/mol and 38,000 g/mol respectively. The higher M_c for Sample 5 (a result of low amount of crosslinker) leads to a lower modulus, whereas the lower weight fraction protein (a result of a lower concentration during crosslinking) does not affect the M_c , and also leads to a low modulus. The lower weight fraction protein compensates for the lower crosslinker concentration in the modulus difference in M_c , allowing similar moduli.

For Method II films, the theoretical M_c ranges from 7000 g/mol to 3000 g/mol with increasing crosslinker concentration. This encompasses the M_c for elastin, which is 6000-7000 g/mol [11, 17]. Although the modulus and M_c are similar in these films, the water content is much higher.

The expected M_c for the proteins is 2500 g/mol assuming all crosslinks are effective and there are no chain ends. The M_c for the most highly crosslinked samples (Method II, 100:1 stoichiometry) is very close to the expected at 3000 g/mol.

3.4 Summary and Conclusions

The films prepared in this work yielded Young's moduli ranging from 0.07 MPa to 0.97 MPa. The residual lysine content quantified the extent of crosslinking to be between 42 % and 89 % depending on crosslinking conditions. The buffer content of the crosslinked films was between 19.5 % and 38.9 % and the theoretical molecular weight between crosslinks (M_c) was determined to vary from 38000 g/mol to 3000 g/mol. The modulus and M_c of the proteins are in the same range as is reported for natural elastin.

The crosslinked proteins show interesting and promising mechanical properties for the application of a vascular graft. By changing the method and conditions of crosslinking, the moduli and M_c can be controlled within the range expected for native elastin. The theoretical M_c is very close to what would be expected for an ideally crosslinked network of the proteins. The CS5 and SC5 proteins show no difference in mechanical properties indicating the scrambling of the cell-binding domain does not affect the mechanical properties.

Sample	NHS/Lysine Stoichiometry	Protein Solution Conc.(w/v)	Reaction Temp. (C)	Reaction Time (hr)	Wt. Fraction ^a Protein (w/w)	Reacted Lysines(%)	Mc x1000 (g/mol)
Method I: Films crosslinked in PBS with BS3							
CS5							
1	0.5 : 1	0.4	25	>12	0.30 ± 0.03	42 ± 7	38
2	1 : 1	0.4	25	>12	0.29 ± 0.02	75 ± 7	14
3	1.5 : 1	0.4	25	>12	0.25 ± 0.03	76 ± 8	11
4	1 : 1	0.4	4	>12	0.32 ± 0.02	74 ± 7	15
5	1 : 1	0.2	25	>12	0.20 ± 0.02	61 ± 15	20
SC5							
6	0.5 : 1	0.4	25	>12			
7	1 : 1	0.4	25	>12			
8	1.5 : 1	0.4	25	>12			
9	1 : 1	0.4	4	>12			
10	1 : 1	0.2	25	>12			
Method II: Films immersed in DMF/DSS crosslinking solution							
CS5							
11	5 : 1	dry film	25	>24	0.32		7
12	10 : 1	dry film	25	>24	0.37 ± 0.01		4
13	100 : 1	dry film	25	>24	0.39 ± 0.02	90 ± 7	3
Elastin							6 ^b

^a In films equilibrated at 37 °C.

^b Reference [11].

Table 3.1 Physical properties of crosslinked CS5 and SC5 protein films.

Sample	# Samples tested	Tensile Modulus E (MPa)	Shear Modulus G (MPa)
--------	------------------	----------------------------	--------------------------

Method I: Films crosslinked in PBS with BS3

CS5 Protein

1	5	0.07 ± 0.03	0.022 ± 0.003
2	8	0.17 ± 0.01	0.055 ± 0.001
3	5	0.19 ± 0.01	0.060 ± 0.001
4	6	0.18 ± 0.02	0.060 ± 0.002
5	5	0.08 ± 0.01	0.026 ± 0.001

SC5 Protein

6	3	0.05 ± 0.02	0.015 ± 0.001
7	5	0.15 ± 0.02	0.052 ± 0.005
8	2	0.16 ± 0.02	0.055 ± 0.005
9	3	0.17 ± 0.03	0.058 ± 0.002
10	2	0.08 ± 0.02	0.035 ± 0.003

Method II: Films immersed in DMF/DSS crosslinking solution

CS5 Protein

11	4	0.35 ± 0.31	0.12 ± 0.08
12	6	0.77 ± 0.12	0.25 ± 0.05
13	5	0.97 ± 0.31	0.32 ± 0.10

Elastin^a 0.30 - 0.60

^a Reference [11, 14, 16].

Table 3.2 Mechanical properties of crosslinked CS5 and SC5 protein films.

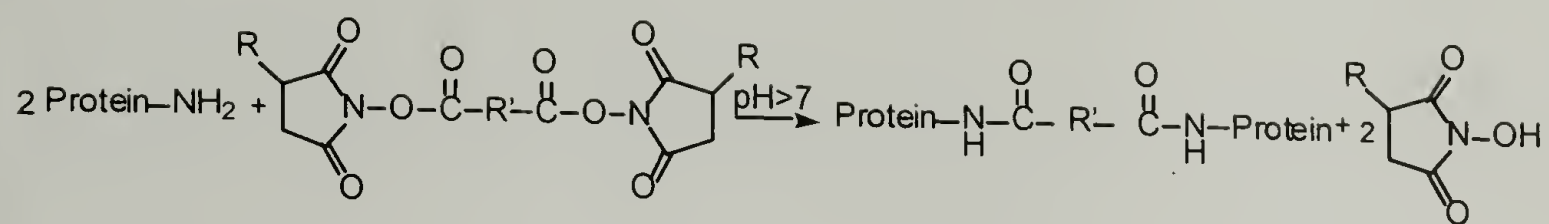


Figure 3.1 Reaction scheme for crosslinking the lysine residues of the protein with bifunctional NHS esters. R' is (CH₂)₆, for DSS, R=H; for BS3, R=SO₃⁻Na⁺.

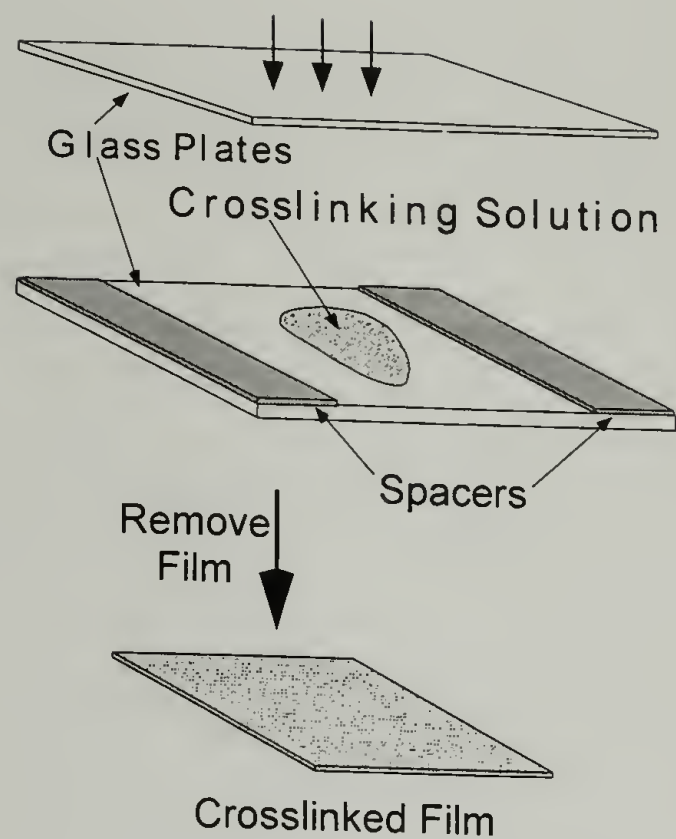


Figure 3.2 Film casting by Method I.

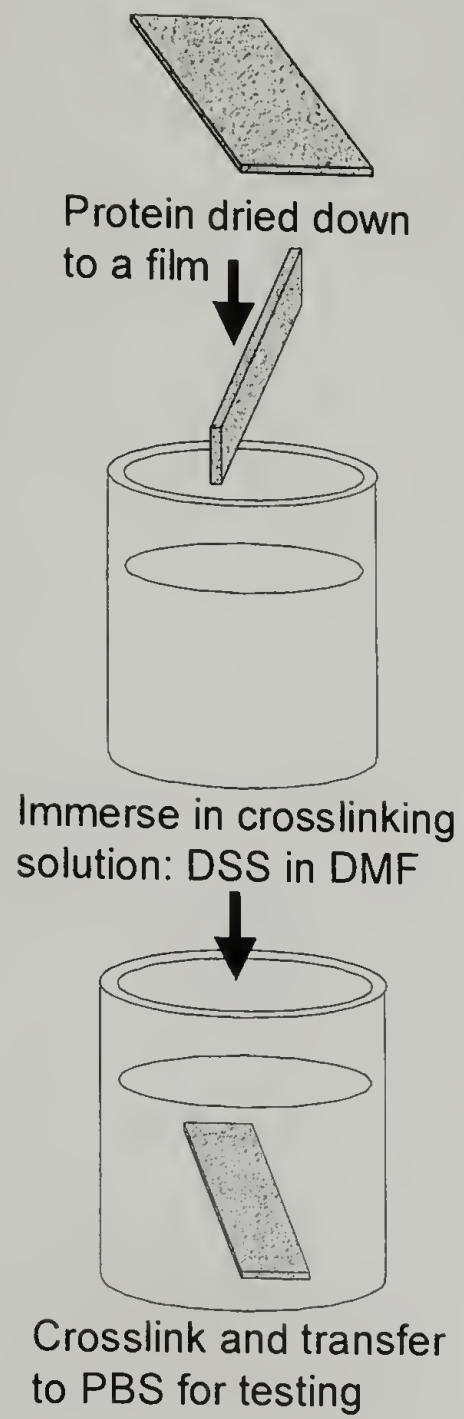


Figure 3.3 Film casting by Method II.

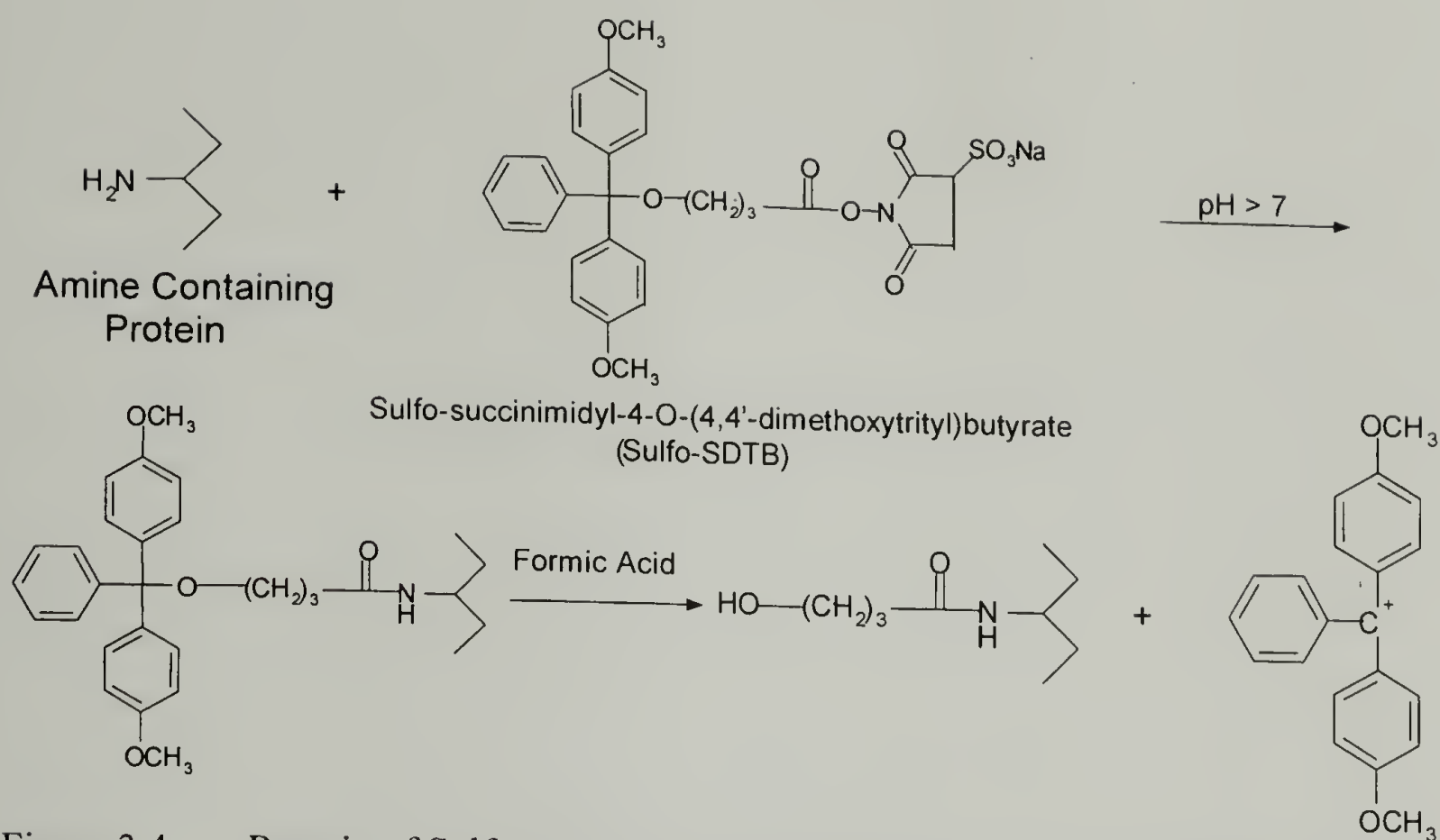


Figure 3.4 Reaction of Sulfo-SDTB for detection of residual lysines in crosslinked films by measuring absorbance at 498 nm of the dimethoxytrityl cation product.

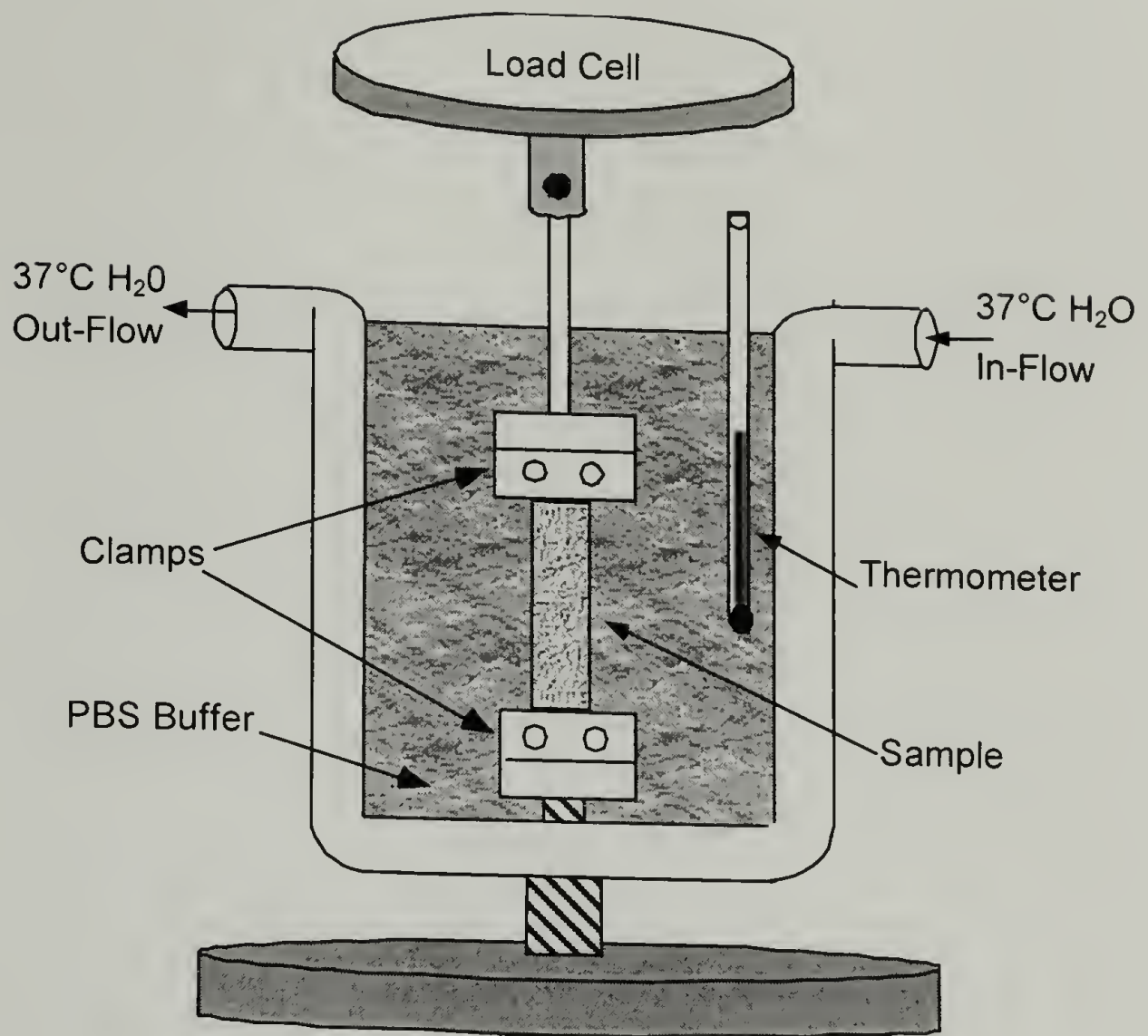


Figure 3.5 Tensile testing apparatus allowing uniaxial tensile tests under simulated physiological conditions (37 °C, PBS pH 7.4).

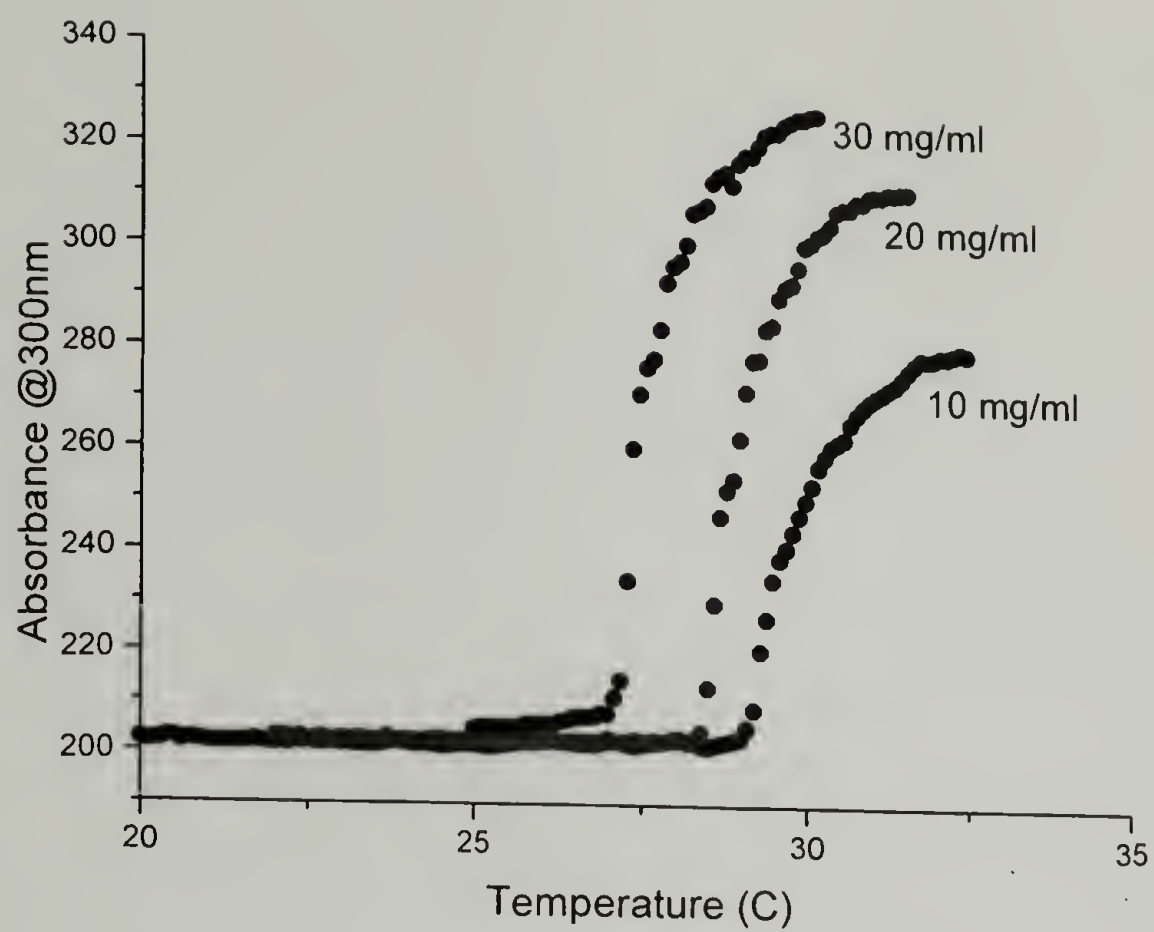


Figure 3.6 LCST behavior of CS5 protein at 10, 20, and 30 mg/ml concentrations.

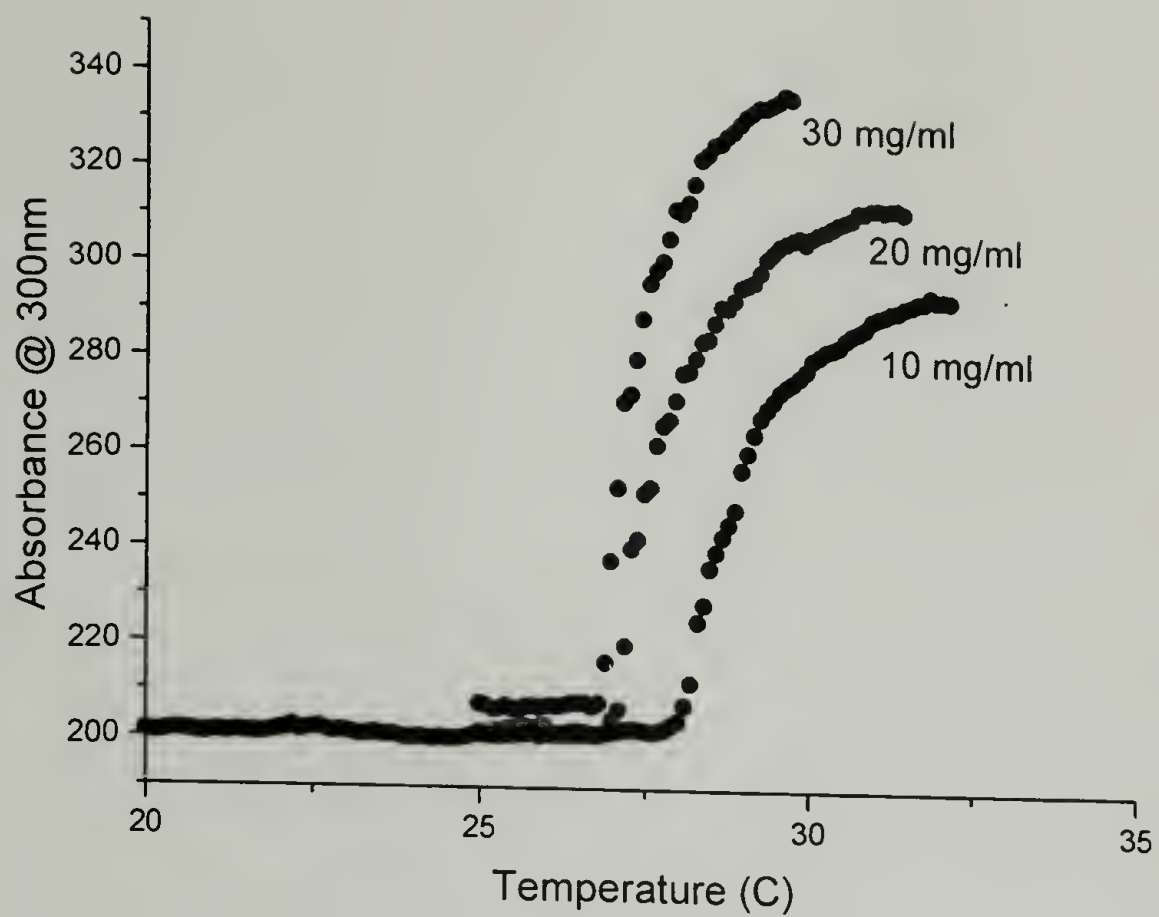


Figure 3.7 LCST behavior of SC5 protein at 10, 20, and 30 mg/ml concentrations.

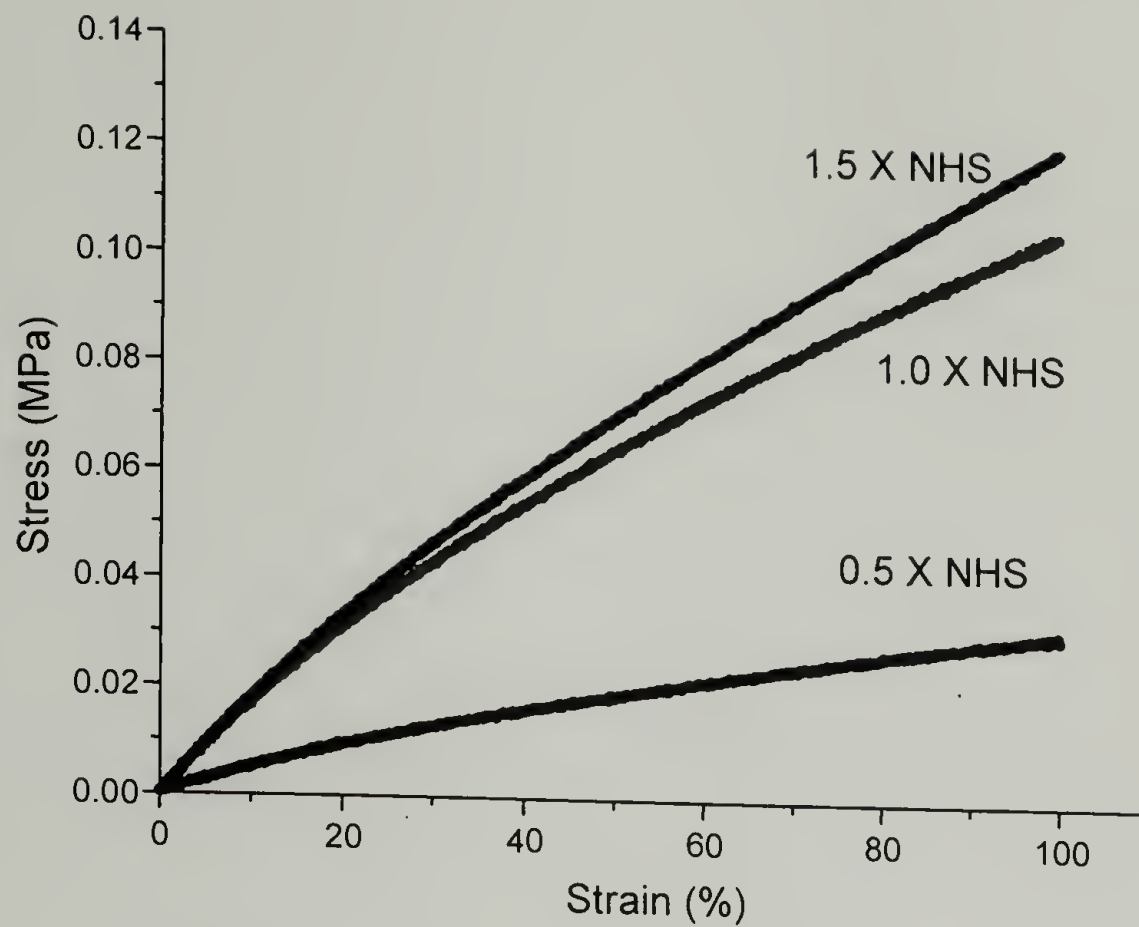


Figure 3.8 Stress-strain behavior of CS5 protein films crosslinked by Method I at 0.5:1, 1:1, and 1.5:1 NHS to lysine stoichiometries.

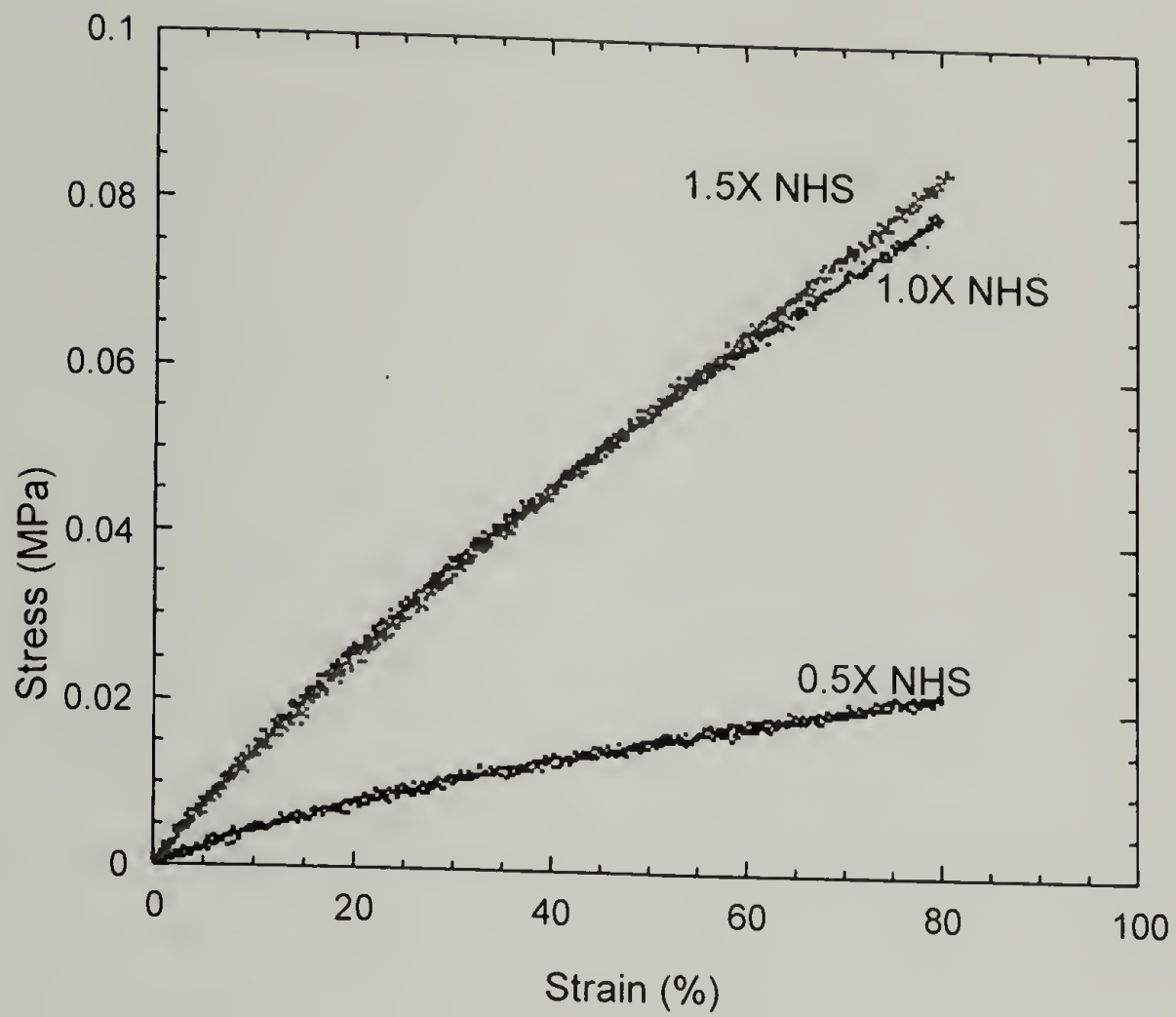


Figure 3.9 Stress-strain behavior of SC5 protein films crosslinked by Method I at 0.5:1, 1:1, and 1.5:1 NHS to lysine stoichiometries.

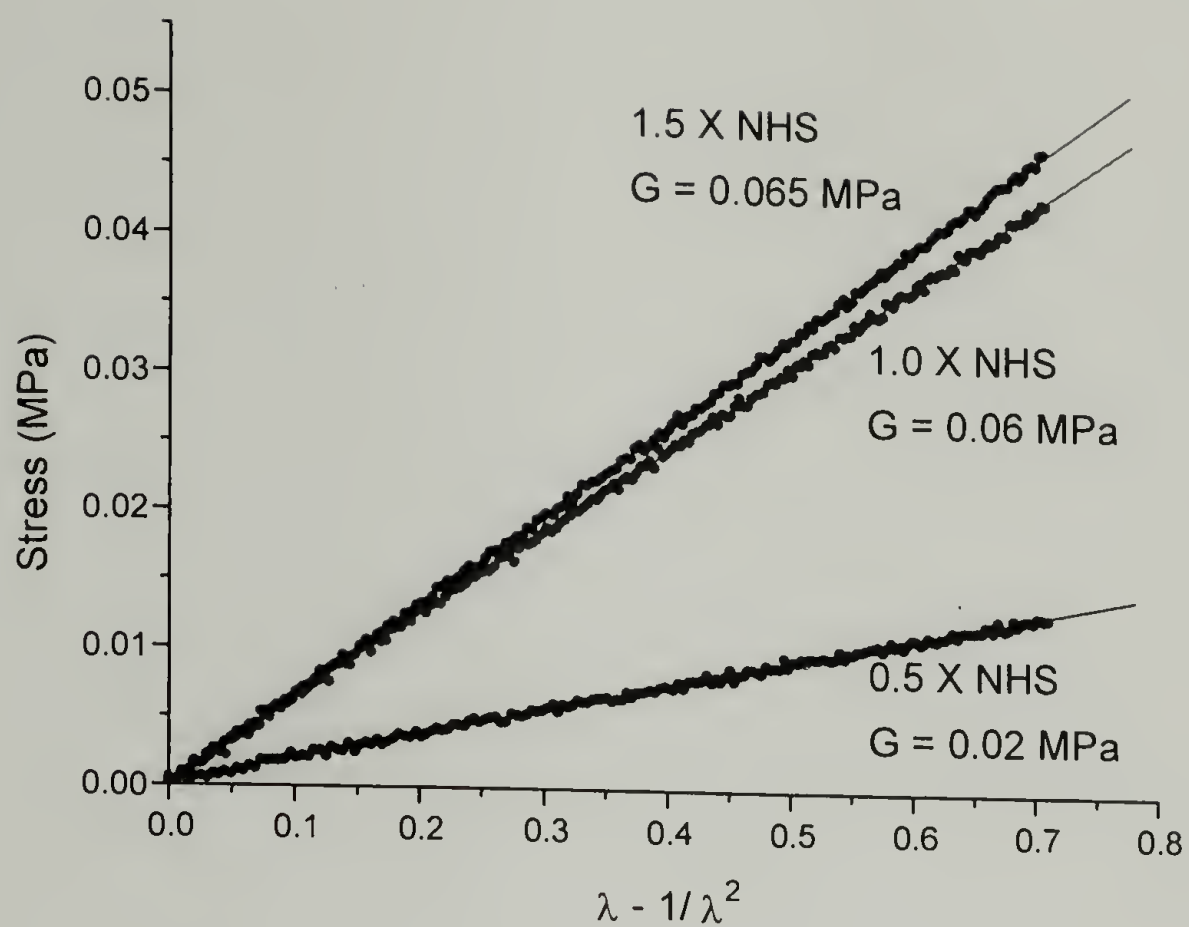


Figure 3.10 Determination of shear modulus, G , of CS5 protein films by measuring the slope of the line formed by plotting stress vs. $\lambda - 1/\lambda^2$.

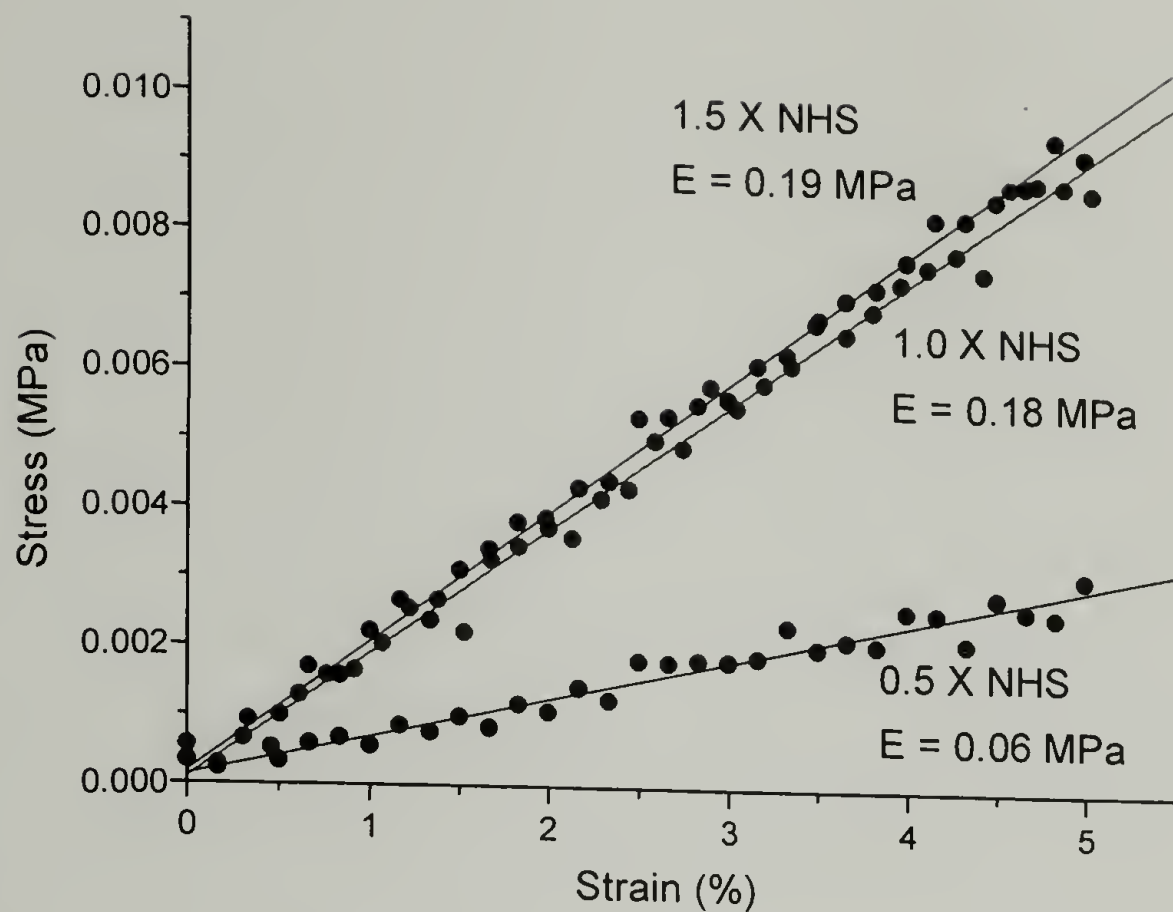


Figure 3.11 Determination of tensile or Young's modulus, E , of CS5 protein films by measuring the slope of the line formed by plotting stress vs. strain for the first 5 % strain.

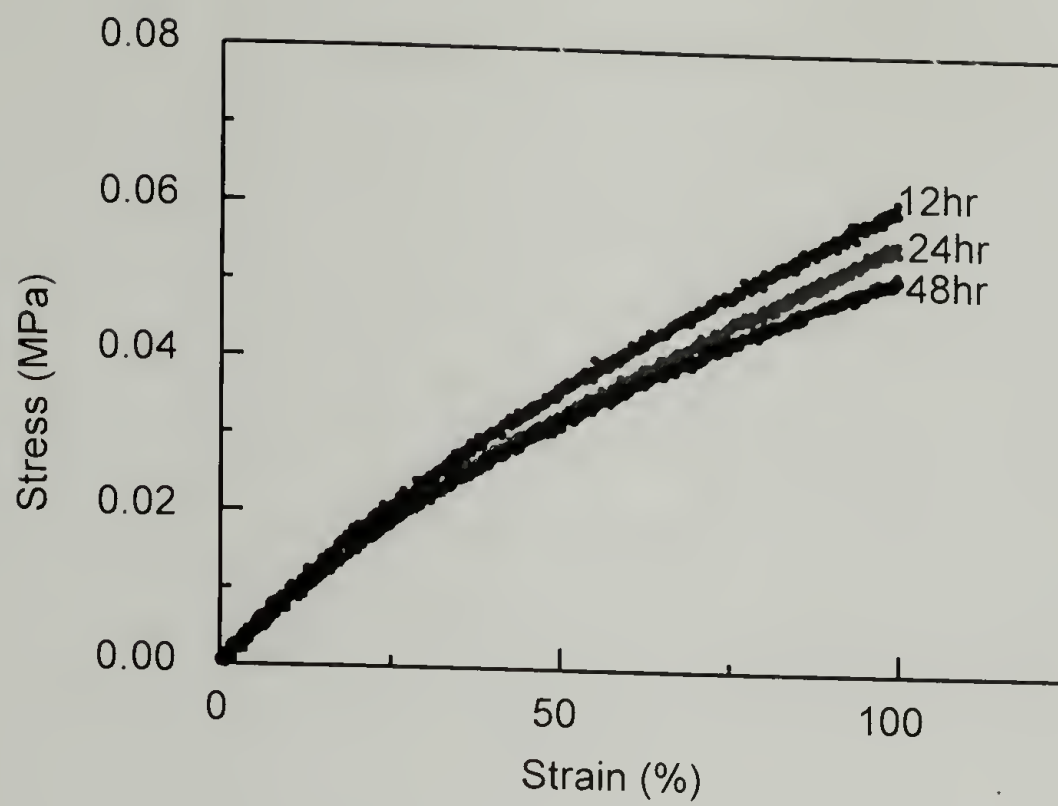


Figure 3.12 Stress-strain behavior of CS5 protein films crosslinked by Method I for 12, 24, and 48 hr.

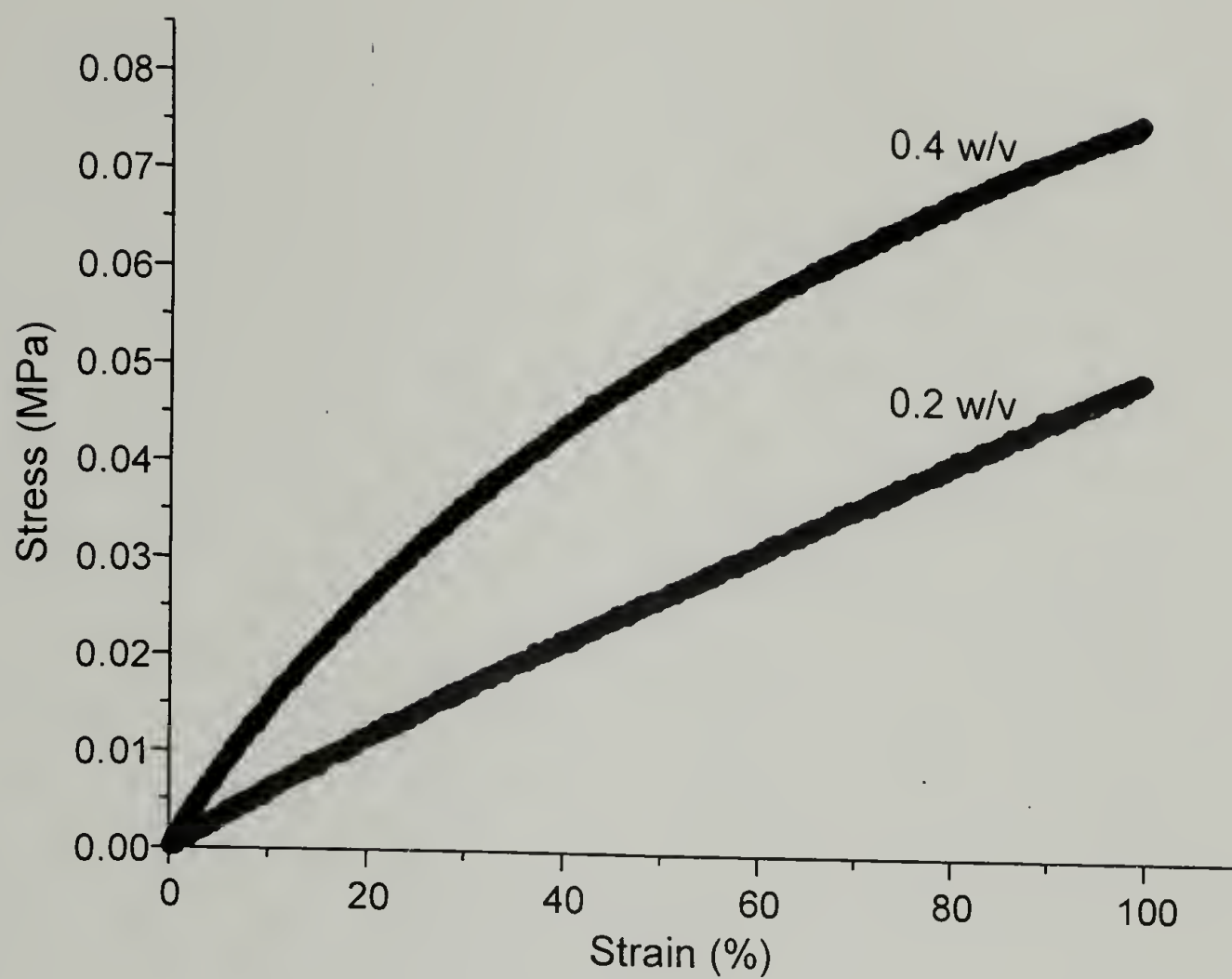


Figure 3.13 Stress-strain behavior of CS5 protein films crosslinked by Method I at 0.2 w/v and 0.4 w/v concentrations.

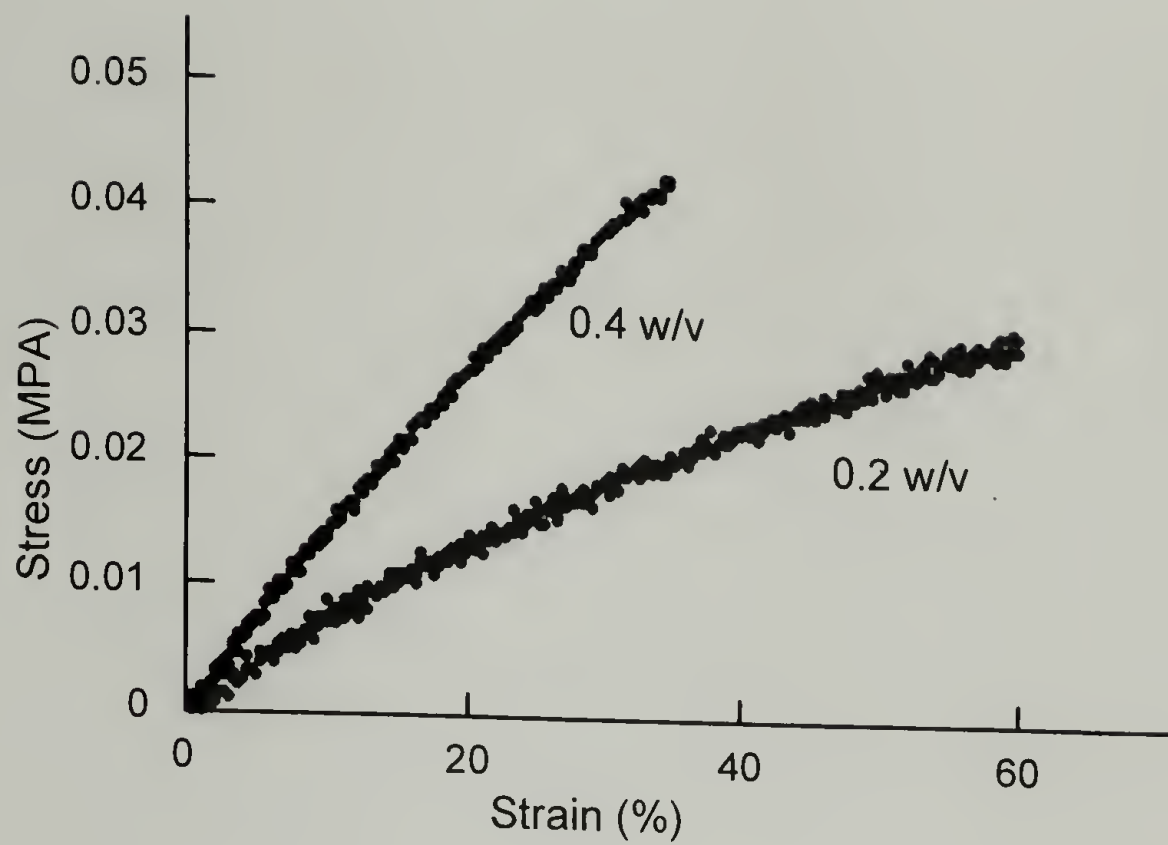


Figure 3.14 Stress-strain behavior of SC5 protein films crosslinked by Method I at 0.2 w/v and 0.4 w/v concentrations.

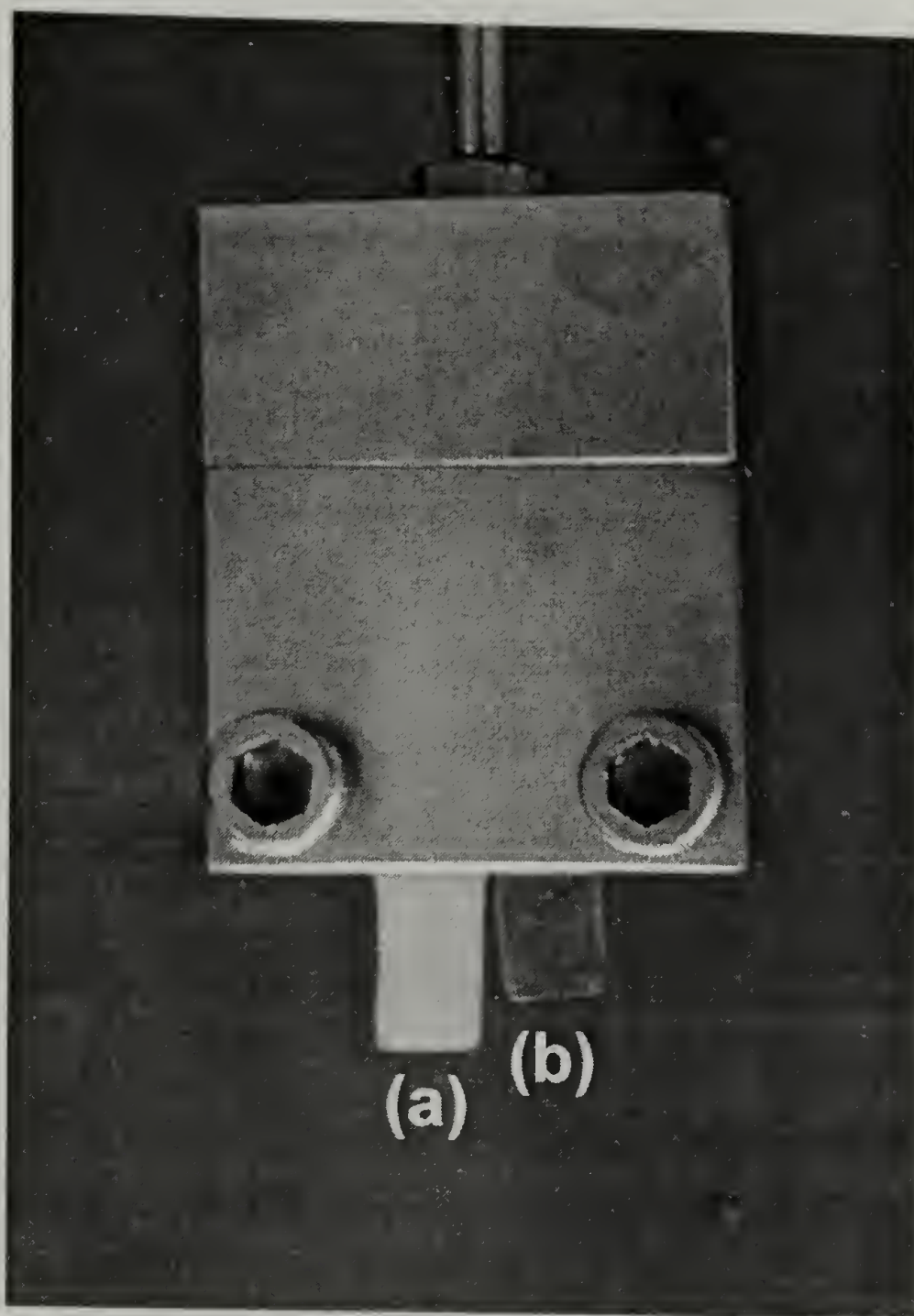


Figure 3.15 Two films clamped in an Instron testing grip, exhibiting difference in appearance between (a) films crosslinked above the LCST (25 °C) and (b) films crosslinked below the LCST (4 °C)

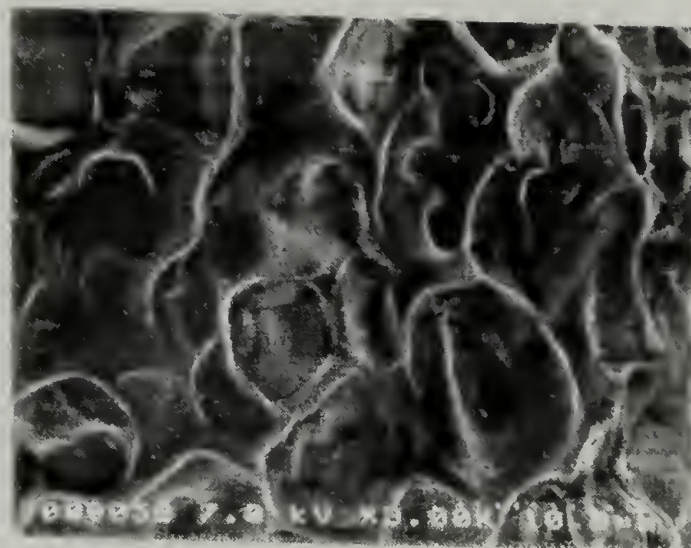
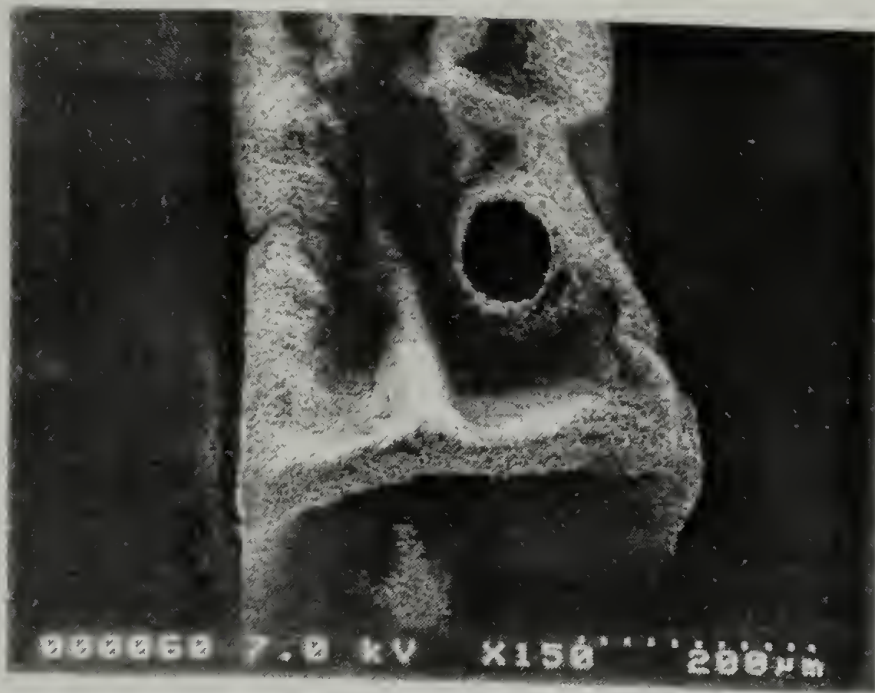


Figure 3.16 SEM micrographs of a CS5 film crosslinked by Method I above the LCST (25 °C).

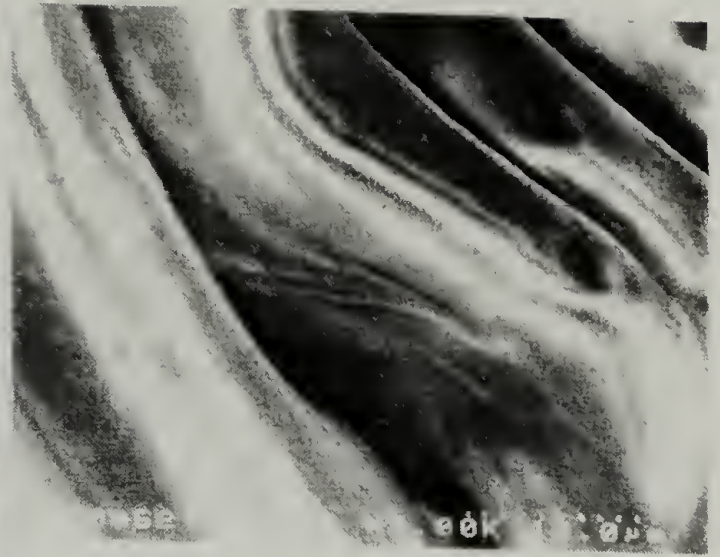
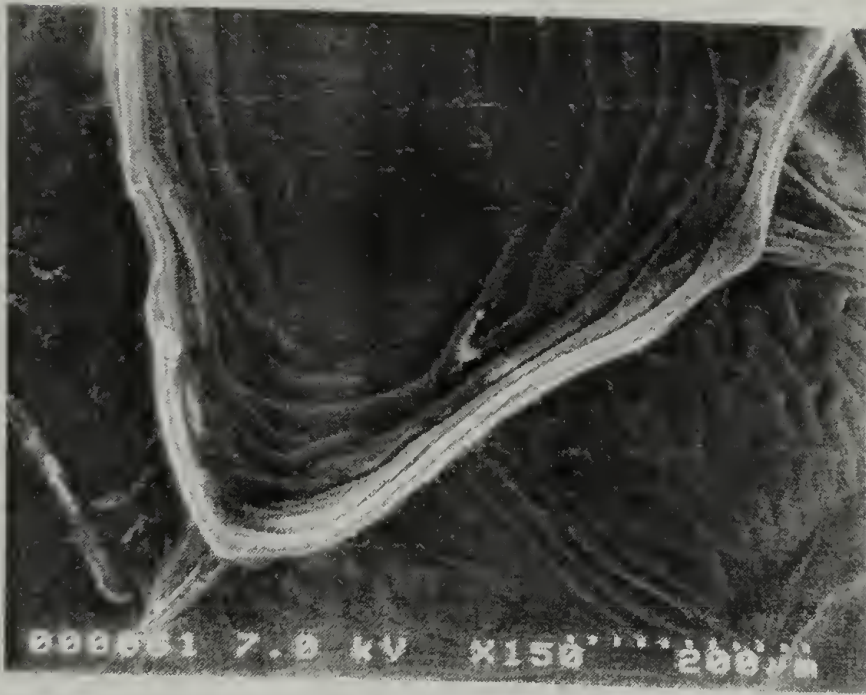


Figure 3.17 SEM micrographs of a CS5 film crosslinked by Method I below the LCST (4 °C).

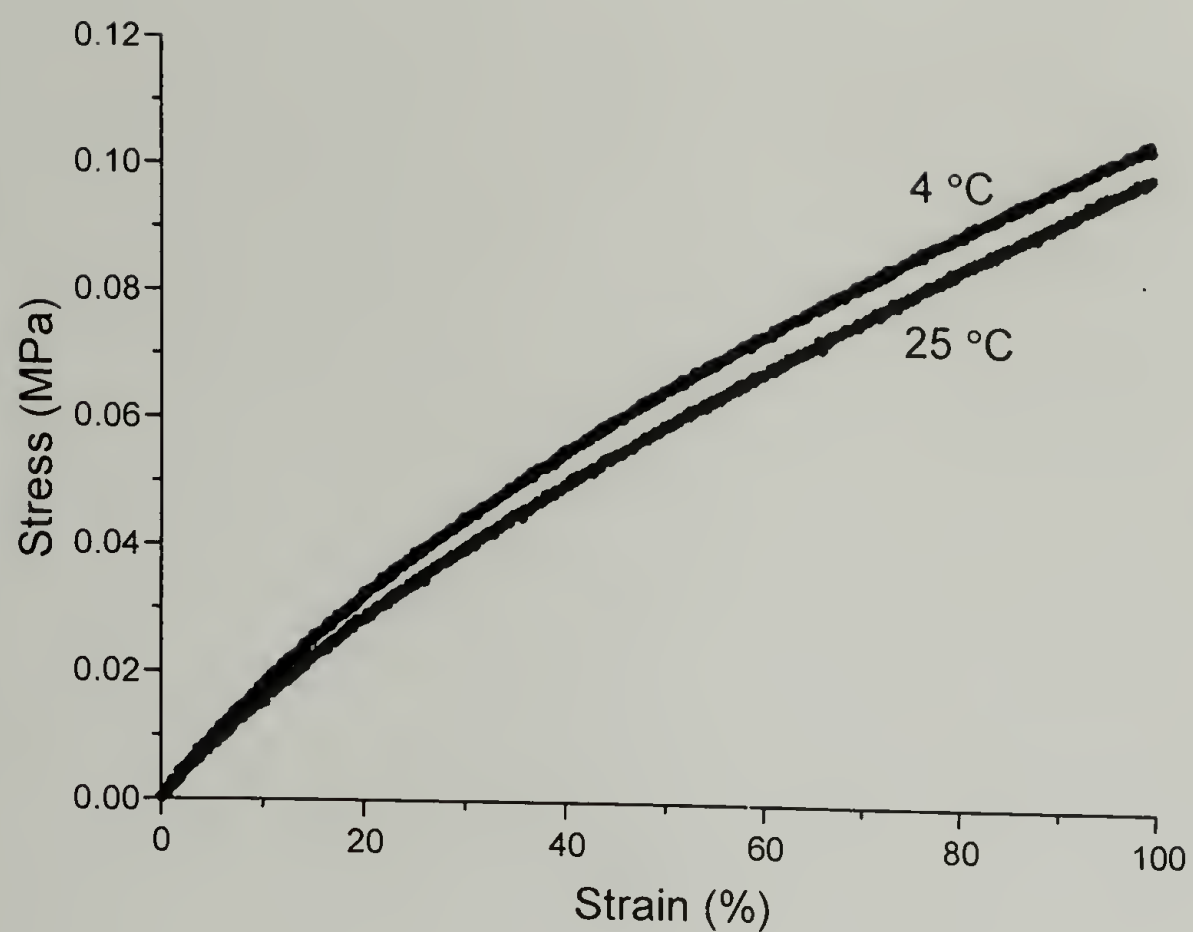


Figure 3.18 Stress-strain behavior of CS5 protein films crosslinked by Method I at 4 °C and 25 °C.

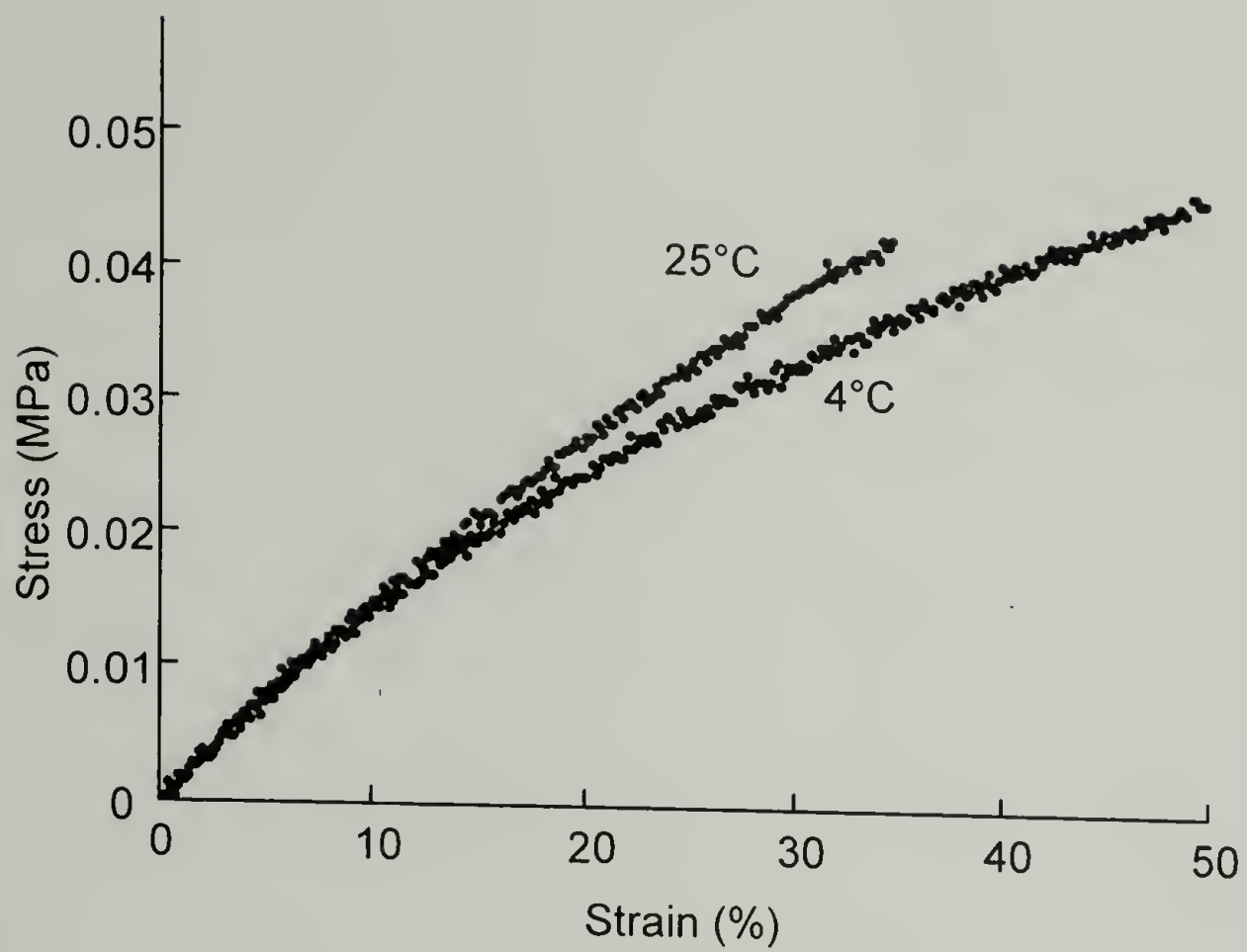


Figure 3.19 Stress-strain behavior of SC5 protein films crosslinked by Method I at 4 °C and 25 °C.

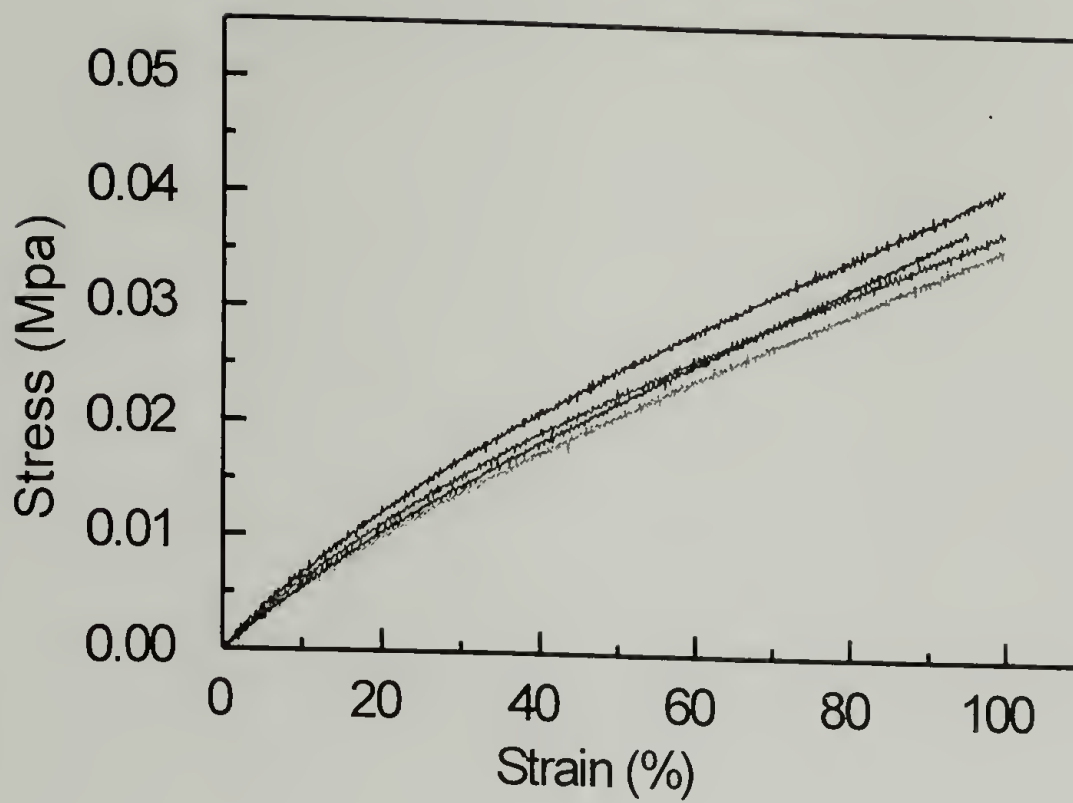


Figure 3.20 Stress-strain behavior of a 0.2 w/v crosslinked CS5 protein film tested at 15, 25, 37, and 45 °C.

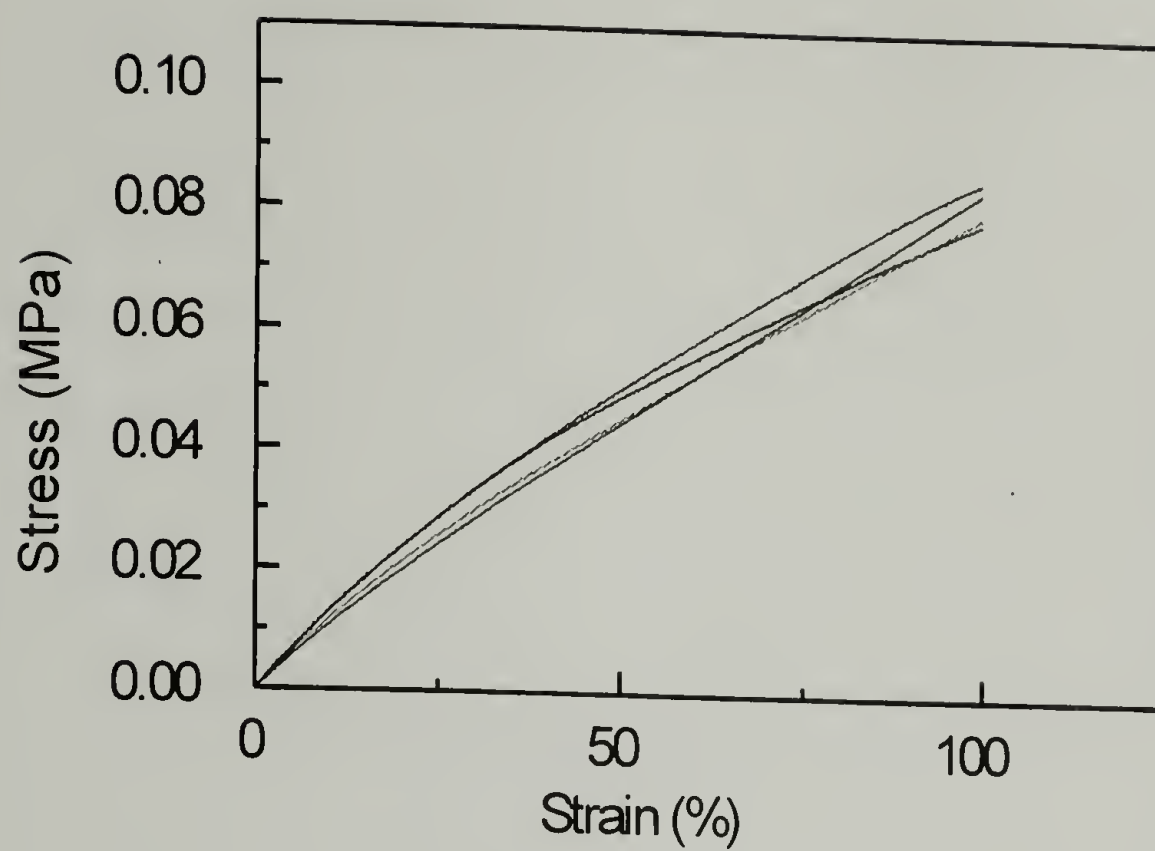


Figure 3.21 Stress-strain behavior of a 0.4 w/v crosslinked CS5 protein film tested at 15, 25, 37, and 45 °C.

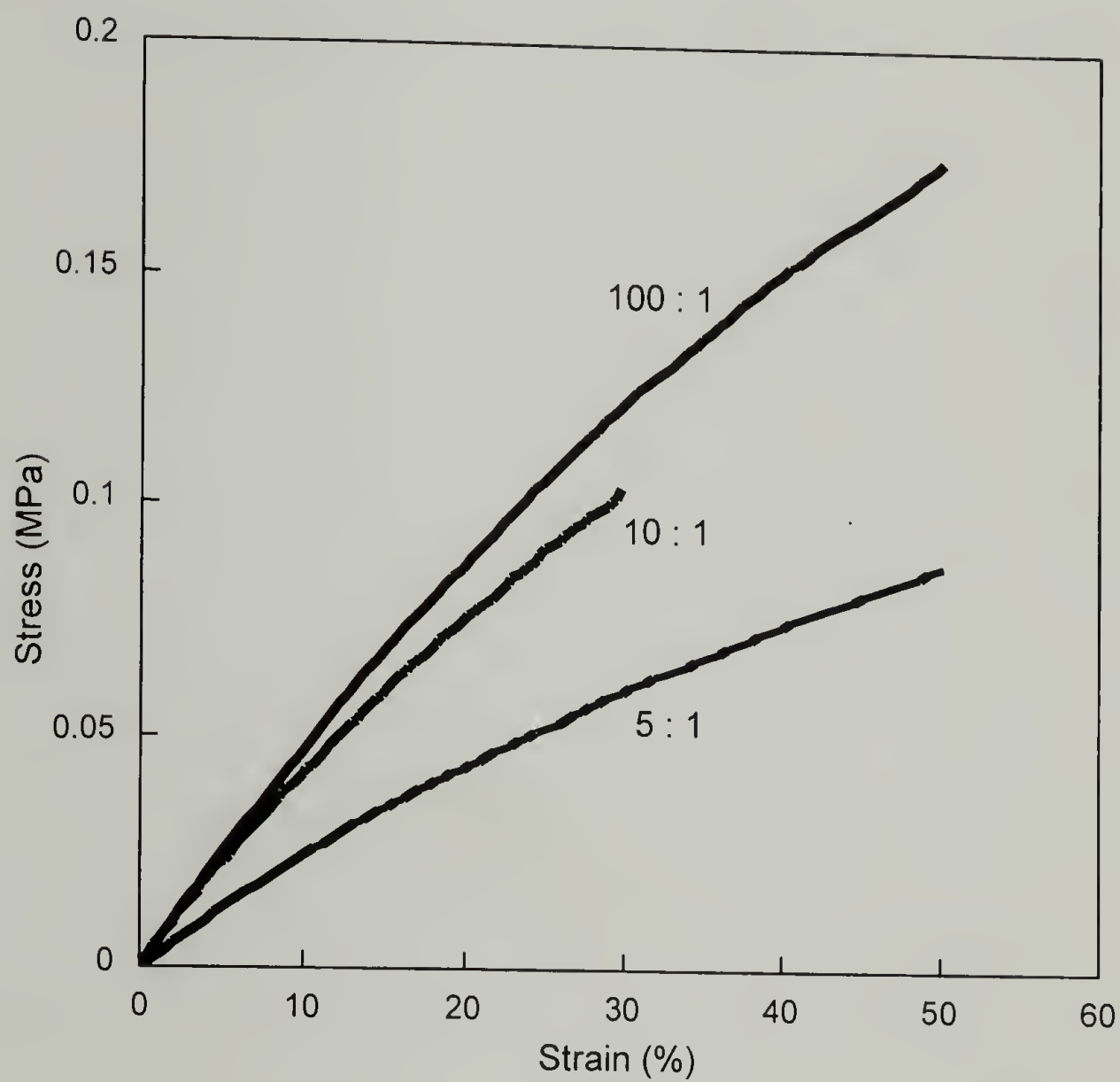


Figure 3.22 Stress-strain behavior of films crosslinked by Method II in solutions with 100:1, 10:1 and 5:1 NHS to lysine stoichiometries.

3.5 References

1. Huang, C., *Physicochemical studies of collagen and collagen-mucopolysaccharide composite materials: model materials for skin*, in *Mechanical Engineering*. 1974, MIT: Cambridge, MA. p. 376.
2. Guar, R.K. and K.C. Gupta, *A Spectrophotometric Method for the Estimation of Amino Groups on Polymer Supports*. *Anal. Biochem.*, 1989. **180**: p. 253-258.
3. Sarin, V.K., et al., *Quantitative Monitoring of Solid-Phase Peptide Synthesis by the Ninhydrin Reaction*. *Analytical Biochemistry*, 1981. **117**: p. 147-157.
4. Lustenberger, P., P. Formstecher, and M. Dautrevaux, *Quantitative Determination of Alkylamino Side-Chains Coupled to Agarose Beads*. *Journal of Chromatography*, 1980. **193**: p. 451-457.
5. McMillan, R.A. and V.P. Conticello, *Synthesis and Characterization of Elastin-Mimetic Protein Gels Derived from a Well-Defined Polypeptide Precursor*. *Macromolecules*, 2000. **33**(13): p. 4809-4821.
6. Panitch, A., et al., *Design and Biosynthesis of Elastin-like Artificial Extracellular Matrix Proteins Containing Periodically Spaced Fibronectin CS5 Domains*. *Macromolecules*, 1999. **32**(5): p. 1701-1703.
7. Welsh, E.R. and D.A. Tirrell, *Engineering the Extracellular Matrix: A Novel Approach to Polymeric Biomaterials. I. Control of the Physical Properties of Artificial Protein Matrices Designed to Support Adhesion of Vascular Endothelial Cells*. *Biomacromolecules*, 2000. **1**(1): p. 23-30.
8. Urry, D.W., et al., *Hydrophobicity Scale for Proteins Based on Inverse Temperature Transitions*. *Biopolymers*, 1992. **32**: p. 1243-1250.
9. Cox, G.W., et al., *Characterization of IL-2 receptor expression and function on murine macrophages*. *Journal of Immunology*, 1990. **145**: p. 1719-1726.
10. Knoller, S., S. Shpungin, and E. Pick, *The Membrane-Associated Component of the Amphiphile-Activated, Cytosol-Dependent Superoxide-Forming NADPH Oxidase of Macrophages is Identical to Cytochrome b559*. *Journal of Biological Chemistry*, 1991. **266**: p. 2785-2804.
11. Gosline, J.M. and J. Rosenbloom, *Elastin*, in *Extracellular Matrix Biochemistry*, K.A. Piez and A.H. Reddi, Editors. 1984, Elsevier Science Publishing Co.: New York, NY.

12. Aklonis, J.J. and W.J. MacKnight, *Introduction to Polymer Viscoelasticity*. 1983: John Wiley & Sons.
13. Young, R.J. and P.A. Lovell, *Introduction to Polymers*. Second ed. 1991, London, UK: Chapman and Hall.
14. Fung, Y.C., *Biomechanics: Mechanical Properties of Living Tissues*. Second ed. 1993, New York, NY: Springer-Verlag New York, Inc.
15. Gosline, J. and C. French, *Dynamic Mechanical Properties of Elastin*. Biopolymers, 1979. **18**: p. 2019-2103.
16. Abbott, W.M. and R.P. Cambria, *Control of Physical Characteristics (Elasticity and Compliance) of Vascular Grafts, in Biologic and Synthetic Vascular Prostheses*, ed. J.C. Stanley. 1982, New York: Gurne and Stratton. 189-220.
17. Winlove, C.P. and K.H. Parker, *Physiochemical properties of vascular elastin*, in *Connective Tissue Matrix : Part 2*, D.W.L. Hukins, Editor. 1990, The MacMillan Press Ltd.

CHAPTER 4

MECHANICAL PROPERTIES OF CS1 PROTEIN

4.1 Introduction and Objectives

Mechanical properties of the CS1 protein were explored to determine the potential for use as a vascular graft material. Bis(sulfosuccinimidyl)suberate was used to crosslink the protein into films for uniaxial tensile testing. The amount of crosslinker, protein weight fraction, and method of crosslinking were varied to yield differing mechanical properties. The residual lysine content was measured spectrophotometrically to quantify extent of crosslinking. The buffer content of the crosslinked films was measured and the theoretical molecular weight between crosslinks (M_c) was determined.

4.2 Experimental Section

4.2.1 Measuring the LCST

See section 3.2.1

4.2.2 Film Casting

4.2.2.1 Method I

See Section 3.2.3.1, except above the LCST refers to 37 °C instead of 25 °C.

4.2.2.2 Method III

Method III, shown in Figure 4.1, involved crosslinking a 0.1, 0.2, or 0.3 w/v solution of protein in PBS with a 1:1 NHS/lysine ratio using bis(sulfo-succinimidyl) suberate (BS3) (Pierce, Rockford, IL) in a teflon mold. The solution was spun at 2000 g for 2 min on a plate spinner to create a flat film. This was then placed on a 60 °C hotplate overnight. Films were rehydrated in cold PBS for at least 2 hrs prior to bringing them to 37 °C for testing.

4.2.3 Film Characterization

4.2.3.1 Weight Fraction Protein

See Section 3.2.4.1.

4.2.3.2 Residual Lysine Content

See Section 3.2.4.2.

4.2.4 Tensile Testing

See Section 3.2.5.

4.3 Results and Discussion

4.3.1 LCST Behavior

Figure 4.2 shows the LCST behavior of the protein at 10, 20, and 30 mg/ml concentrations. The onset of the transition occurs between 36 °C and 37 °C for each of the concentrations with the slope of the curve increases with increasing concentration. The CS1 has an LCST 10 °C higher than CS5 and SC5.

4.3.2 Film Characterization

4.3.2.1 Weight Fraction Protein

Table 4.1 gives the weight fraction protein in the crosslinked films. In general, the CS1 films behaved similarly to the CS5 films. However, there is no difference in

weight fraction protein with a decrease in crosslinker in Samples 1-3. This indicates the trend seen previously is likely within error of the measurement. Like the CS5, the CS1 films increase in weight fraction protein with an increase in crosslinking solution concentration (cf. Samples 2, 5). As was seen with the CS5 films, the protein concentration during crosslinking is the most significant factor determining the final water content of the crosslinked film.

For films prepared by Method III, the higher the concentration during crosslinking, the higher the weight fraction protein in the crosslinked film giving a range of 25 to 32 %. In agreement with equation 3, an increase in modulus is observed with an increase in weight fraction protein.

4.3.2.2 Residual Lysine Content

Table 4.1 shows the percentage of lysines reacted in the films. Again, CS1 shows similar levels of reacted lysines as the CS5 films although the values for Method I films are slightly higher and the values for Method III films are slightly lower. Sample 1 shows 46 % of the lysines reacted which is approximately half of that of Sample 2. As with the CS5 results, this extent of reaction is consistent with the use of half the crosslinker needed to crosslink the sample. Adding 50 percent excess crosslinker as in Sample 3 does not significantly increase the number of reacted lysines. Sample 5 shows 76 % of the lysines reacted, lower than that of Sample 2, because at lower concentrations hydrolysis would compete more strongly. The temperature of reaction does not affect the

percentage of reacted lysines in the films (cf. Samples 4, 2). Samples 6 – 8 show 85 % reacted lysines, which seems lower than would be expected with the presence of excess crosslinker.

4.3.3 Mechanical Properties of Films

4.3.3.1 Treatment of Mechanical Testing Data

See Section 3.3.4.1.

4.3.3.2 Mechanical Properties of Method I Films

4.3.3.2.1 Variation of NHS to Lysine Stoichiometry

Figure 4.3 shows the stress-strain behavior of films crosslinked using Method I in PBS at 37 °C with BS3/lysine stoichiometries of 0.5:1, 1:1, and 1.5:1. Figure 4.4 shows the determination of G, and Figure 4.5 shows the determination of E. The tensile modulus is again one third of the shear modulus agreeing with theory and yielding tensile moduli ranging from 0.06 to 0.17 MPa. The moduli are within error of moduli for the CS5 films crosslinked by the same process. The modulus of Sample 1 is less than half of the modulus for Sample 2, and increasing the crosslinker amount (Sample 3) does not significantly change the modulus from Sample 2. This was previously described in Chapter 3 for CS5 films and similarly, although the high amount of crosslinker might be

expected to decrease the modulus by increasing tethered ends and reducing the number of effective crosslinks, it seems this effect is not significant. As with the CS5 it is possible competing hydrolysis and/or incomplete reaction negate this effect. Since a 1:1 ratio should fully crosslink the sample under ideal crosslinking, the fact that an increase in crosslinker does not significantly increase the modulus indicates fairly efficient crosslinking.

4.3.3.2.2 Variation of Crosslinking Time

The effect of crosslinking time on the mechanical properties was explored by allowing the films to crosslink for 12, 24, and 48 hr. Figure 4.6 shows the stress-strain curves illustrating no difference in the mechanical properties with increasing reaction time. This ensures the reaction was complete for each of the studies since the films were allowed at least a 12 hr reaction time.

4.3.3.2.3 Variation of Protein Concentration

Figure 4.7 shows the tensile properties of films cast at both 0.2 and 0.4 w/v protein in PBS at 37 °C. As with the CS5 films, the modulus for the 0.4 w/v sample is approximately twice that for the 0.2 w/v sample. From Equation 3, since the modulus is proportional to the chain density, a sample with twice the chain density and other properties remaining the same would have twice the modulus.

4.3.3.2.4 Variation of Crosslinking Temperature

In aqueous solution (PBS) the protein exhibits an LCST as mentioned previously. For the CS1 protein, at 0.4 w/v the LCST is below 37 °C, and as the lysines are neutralized by crosslinking, the LCST is lowered further. The previously described films were crosslinked above the LCST (at 37 °C) where the films have a completely opaque, white appearance. Conversely, protein films crosslinked below the LCST (at 4 °C), after crosslinking do not appear to go through the LCST and remain clear, even after raising the temperature. Figure 4.8 shows the tensile behavior of films crosslinked above (37 °C) and below the LCST (4 °C). As with the CS5 films, although the appearance of the samples is very different, the modulus is unaffected. Again, it is possible that tests other than uniaxial tensile tests could elucidate some mechanical differences not shown with this test.

4.3.3.3 Mechanical Properties of Method III Films

Naturally occurring elastin has a modulus in the range of 0.3-0.6MPa [1-3]. Prepared films by Method II encompass this range, but had a higher than desired standard deviation (see Table 3.2). Therefore the next set of films were made using Method III to improve the film quality and maintain the appropriate modulus. Figure 4.9 shows the mechanical behavior of these films crosslinked at 0.1, 0.2, and 0.3 w/v protein. As the concentration of protein is increased, the modulus also increases, giving a range of 0.21-0.58 MPa, which lies close to or within the desired range of moduli.

4.3.4 Theoretical Mc

Using Equation 3, the theoretical Mc was determined. The Mc for the crosslinked films is shown in Table 4.1. As is seen with the CS5 protein, for Method I, Sample 1 has a lower modulus than Sample 2 and 3 and a similar protein weight fraction. This is a result of a larger Mc as can be calculated from Equation 3. Although the moduli of Samples 1 and 5 are similar, Mc is 35,000 g/mol and 22,000 g/mol respectively. Similar to the CS5 films, the lower weight fraction protein compensates for this difference in Mc, allowing similar moduli.

For films prepared by Method III, the theoretical Mc ranges from 10000 g/mol to 3000 g/mol with increasing protein concentration. This encompasses the Mc for elastin of 6000-7000 g/mol as well as the known modulus [3, 4]. Although the modulus and Mc are similar in these films, the water content is much higher.

The expected Mc for the proteins is 2500 g/mol assuming all crosslinks are effective and there are no chain ends. The Mc for the highest crosslinked samples (Sample 8) is very close to the expected at 3000 g/mol.

4.4 Summary and Conclusions

By varying amount of crosslinker, protein weight fraction, and method of crosslinking, CS1 films yielded Young's moduli ranging from 0.07 MPa to 0.58 MPa. The residual lysine content was measured spectrophotometrically to quantify the extent of crosslinking to be between 46 % and 85 %. The buffer content of the crosslinked films

was measured and the theoretical molecular weight between crosslinks (M_c) was determined to vary from 35000 g/mol to 3000 g/mol. The M_c is very close to what would be expected for an ideally crosslinked network of the protein. The mechanical properties of the CS1 films are within error of the CS5 and SC5 films (cf. Chapter 3-Sample 1-10, Chapter 4 – Samples 1-5). The modulus and M_c of the CS1 protein films prepared by Method III are in the same range as is reported for natural elastin.

The crosslinked proteins show interesting and promising mechanical properties for application in vascular grafts. By changing the method and conditions of crosslinking, the moduli and M_c can be controlled within the range expected for native elastin. The M_c is very close to what would be expected for an ideally crosslinked network of the protein. The CS1 compared to the CS5 and SC5 proteins show no significant difference in mechanical properties indicating the differing cell-binding domain does not affect the mechanical properties. Although not surprising, it is important information for the future incorporation of alternative cell-binding domains.

Sample	NHS/Lysine Stoichiometry	Protein Solution Conc.(w/v)	Reaction Temp. (C)	Reaction Time (hr)	Wt. Fraction Protein (%)	Mc x1000 (g/mol)	Reacted Lysines(%)
Method I: Films crosslinked in PBS with BS3							
1	0.5:1.0	0.4	37	>12	0.28 \pm 0.05	35	6 \pm 8
2	1.0:1.0	0.4	37	>12	0.30 \pm 0.02	15	83 \pm 7
3	1.5:1.0	0.4	37	>12	0.28 \pm 0.02	13	81 \pm 8
4	1.0:1.0	0.4	4	>12	0.28 \pm 0.05	13	83 \pm 7
5	1.0:1.0	0.2	37	>12	0.22 \pm 0.03	22	86 \pm 15
Method III: Films spun flat and dried							
6	1.0:1.0	0.1	60	>12	0.25 \pm 0.02	10	84 \pm 6
7	1.0:1.0	0.2	60	>12	0.27 \pm 0.04	5	83 \pm 5
8	1.0:1.0	0.3	60	>12	0.32 \pm 0.03	3	85 \pm 7
Elastin						6 ^a	

^a Reference [3].

Table 4.1 Physical properties of crosslinked CS1 protein films.

Sample #	# Sample Determinants	Tensile Modulus E (MPa)	Shear Modulus G(MPa)
Films Crosslinked by Method I			
1	3	0.06 ± 0.02	0.027 ± 0.003
2	5	0.16 ± 0.01	0.052 ± 0.001
3	4	0.17 ± 0.03	0.058 ± 0.001
4	4	0.16 ± 0.01	0.056 ± 0.002
5	3	0.07 ± 0.01	0.027 ± 0.002
Films Crosslinked by Method III			
6	3	0.21 ± 0.06	0.07 ± 0.008
7	4	0.41 ± 0.05	0.14 ± 0.005
8	3	0.58 ± 0.07	0.28 ± 0.004
Native Elastin		$0.30 - 0.60^a$	

^a Reference [1-3].

Table 4.2 Mechanical properties of crosslinked CS1 protein films.

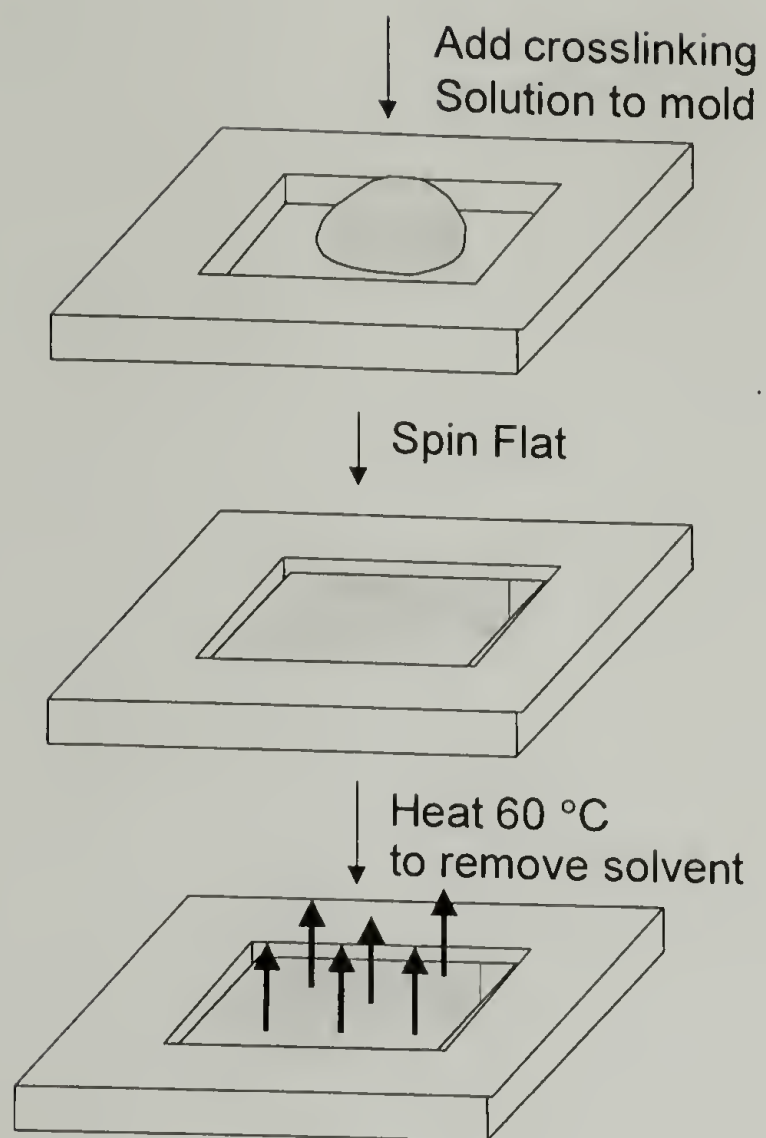


Figure 4.1 Film casting by Method III.

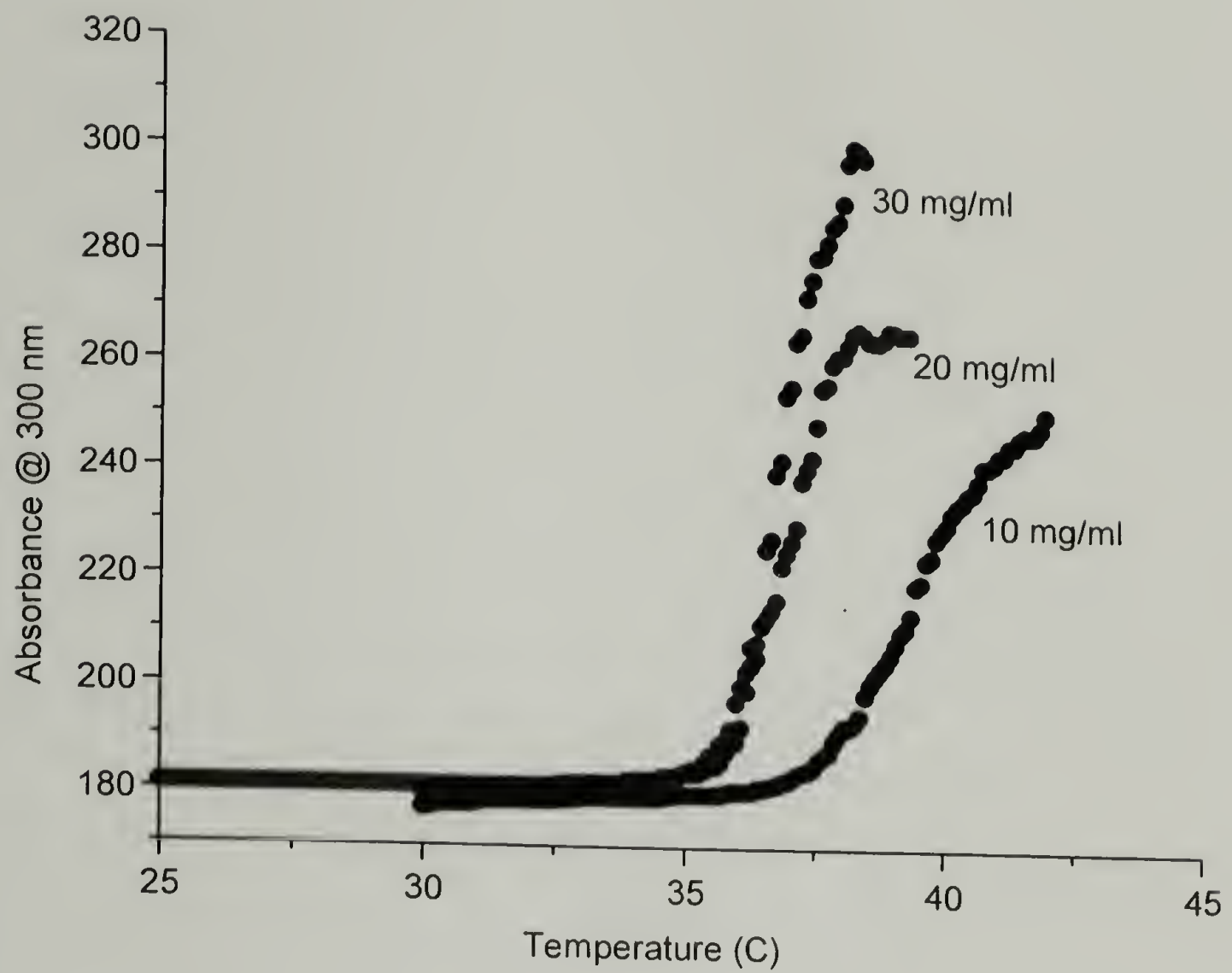


Figure 4.2 LCST behavior of the CS1 protein at 10, 20, and 30 mg/ml concentrations.

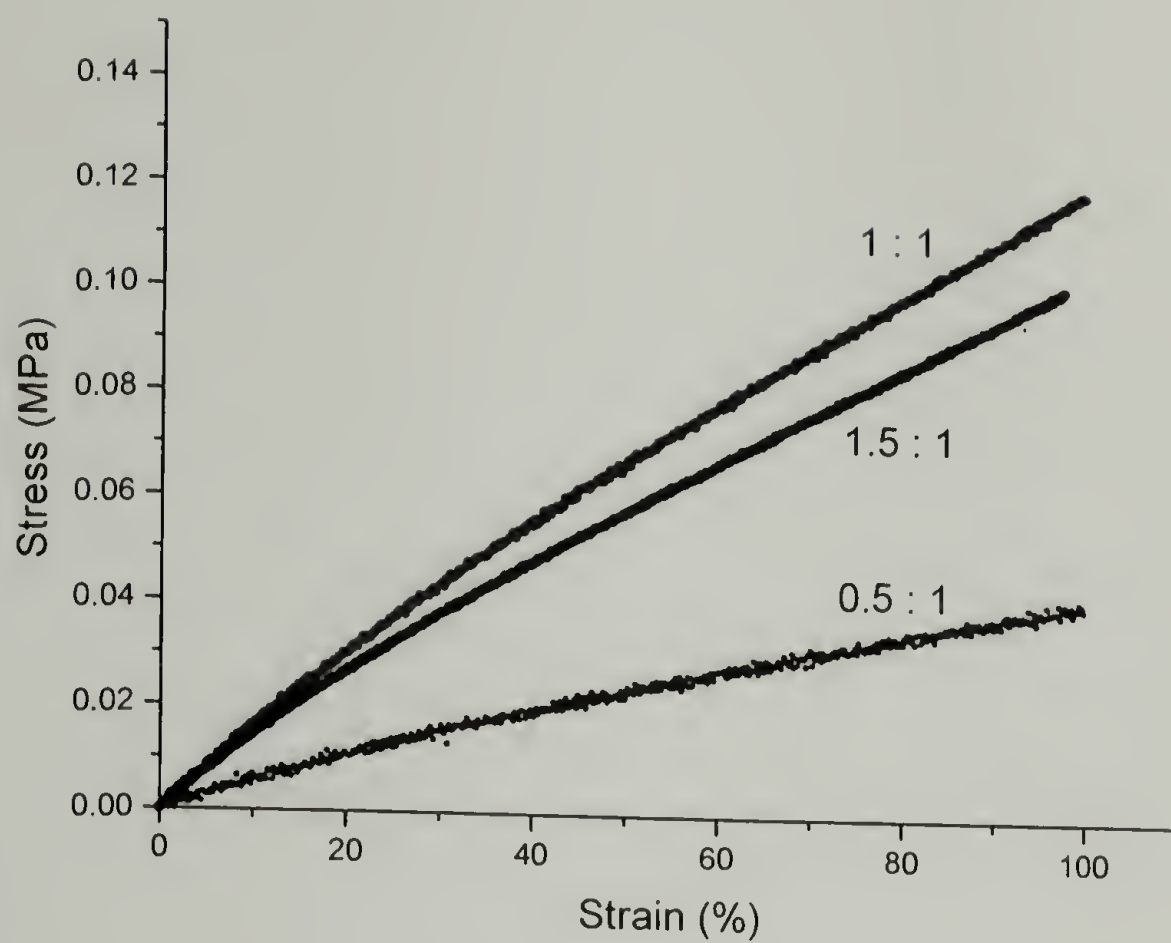


Figure 4.3 Stress-strain behavior of CS1 protein films crosslinked by Method I at 0.5:1, 1:1, and 1.5:1 NHS to lysine stoichiometries.

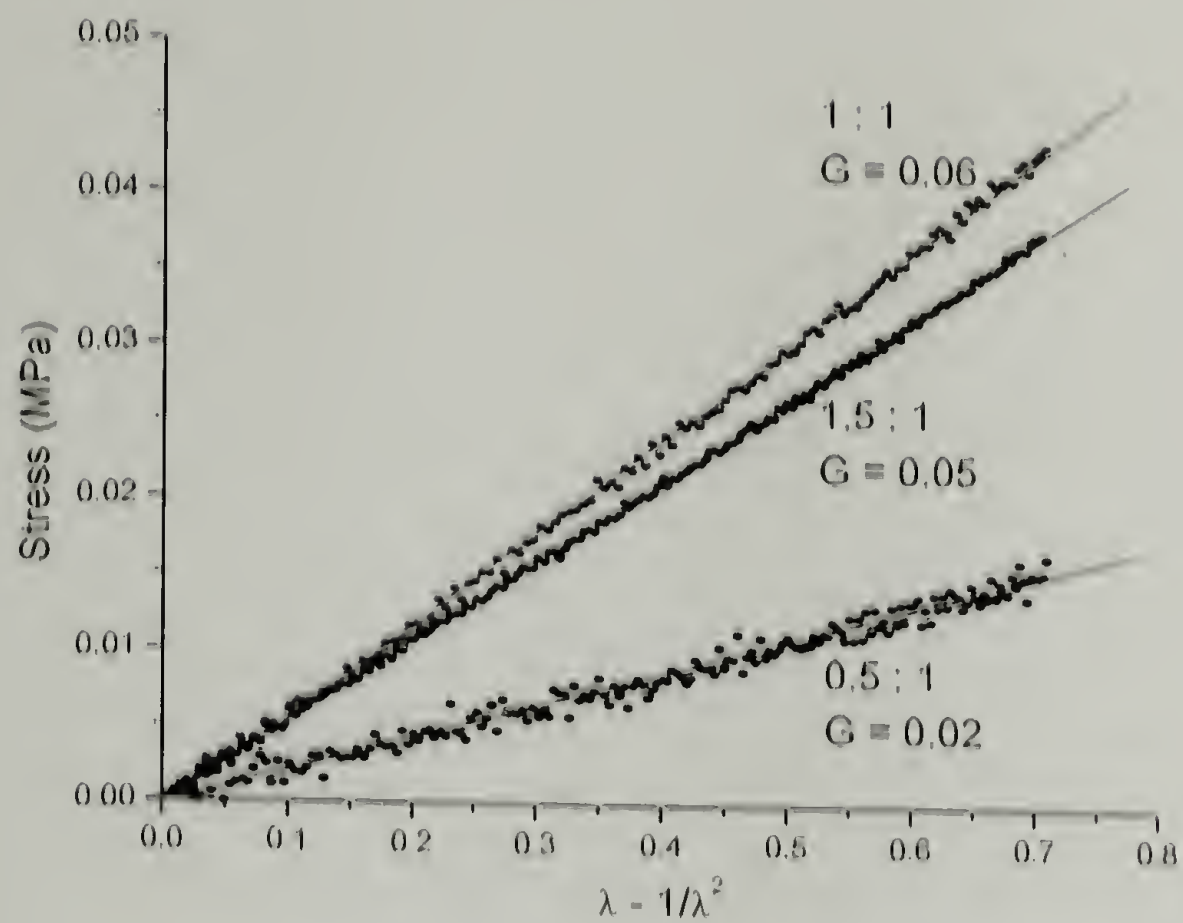


Figure 4.4 Determination of shear modulus, G , of crosslinked CSI protein films.

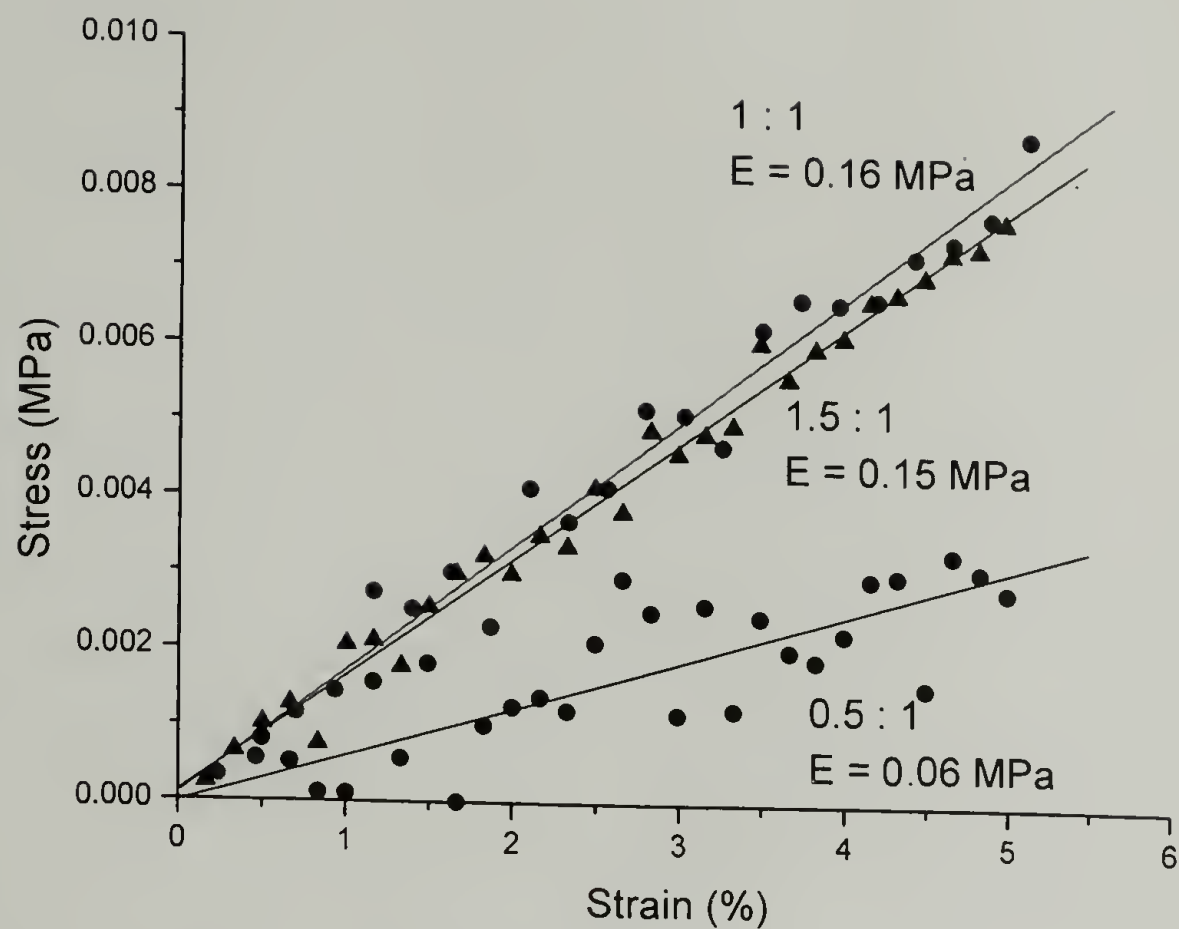


Figure 4.5 Determination of the tensile or Young's modulus, E , of crosslinked CS1 films.

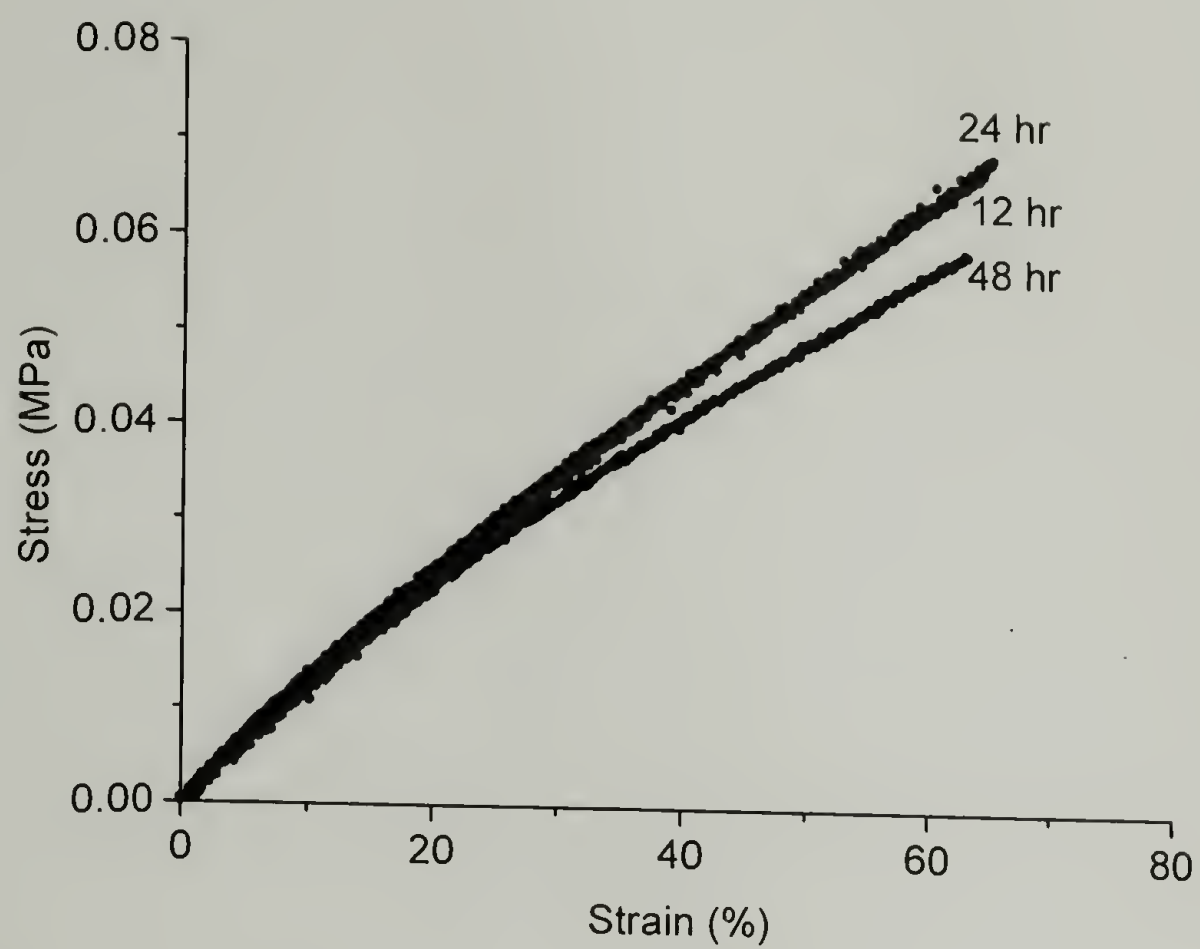


Figure 4.6 Stress-strain behavior of CS1 protein films crosslinked by Method I for 12, 24, and 48 hr.

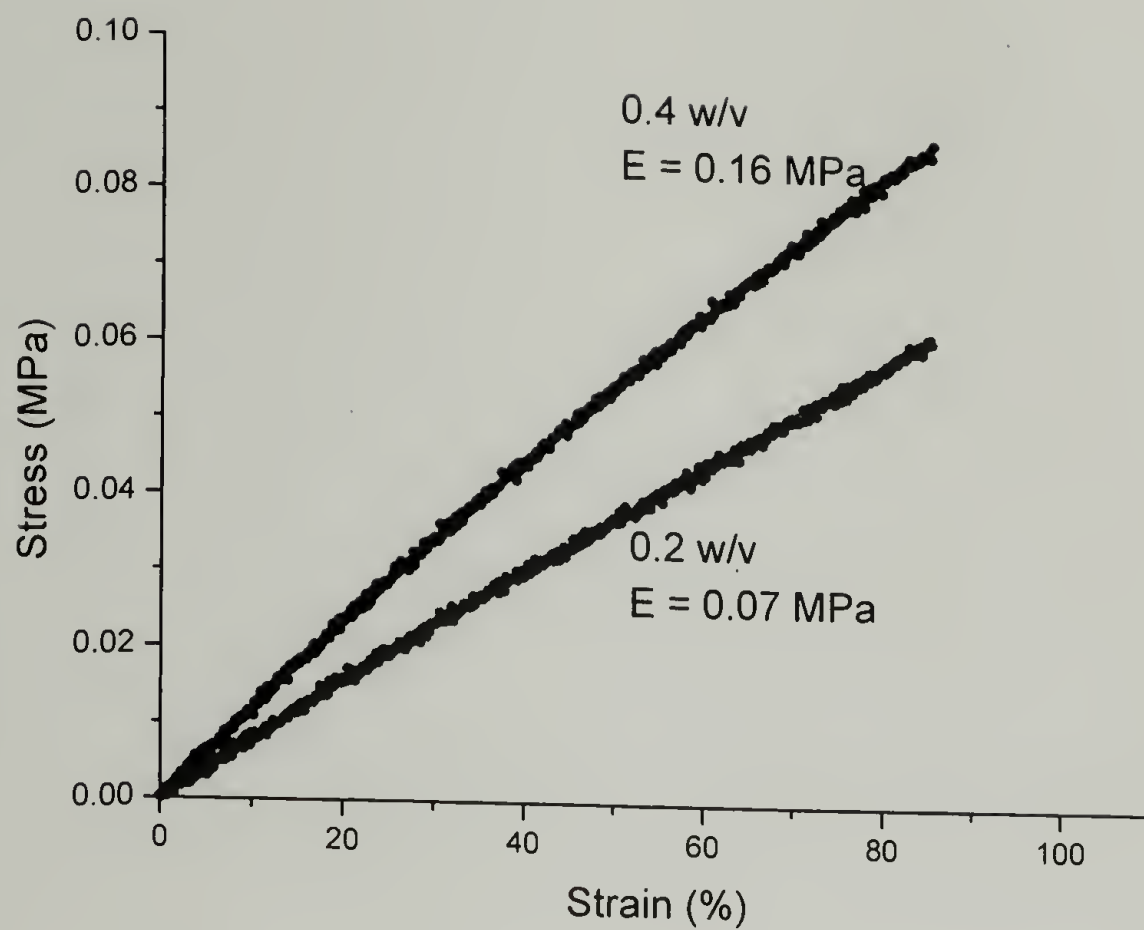


Figure 4.7 Stress-strain behavior of CS1 protein films crosslinked by Method I at 0.2 w/v and 0.4 w/v concentrations.

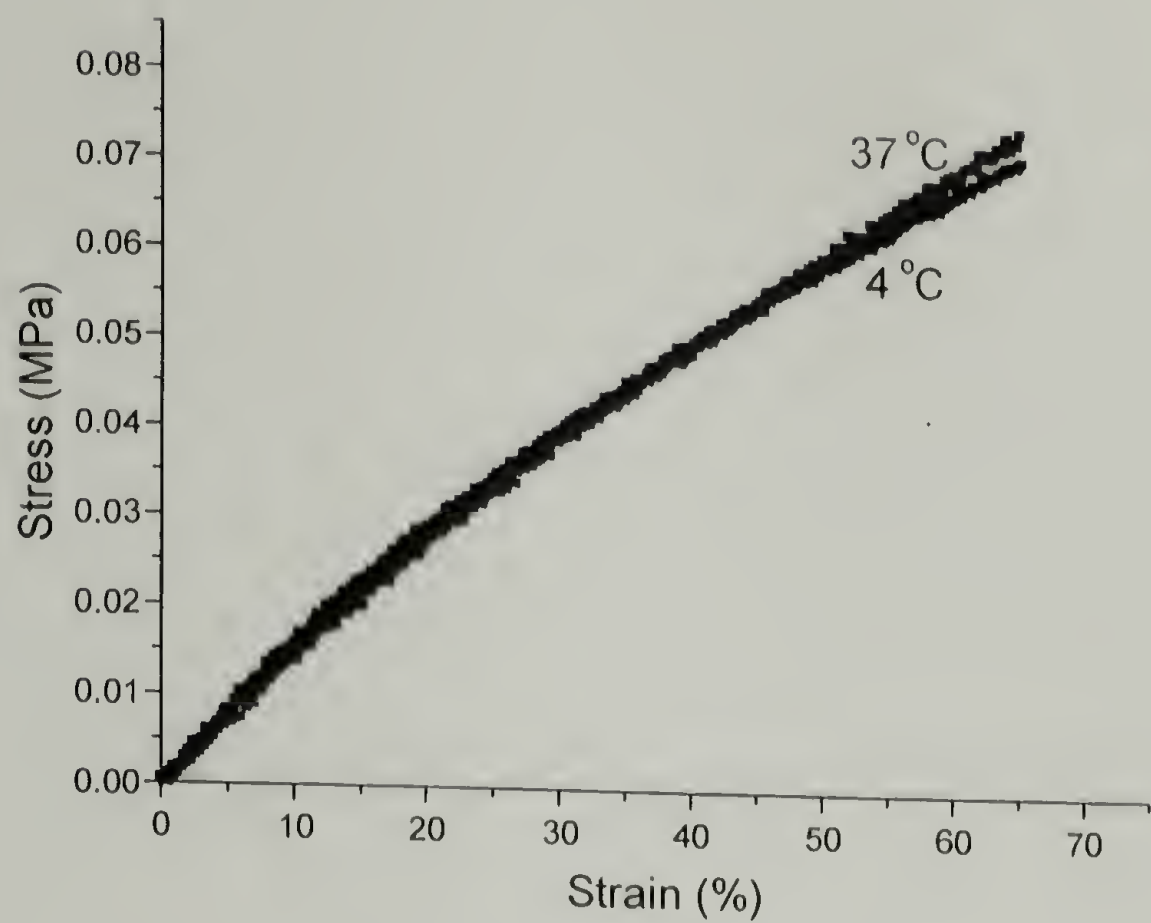


Figure 4.8 Stress-strain behavior of CS1 protein films crosslinked by Method I at 4 °C and 37 °C.

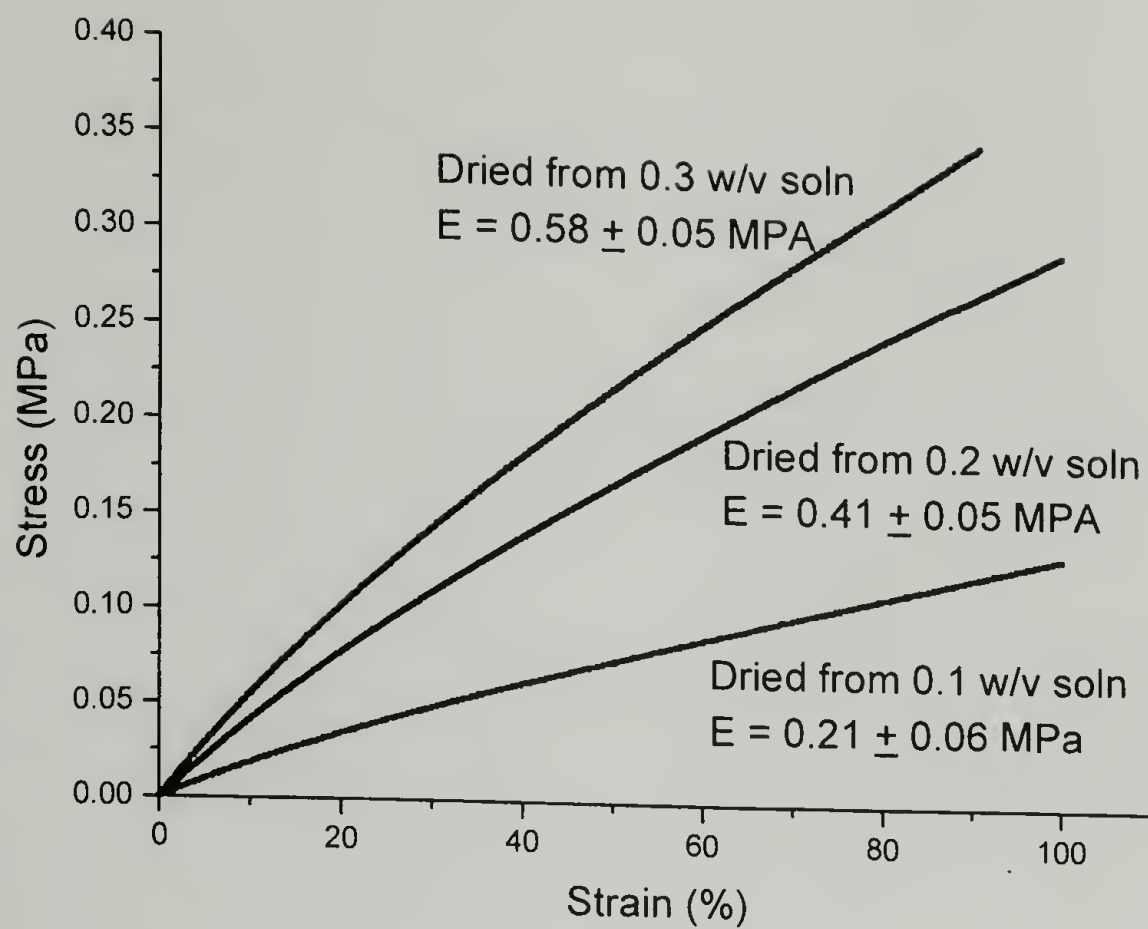


Figure 4.9 Stress-strain behavior of CS1 protein films crosslinked by Method III at 0.1, 0.2, and 0.3 w/v protein concentrations.

4.5 References

1. Abbott, W.M. and R.P. Cambria, *Control of Physical Characteristics (Elasticity and Compliance) of Vascular Grafts*, in *Biologic and Synthetic Vascular Prostheses*, ed. J.C. Stanley. 1982, New York: Gurne and Stratton. 189-220.
2. Fung, Y.C., *Biomechanics: Mechanical Properties of Living Tissues*. Second ed. 1993, New York, NY: Springer-Verlag New York, Inc.
3. Gosline, J.M. and J. Rosenbloom, *Elastin*, in *Extracellular Matrix Biochemistry*, K.A. Piez and A.H. Reddi, Editors. 1984, Elsevier Science Publishing Co.: New York, NY.
4. Winlove, C.P. and K.H. Parker, *Physiochemical properties of vascular elastin*, in *Connective Tissue Matrix : Part 2*, D.W.L. Hukins, Editor. 1990, The MacMillan Press Ltd.

CHAPTER 5

THIOLATION OF CS5 PROTEIN FOR DISULFIDE CROSSLINKING

5.1 Introduction and Objectives

By thiolating the lysines in CS5, the effect of disulfide crosslinking on the mechanical properties can be investigated. Disulfide bonding is a mechanism of crosslinking and stabilization found in native proteins [1]. A disulfide group is relatively unreactive and stable under the physiological conditions experienced by the ECM. This stability is the general basis of its biochemical function, maintaining protein structure. Proteins containing disulfide bonds are thus sufficiently stable to be found in the ECM. Many important proteins contain cysteines that function in both intra- and inter-molecular disulfide bonding [2].

By modifying the lysines to thiols after the protein is expressed and purified, the complication of purifying a cysteine rich protein is eliminated. Initially the intended design of this thesis involved incorporation of cysteine in the place of the lysines in the CS5. This strategy proved to be very difficult to implement. The protein was never successfully purified and the lysine motif was adopted as an alternative. Once the lysine is modified to a thiol, it can be disulfide bonded or reacted with maleimide derivatives for further modification. The modification reagent of choice is N-succinimidyl S-acetylthioacetate (SATA). The protected thiol moiety allows processing and deprotection without thiol reductants such as β -mercaptoethanol or dithiothreitol [3].

5.2 Experimental Section

5.2.1 Protein Thiolation

The CS5 protein (100 mg) was placed in a 4 ml vial with a small stir bar and dried overnight at 50 °C in a vacuum oven. The oven was purged with nitrogen and the vial quickly capped. Anhydrous DMSO (2 ml) was added to the vial to dissolve the protein. Approximately a five fold excess of the modifying reagent N-succinimidyl S-acetylthioacetate (SATA) (50mg) was dissolved in 1 ml anhydrous DMSO and added to the protein solution. This was stirred overnight to produce a yellowish solution. The solution was added drop-wise to 4 °C H₂O while stirring. The resulting solution was dialyzed against 4 °C H₂O for six, 4-liter H₂O changes. The dialyzed solution was centrifuged (1 hr, 4 °C, 30000g), and the supernatant frozen and finally lyophilized. The reaction scheme for the SATA modification is shown in Figure 5.1 and the modified protein is designated CS5-SATA.

5.2.2 NMR of Thiolated Protein

NMR spectra of the CS5, and CS5-SATA proteins were taken on a Varian Inova 600 MHz NMR Spectrometer in deuterated DMSO at 25 mg/ml.

5.2.3 Measuring the LCST

See Section 3.2.1.

5.2.4 Film Casting

Films were cast using Method IV as shown in Figure 5.2. Protein (45 mg) was dissolved in DMSO at 300 mg/ml and put into a teflon mold. The film was dried overnight at 60 °C. The dried film was immersed in 10 ml of 25 °C deacetylation solution (50 mM sodium phosphate, 25 mM EDTA, 0.5 M hydroxylamine HCl, pH 7.5) and mildly agitated for 12 hr. The film was transferred to 20 ml cold PBS twice for 1 hr to rinse the film.

5.2.5 Film Characterization

5.2.5.1 Reduction of Disulfides

The disulfide crosslinked film (20 mg) was immersed in 10 ml 4 M urea and 10% β -mercaptoethanol for 5 min at 25 °C.

5.2.5.2 Weight Fraction Protein

See Section 3.3.4.1.

5.2.5.3 Residual Lysine Content

See Section 3.3.3.2.

5.2.6 Mechanical Testing

See Section 3.2.5.

5.3 Results and Discussion

5.3.1 Protein Thiolation

The protein was reacted with SATA to produce a protected thiol. This allowed processing of the protein into films or tubes prior to disulfide bonding. Once the processing was complete, the thiol could be deacetylated to liberate the free thiol and allow disulfide bonding to occur spontaneously.

5.3.2 NMR Analysis of Thiolated Protein

The NMR spectra of SATA, CS5, and CS5-SATA are shown in Figure 5.3. By using the known shifts for isoleucine in this type of protein [4] and the fact that there are

54 isoleucines to each lysine, it can be determined that the CS5 is approximately 50 - 60 % modified under the conditions used here.

5.3.3 LCST Behavior

Modification of the protein drastically changes the concentration dependent behavior of the LCST. The LCST behavior of SATA-CS5 is shown in Figure 5.5. The LCST of the 10 mg/ml CS5-SATA is similar to the LCST of the 10 mg/ml CS5 showing an onset at 27 °C. The onset of the LCST drops to 20 °C and 7 °C as the concentration of the CS5-SATA is increased to 20 mg/ml and 30 mg/ml, respectively. This is very different than the LCST of the CS5 that only varies down to 26 °C with the same increase in concentration. It is possible the stability of the protecting group is compromised under these conditions and disulfide bonding occurs, an effect that is enhanced with increasing concentration. This is supported by the fact that the protein becomes increasingly difficult to rinse from the test cell without a denaturant and reducing agent.

5.3.4 Film Casting

The modified protein dissolves readily in DMSO to form a thick, amber solution. The film dries clear and remains clear after immersion in the 25 °C deacetylation solution. This indicates disulfides form spontaneously after deacetylation since the

protein does not appear to go through an LCST after immersion. If the film is not completely dry of the DMSO, the disulfides do not seem to form immediately, or the concentration is not high enough, and the film turns opaque.

5.3.5 Film Characterization

5.3.5.1 Reduction of Disulfides

When immersed in a solution of 4 M urea or DMSO, the disulfide crosslinked films remain stable, swelling relative to the solvent as would be expected of a crosslinked matrix. If the film is immersed in a solution of 4 M urea and 10 % β -mercaptoethanol it completely dissolves within minutes.

5.3.5.2 Weight Fraction Protein

The protein weight fraction in the hydrated films is 33 % and is shown in Table 5.1. This is similar to the weight fraction protein in the higher crosslinked CS5 films.

5.3.5.3 Residual Lysine Content

The percentage of reacted lysines is shown in Table 5.1. Approximately 90 % of the lysines are reacted with SATA. This assay is not consistent with the NMR data, which showed 50 - 60 % reaction with the SATA.

5.3.6 Mechanical Properties and Theoretical Me

The mechanical properties of the CS5-SATA films are tabulated in Table 5.2. Treatment of the mechanical data is described in Section 3.3.4.1.

The stress-strain behavior of a disulfide crosslinked film is shown in Figure 5.7. Figure 5.8 shows the determination of G , and Figure 5.9 shows the determination of E . The tensile modulus is indeed one third of the shear modulus agreeing well with theory and yielding an average tensile modulus of 0.46 MPa. Films made from the thiolated protein have a Young's modulus that lies within the range reported for native elastin and in the higher range given for crosslinked CS5 protein films. The shear modulus was determined using up to 25 % strain since the curve of the stress vs. $\lambda - 1/\lambda^2$ became nonlinear at higher strains.

The shape of the stress-strain curve is typical of nonlinear viscoelastic behavior of reinforced nonhomogeneous elastomers. The Payne effect describes a strain-dependent contribution to the modulus based on an agglomeration-deagglomeration mechanism between aggregates within a filler network [5]; at high strain amplitude, the stress plateaus, or there is a decrease in modulus. Since the films are completely clear and homogeneous in appearance, this may indicate an effect from disulfide exchange.

The M_c for the crosslinked thiolated protein is 6000 g/mol, which is similar to that reported for natural elastin, and the results for the CS5 films crosslinked by Method II.

5.4 Conclusions and Summary

Disulfide crosslinking of thiolated protein produces coherent, stable films.

Mechanical testing of the films yields moduli and M_c in the range reported for native elastin. The NMR analysis shows 50 - 60 % thiolation and a M_c of 6000 g/mol. This M_c agrees with a 50-60 % modification since the M_c would be 2500 for a film with 100 % modification and crosslinking. The shape of the stress-strain curve is unusual for a homogeneous material, indicating possible effects of disulfide exchange.

Sample	Deacetylation Time	Wt. Fraction Protein	Mc x1000 (g/mol)	NMR-Reacted Lysines(%)	SDTB-Reacted Lysines(%)
SATA Modified Protein	12 hr	32.5 ± 4.3	6	50 - 60	90.9 ± 2.5
Elastin			6 - 7 ^a		

^a Reference [6].

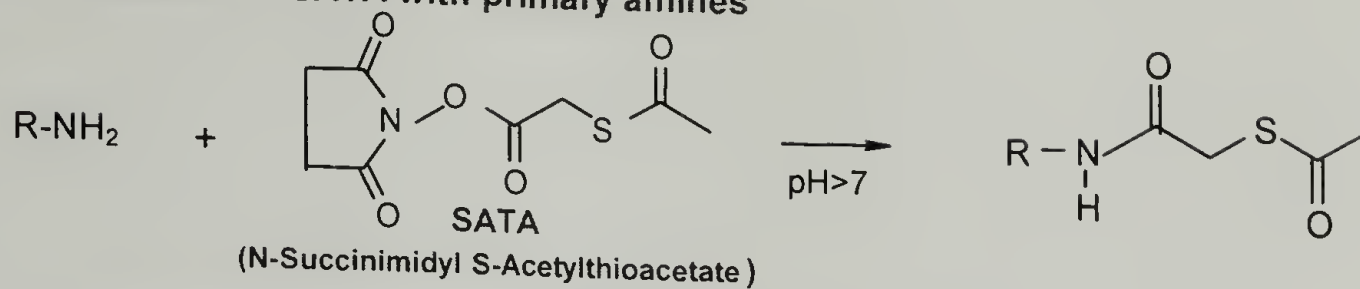
Table 5.1 Physical properties of disulfide crosslinked CS5-SATA protein films.

Sample	# Sample Determinants	Tensile Modulus E (MPa)	Shear Modulus G(MPa)
SATA Modified Protein	3	0.46 ± 0.03	0.15 ± 0.01
Elastin		$0.30 - 0.60^a$	

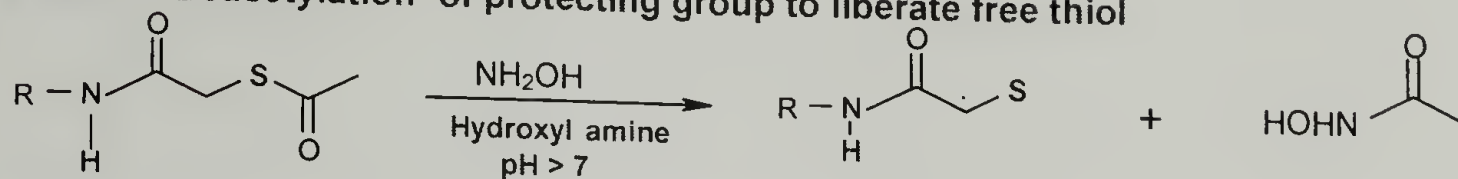
^a Reference [6-8].

Table 5.2 Mechanical properties of disulfide crosslinked CS5-SATA protein films.

STEP 1: Reaction of SATA with primary amines



STEP 2: Deacetylation of protecting group to liberate free thiol



STEP 3: Spontaneous formation of disulfide crosslinked matrix

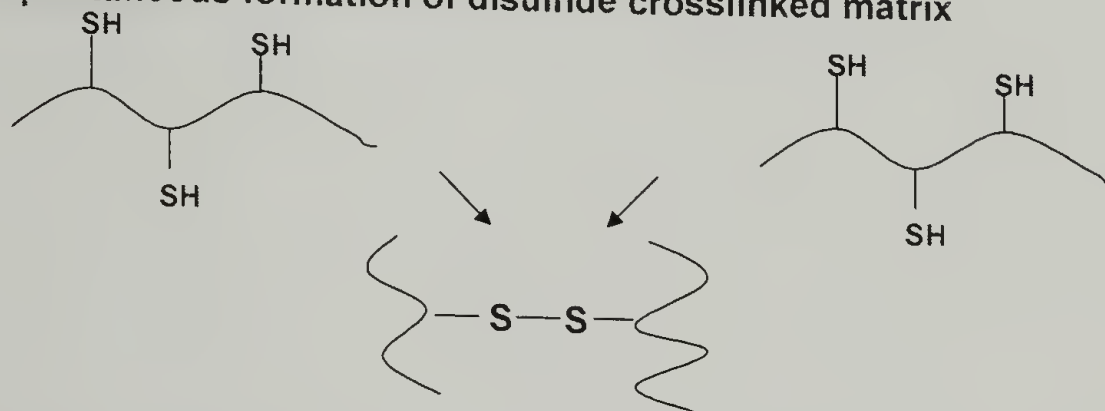


Figure 5.1 SATA-modification reaction scheme for the thiolation of CS5 protein.

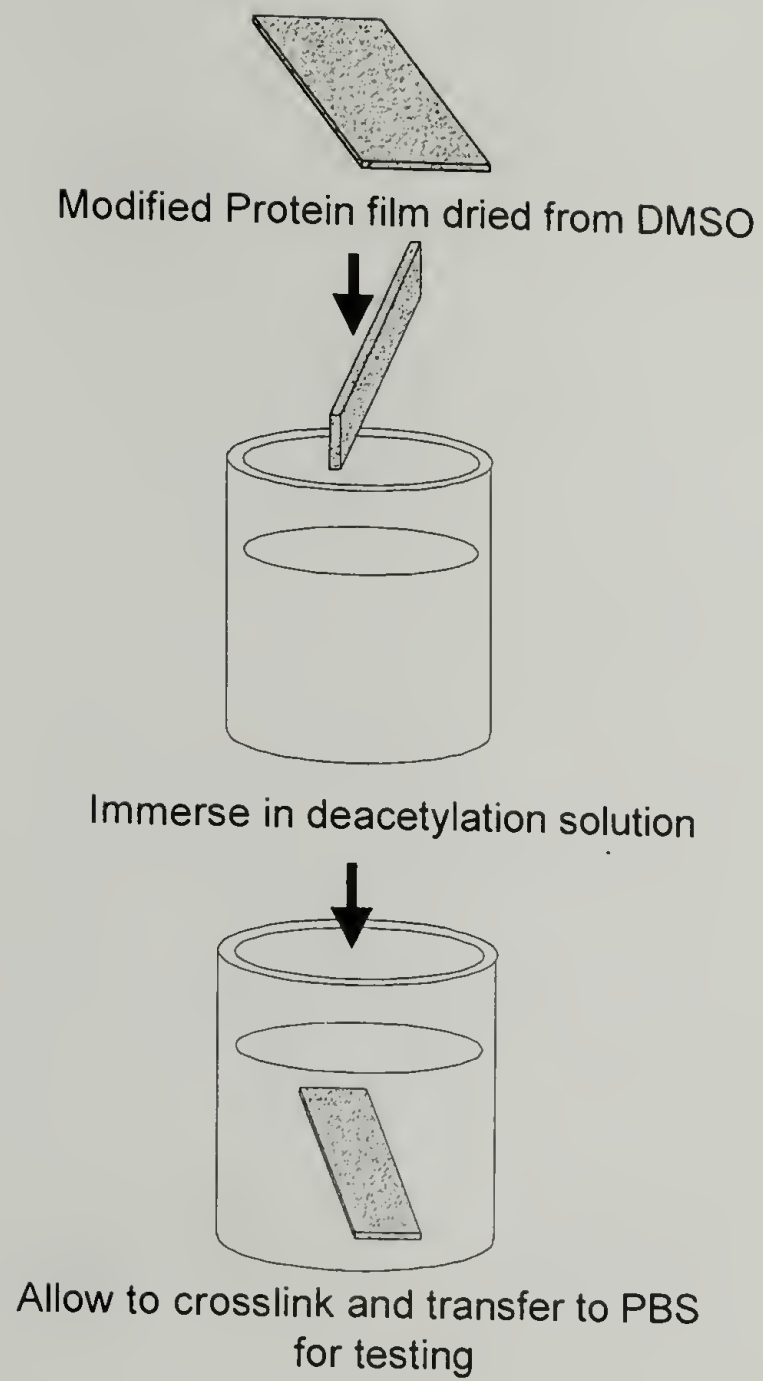


Figure 5.2 Film casting by Method IV.

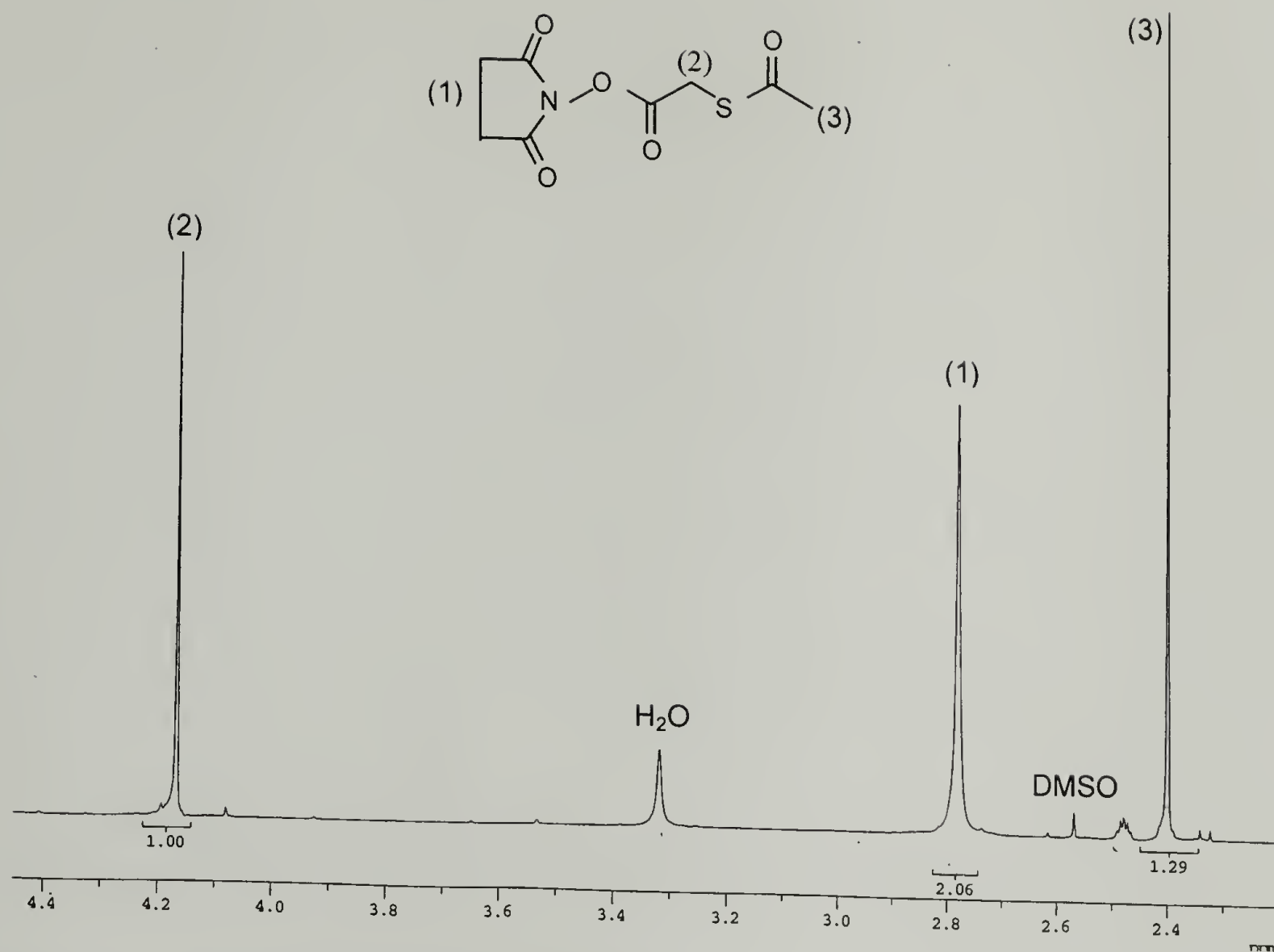


Figure 5.3 NMR spectrum of SATA.

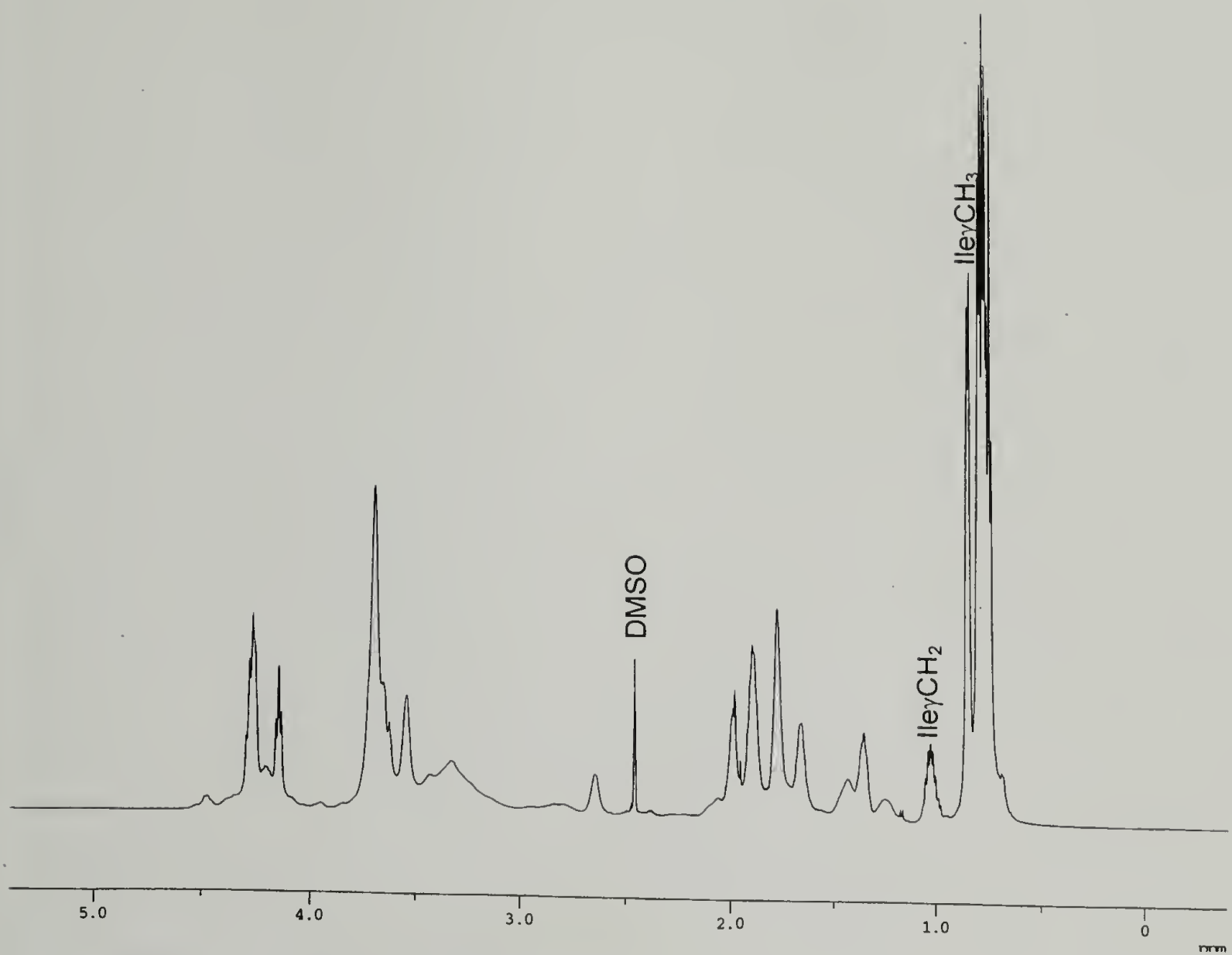


Figure 5.4 NMR spectrum of CS5.

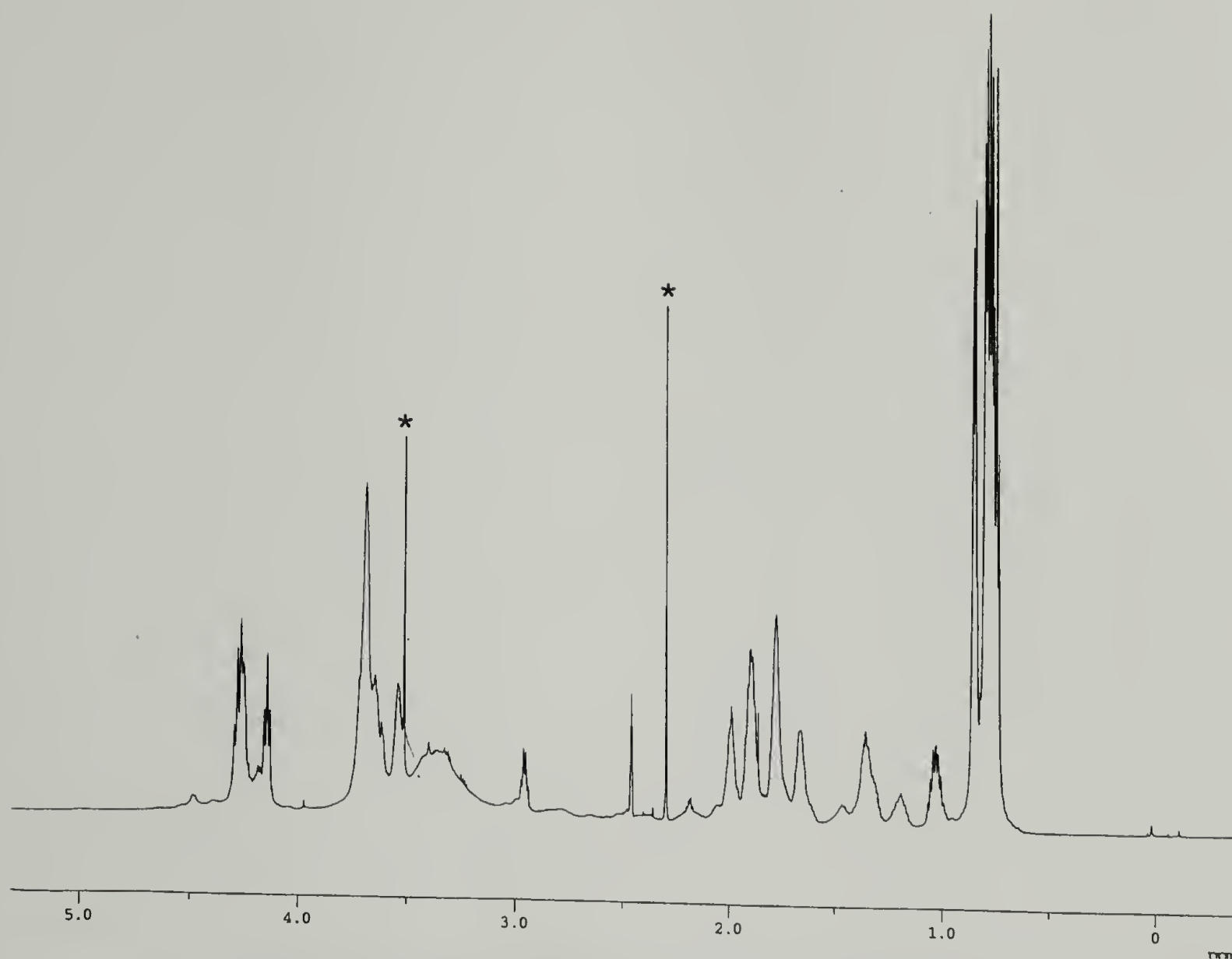


Figure 5.5 NMR spectrum of CS5-SATA. SATA-derived signals are labeled with asterisks.

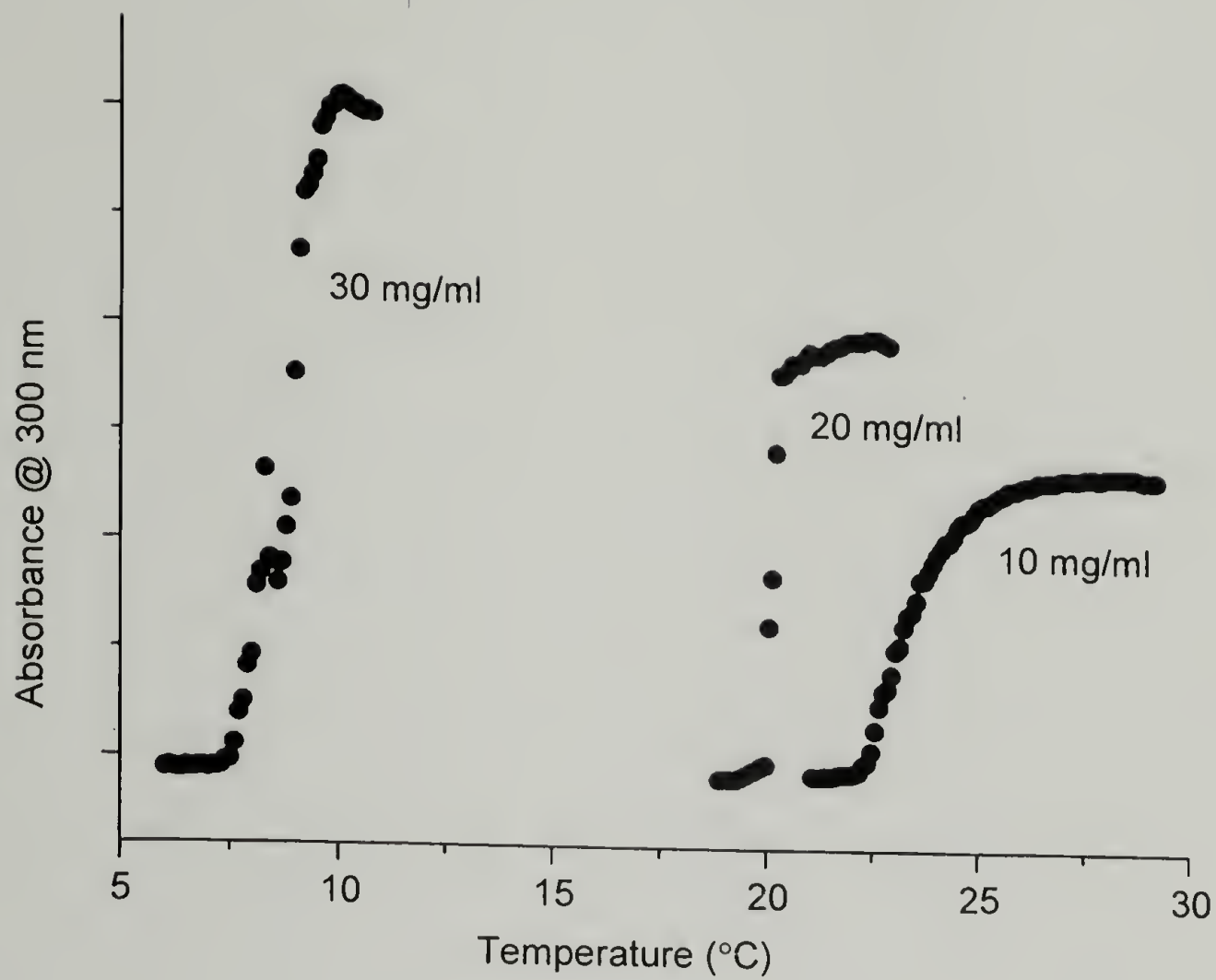


Figure 5.6 LCST behavior of CS5-SATA protein at 10, 20, and 30 mg/ml concentrations.

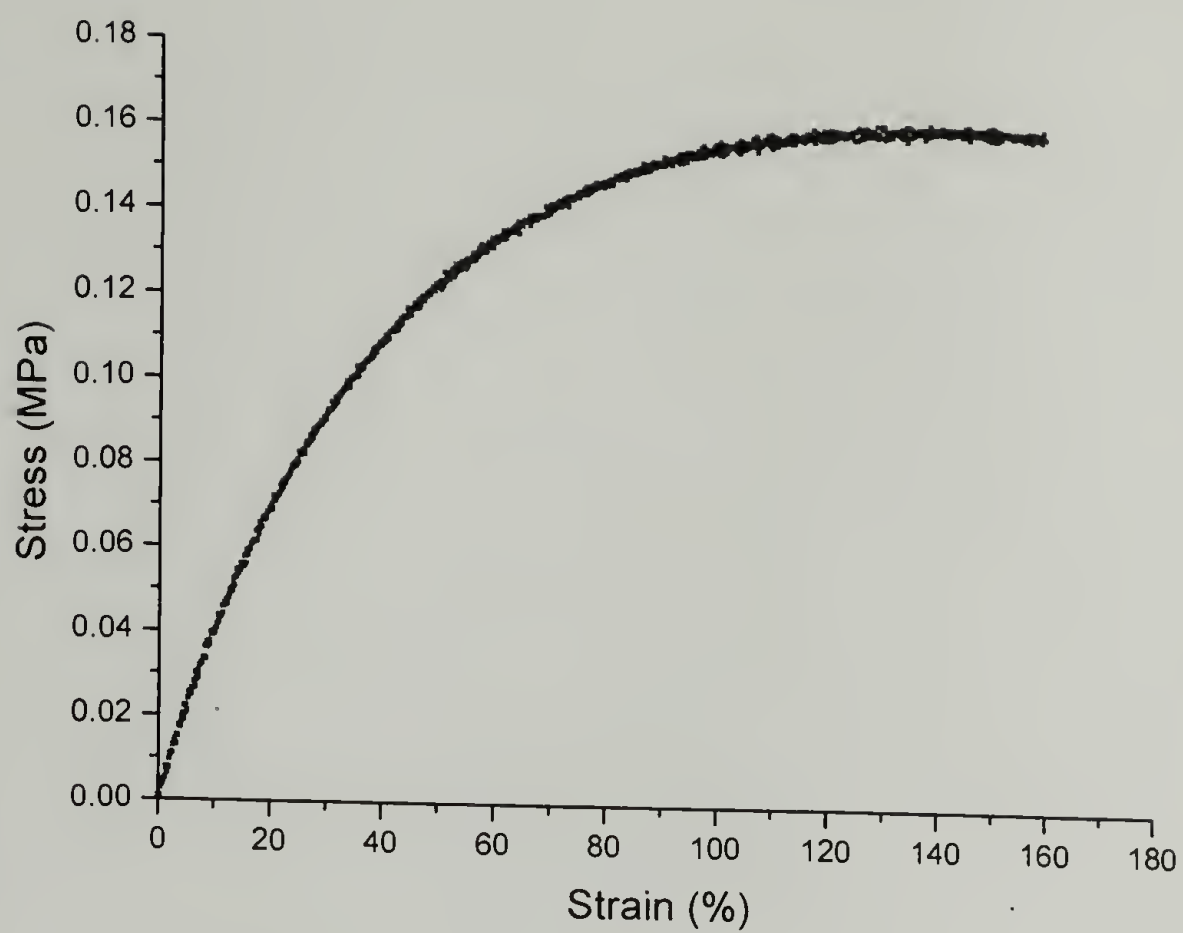


Figure 5.7 Stress-strain behavior of disulfide crosslinked CS5-SATA protein films.

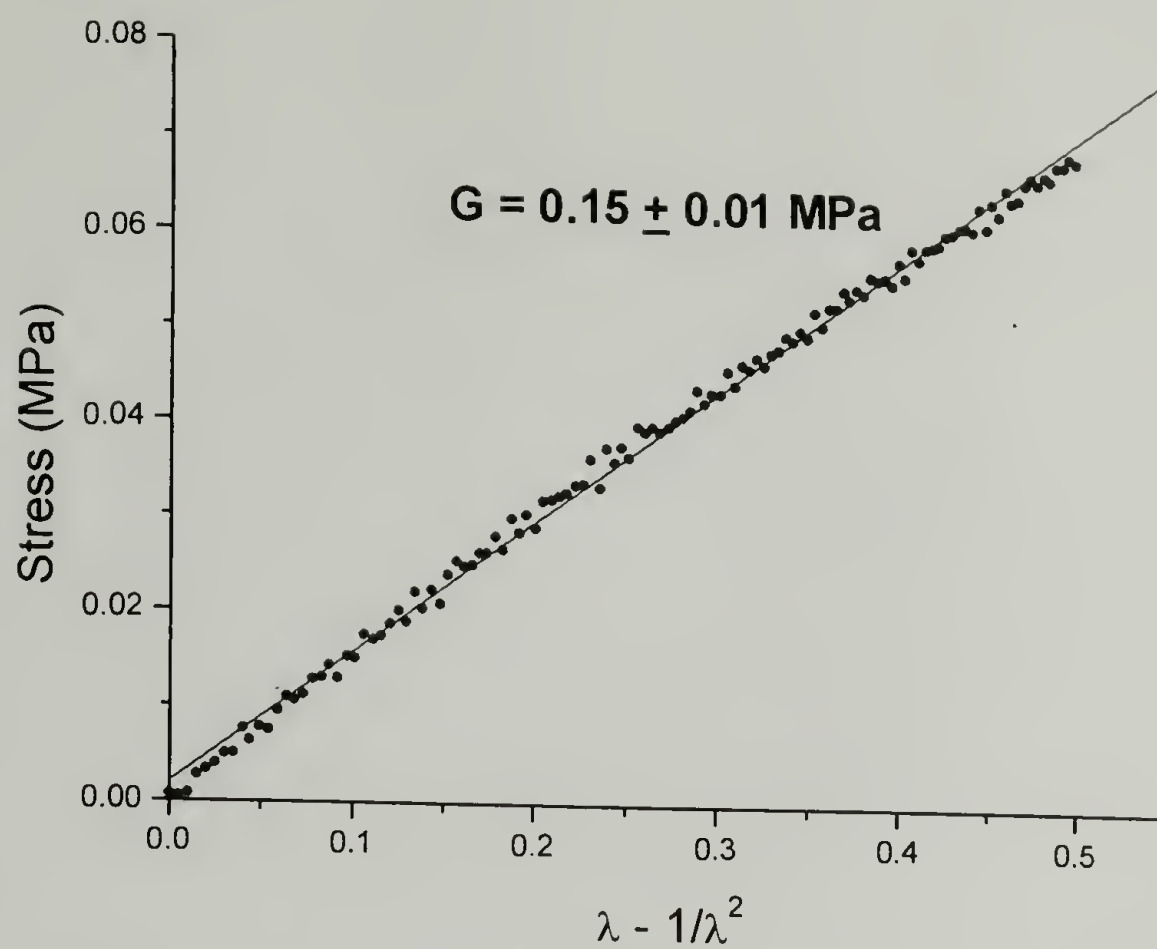


Figure 5.8 Determination of shear modulus, G , of disulfide crosslinked CS5-SATA protein films.

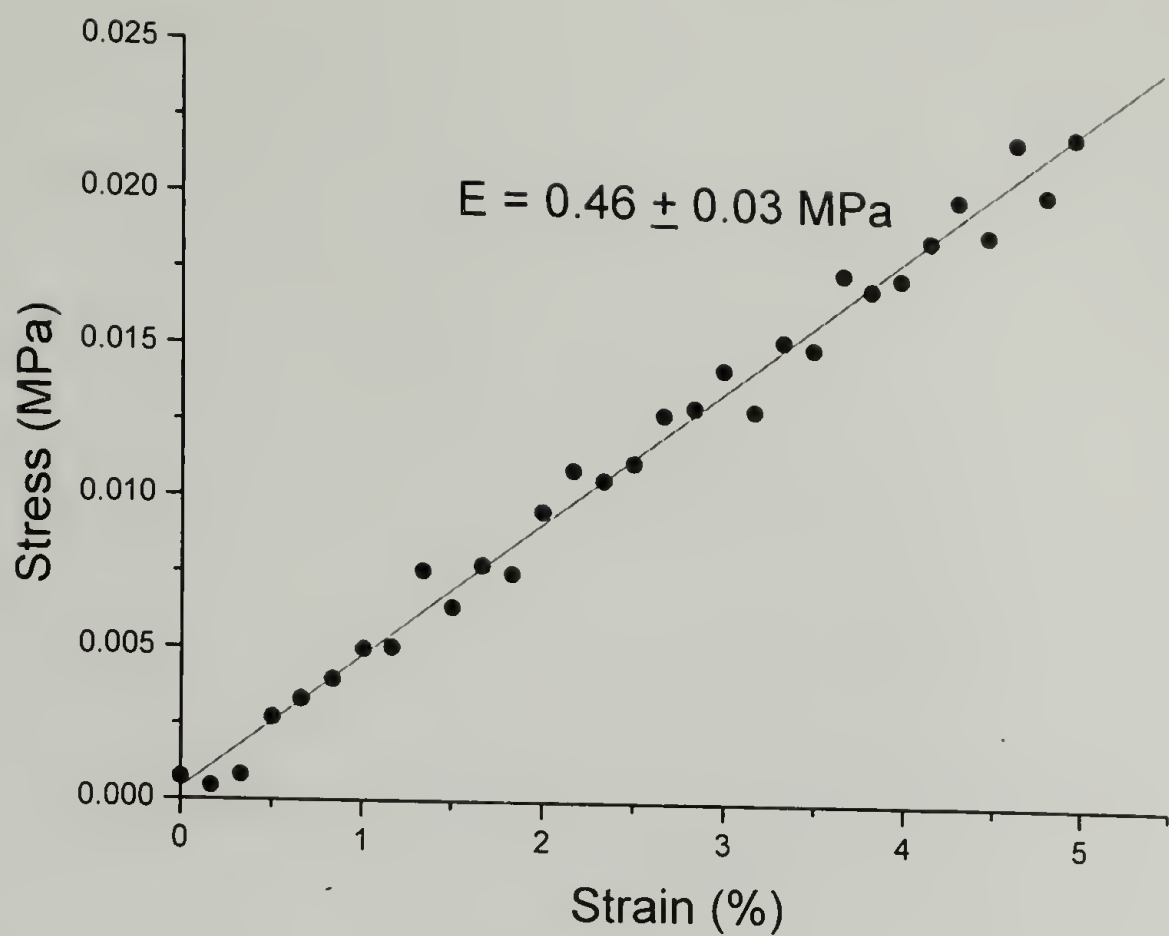


Figure 5.9 Determination of the tensile or Young's modulus, E , of CS5-SATA protein films.

5.5 References

1. Richardson, J.S. *Advances in Protein Chemistry*. Vol. 34. 1981, New York: Academic Press. 167-339.
2. Konig, W. and R. Geiger. *Perspectives in Peptide Chemistry*, ed. A. Eberle, R. Geiger, and T. Weiland. 1981: S Karger. 31-44.
3. Duncan, R., P. Weston, and R. Wrigglesworth, *A new reagent which may be used to introduce sulfhydryl groups into proteins, and its use in the preparation of conjugates for immunoassay*. *Anal. Biochem.*, 1983. **132**(1): p. 68-73.
4. Welsh, E.R. and D.A. Tirrell, *Engineering the Extracellular Matrix: A Novel Approach to Polymeric Biomaterials. I. Control of the Physical Properties of Artificial Protein Matrices Designed to Support Adhesion of Vascular Endothelial Cells*. *Biomacromolecules*, 2000. **1**(1): p. 23-30.
5. Payne, A.R., ed. *Reinforcement of Elastomers.*, ed. G. Kraus. 1965, Interscience: New York. Chapter 3.
6. Gosline, J.M. and J. Rosenbloom, *Elastin*, in *Extracellular Matrix Biochemistry*, K.A. Piez and A.H. Reddi, Editors. 1984, Elsevier Science Publishing Co.: New York, NY.
7. Abbott, W.M. and R.P. Cambria, *Control of Physical Characteristics (Elasticity and Compliance) of Vascular Grafts*, in *Biologic and Synthetic Vascular Prostheses*, ed. J.C. Stanley. 1982, New York: Gurne and Stratton. 189-220.
8. Fung, Y.C., *Biomechanics: Mechanical Properties of Living Tissues*. Second ed. 1993, New York, NY: Springer-Verlag New York, Inc.

CHAPTER 6

HUVEC ADHESION TO CS5 AND SC5 PROTEINS

6.1 Introduction and Objectives

Equally important to the mechanical properties of a vascular graft material are the biologic properties. Adhesion to the REDV sequence has been shown in the CS5 domain[1-5], but this is the first time a scrambled version of the CS5 has been used in an elastin-like protein as the negative control. The adhesion differences between the CS5 and SC5 can be attributed entirely to the scrambling of the REDV to REVD. In this study the adhesion strengths of human umbilical vein endothelial cells (HUVEC) on CS5 and SC5 proteins are investigated and compared to adhesion on fibronectin and BSA.

6.2 Experimental Section

6.2.1 Substrate Preparation

Substrates were prepared for adhesion studies by adsorbing three wells each of a 96-well plate with 75 μ l of 1 mg/ml solutions of fibronectin, CS5, and SC5 for at least 1 hr at 4 °C. The excess protein was removed and 75 μ l 1mg/ml heat inactivated Bovine

Serum Albumin (BSA) was added to the wells containing the adsorbed substrates and 3 additional wells for 30 min. The wells were rinsed with 100 μ l PBS three times and kept in PBS until use.

6.2.2 Culturing HUVEC

HUVEC (Clonetics, San Diego, CA) were used in the adhesion assays from passage two through five. The cells were grown on 100 mm tissue culture polystyrene culture dishes. The culture medium was EGM-2 (Clonetics, San Diego, CA) that contains serum and growth factors.

6.2.3 Fluorescent Labeling of HUVEC

The HUVEC were fluorescently labeled with 2', 7'-bis-(2-carboxyethyl)-5-(and-6)-carboxyfluorescein (BCECF-AM) (Molecular Probes, Inc., Eugene, Oregon). The culture medium was aspirated from the HUVEC, washed twice with 5 ml PBS, and 5 ml of PBS + 0.2 % EDTA was added to the dish. This was allowed to incubate 10 min at 25 °C before tapping the dish to detach the loosened cells and harvesting the detached cells into a centrifuge tube. The cells were centrifuged at 800 g for 5 min. The supernatant was decanted and the cell pellet was redispersed in 1 ml serum and growth factor free medium EBM-2 (Clonetics, San Diego, CA). A 10 mM stock solution of BCECF-AM was prepared in DMSO. A 2 μ l aliquot was added to the redispersed cells and allowed to incubate at 4 °C for 30 min. PBS (10 ml) was added to the cell suspension and this was

centrifuged (800 g, 5 min). This step was repeated and the resultant pellet was counted for cell number and viability in PBS containing Mg^{2+} and Ca^{2+} cations (PBS+).

6.2.4 Plating of HUVEC

HUVEC were plated at a density of 4×10^4 cells/well in PBS+ and incubated 30 min at 37 °C and 5 % CO₂ atmosphere.

6.2.5 Detachment by Centrifugation

Percoll (200 µl) (Sigma Chemical Co., St. Louis, MO) was added gently down the side of each well for three separate prepared 96-well plates after incubation with HUVEC. One plate each was centrifuged at 1 g, 1000 g, and 3000 g for 10 min. After centrifugation, the PBS+ and Percoll/PBS+ interface (includes detached cells) were wicked away with a height-adjusted 4x12 Skatron harvesting frame (Molecular Devices) leaving only a small amount of Percoll in each well. The remaining Percoll was then aspirated from the wells. PBS (100 µl) was added to each well. Plates were either read by a fluorescent plate reader at an excitation/emission of 485/535 nm or stained with Crystal Violet as follows.

6.2.6 Crystal Violet Staining of Adhered HUVEC

After centrifugation the PBS was aspirated from the wells and 100 μ l of a 70 % EtOH/H₂O solution was added to each well and incubated at 25 °C for 15 min. The EtOH solution was removed and 100 μ l of a 1 % crystal violet solution in H₂O was added to each well and incubated for 30 min. The crystal violet solution was removed and washed with 250 μ l H₂O to each well five times. A 2 % SDS solution in H₂O (100 μ l) was added to each well and allowed to solubilize for 12 hr. The plate was read for absorbance at 598 nm on a plate reader.

6.3 Results and Discussion

6.3.1 Substrate Preparation

Adsorption of the protein to the surface of a polystyrene tissue culture plate is a common method for studying the interactions of cells with different proteins [6]. The subsequent addition of heat inactivated BSA blocks nonspecific adhesion sites, allowing the study of the specific interactions of the cell with the test protein.

Fibronectin served as the positive control protein and was expected to show good HUVEC adhesion. HUVEC can adhere through several cell-binding domains within fibronectin targeting different integrins. As described in Chapter 1, the RGD can attach the $\alpha_5\beta_1$ and $\alpha_v\beta_3$ integrins whereas the CS5 and CS1 domains adhere through the $\alpha_4\beta_1$ integrin. BSA blocked polystyrene served as a negative control.

6.3.2 Fluorescent Labeling of HUVEC

The acetoxymethyl ester, BCECF-AM, is membrane permeable and nonfluorescent. As the ester is assimilated into the cell, the intracellular esterases hydrolyze the ester into a membrane impermeable, fluorescent form. For this reason, the dye only fluoresces in viable cells, ensuring metabolically inactive cells are not measured. The fluorescent derivative is pH sensitive; it is possible that downstream events from integrin binding of the cells can affect the intracellular pH. This concern instigated the use of another staining method to substantiate the fluorescence measurements.

The standard curve for labeled HUVEC is shown in Figure 6.2. It shows a linear emission dependence on concentration of cells. Calibration was done on individual experiments and day-to-day differences of absolute values of fluorescence were observed due to variations in uptake of dye. Therefore, the detachment is not expressed in cell numbers, but instead as the mean of three replicated values.

6.3.3 Detachment by Centrifugation

In order to apply a uniform, well defined, detachment force to the HUVEC the PBS+ is displaced with a denser Percoll solution and upon upright centrifugation a

buoyant force is applied to the cells. In this way, the strength of attachment can be investigated by direct centrifugation of the 96-well plate at different relative centrifugal forces [6].

The force applied to each cell can be represented by Archimedes' Theorem:

$$F = (\rho_c - \rho_m) v_c (\text{RCF}) \quad (4) [6].$$

Where ρ_c is the density of the cell, ρ_m is the density of the medium, v_c is the volume of the cell, and RCF are the relative centrifugal force. The cell to substrate adhesion strength must be greater than the applied force for the cell to remain attached. Density marker beads to produce gradients in the Percoll could be used for determining HUVEC density and a Coulter counter for determining volume. For the purposes of this study, the relative attachment forces are being investigated with respect to controls, eliminating the need for absolute numbers. However, as a reference, the density and volume of a cell can be taken from the known values for a human fibrosarcoma cell CCL 121 as 1.046 g/ml and 1.455 nl. The density of the medium (Percoll diluted in 10x PBS) is 1.123 g/ml. Using these numbers to get a general idea, the force at 1g RCF on one cell in Percoll is 0.112 μ dynes.

6.3.4 HUVEC Adhesion to CS5 and SC5 Proteins

The results are background subtracted by negative control wells with no cells added and presented as the mean of three replicated values. The experiment was repeated three times to confirm consistency. Due to variation in absolute numbers, the reported result is from one of the experiments. Table 6.1 gives the relative adhesion of the

different substrates compared to fibronectin. Figure 6.3 shows the relative fluorescence emission versus RCF for fibronectin, CS5, SC5, and BSA. HUVEC adhesion at 1 g to CS5 is similar to fibronectin whereas the adhesion to SC5 is 15 % of adhesion to fibronectin (similar to BSA). As the force is increased to 1000 g the HUVEC still show adhesion to the CS5, but the SC5 shows little or no adhesion, again similar to the BSA. The adhesion to CS5 is 66 % of the adhesion to fibronectin. At 3000 g there is significant detachment of the HUVEC to the CS5, only 23 % of the HUVEC remain compared to fibronectin. Although adhesion is lower to CS5 than to fibronectin, this is not unexpected since there are other types of cell-binding domains in fibronectin and only the REDV in CS5.

Figure 6.4 shows the experimental results of the crystal violet staining method. The trends shown in the fluorescence experiment are confirmed by this method.

The differences between adhesion on CS5 and SC5 indicate adhesion to the CS5 occurs through the REDV cell-binding domain since the only difference in sequence is the REDV scrambled to REVD.

6.4 Summary and Conclusions

HUVEC showed significantly stronger adhesion to CS5 than SC5. SC5 shows little or no HUVEC adhesion at any detachment force, similar to BSA. This result indicates HUVEC is mediated by the REDV sequence in the CS5 domain.

This study complements the results in a recently published article describing HUVEC interactions with CS5 containing elastin-like proteins [7]. It was found that the

soluble peptide GREDVDY inhibited HUVEC adhesion 97 % while no decrease in adhesion was seen with the sequence scrambled GREVDDY.

These results suggest this class of materials could be promising for application in vascular grafts. Studies of cell interactions are being continued on CS5 and SC5 as well as on CS1 and variants with different cell-binding domains.

Substrate	Relative Adhesion at RCF		
	1g	1000g	3000g
Fibronectin	1.00	1.00	1.00
CS5	1.06	0.66	0.23
SC5	0.15	0.05	0.02
BSA	0.00	0.13	0.04
No Cells	0.00	0.00	0.00

Table 6.1 HUVEC adhesion to substrates relative to fibronectin.

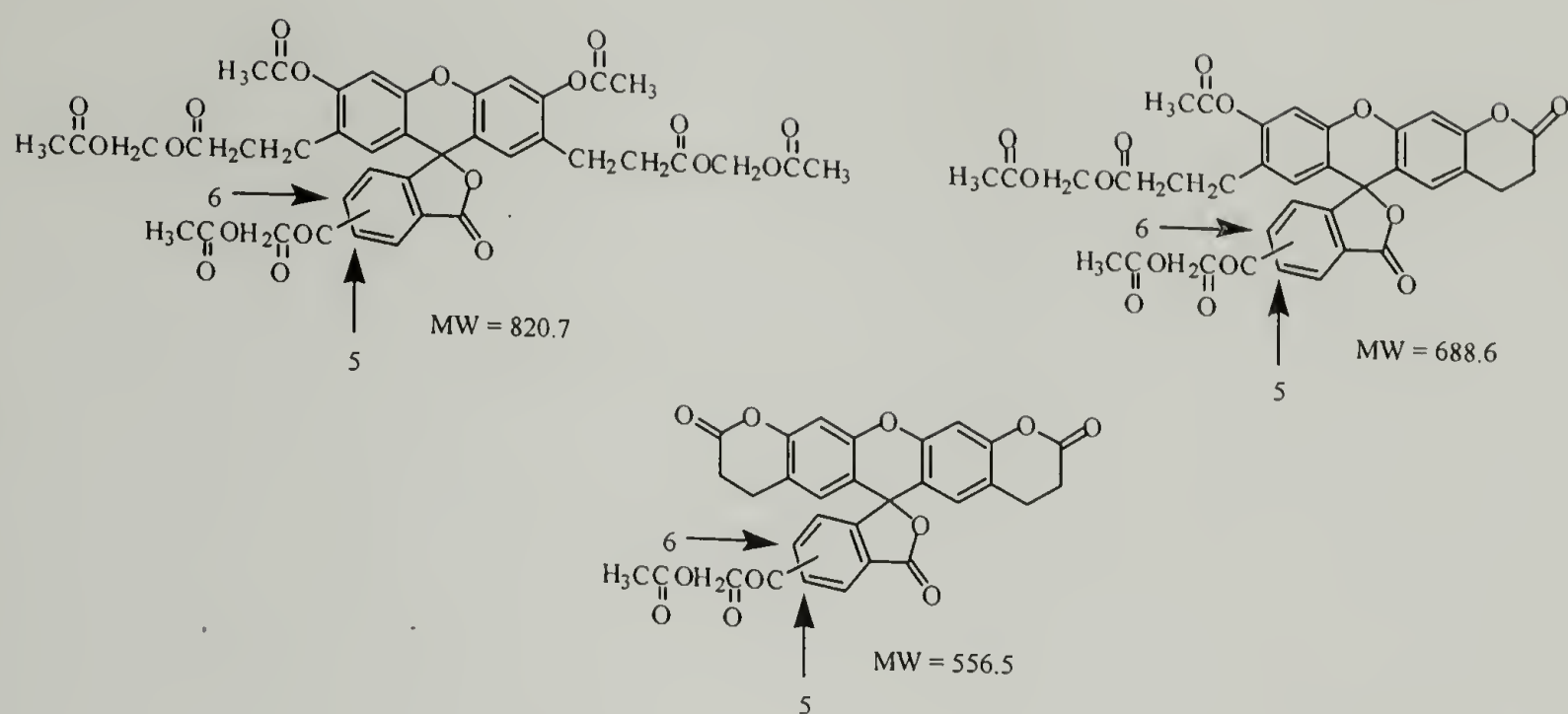


Figure 6.1 The fluorescent label BCECF-AM is a mixture of the above three molecules.

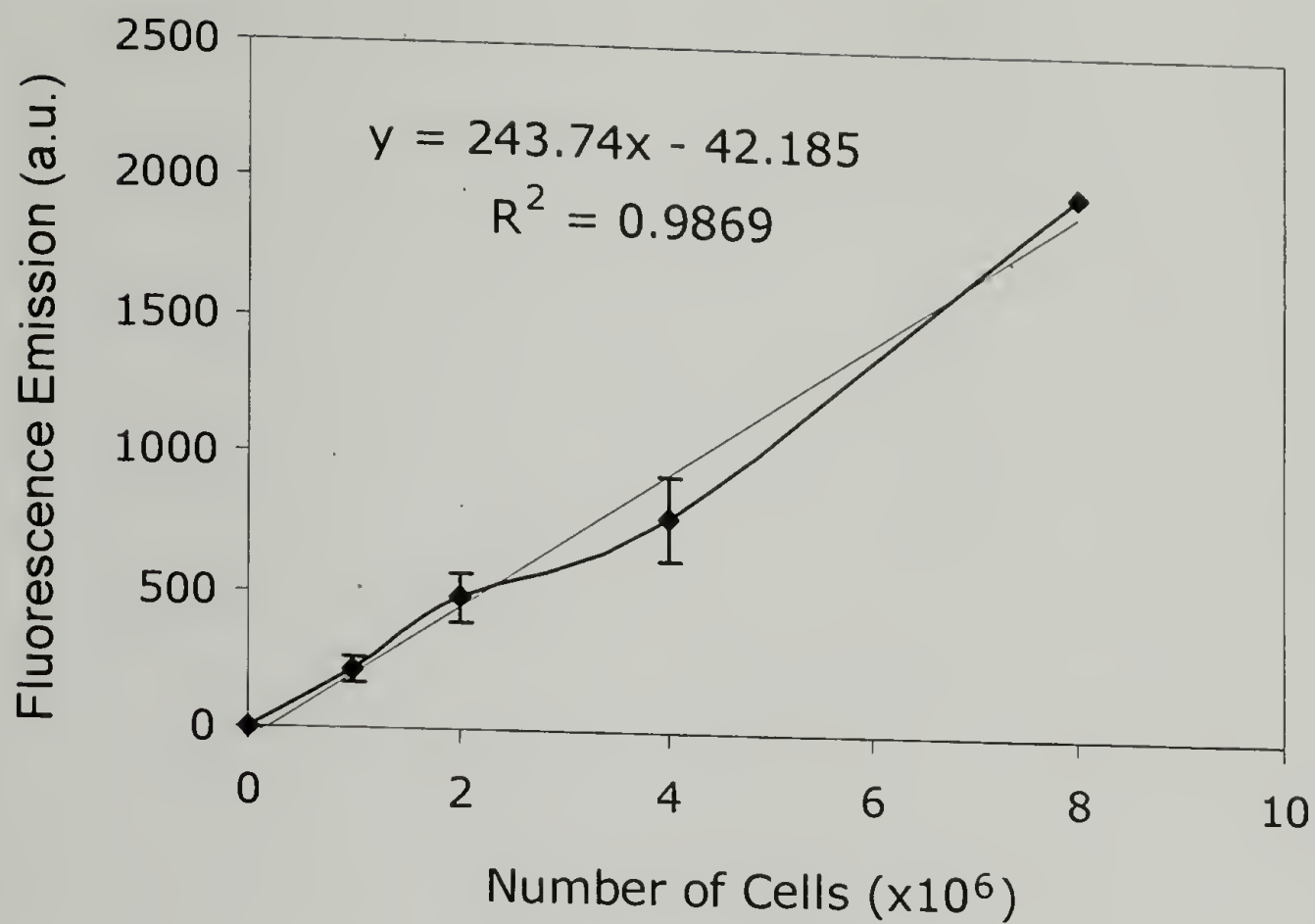


Figure 6.2 Standard curve for the labeled HUVEC showing linear dependence of fluorescence emission at 535 nm with number of cells.

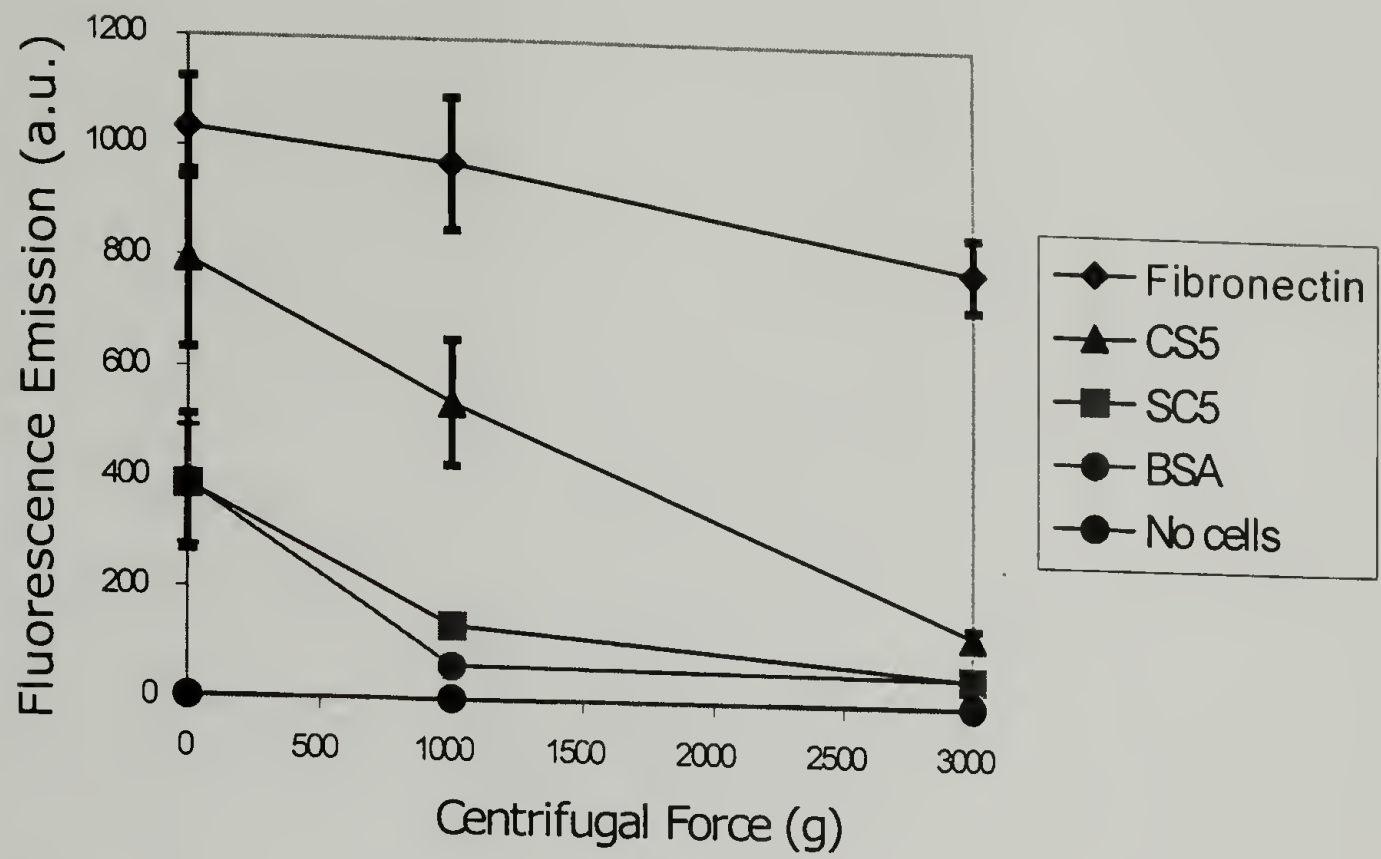


Figure 6.3 HUVEC adhesion, measured in fluorescence, to CS5 and SC5 relative to fibronectin and BSA.

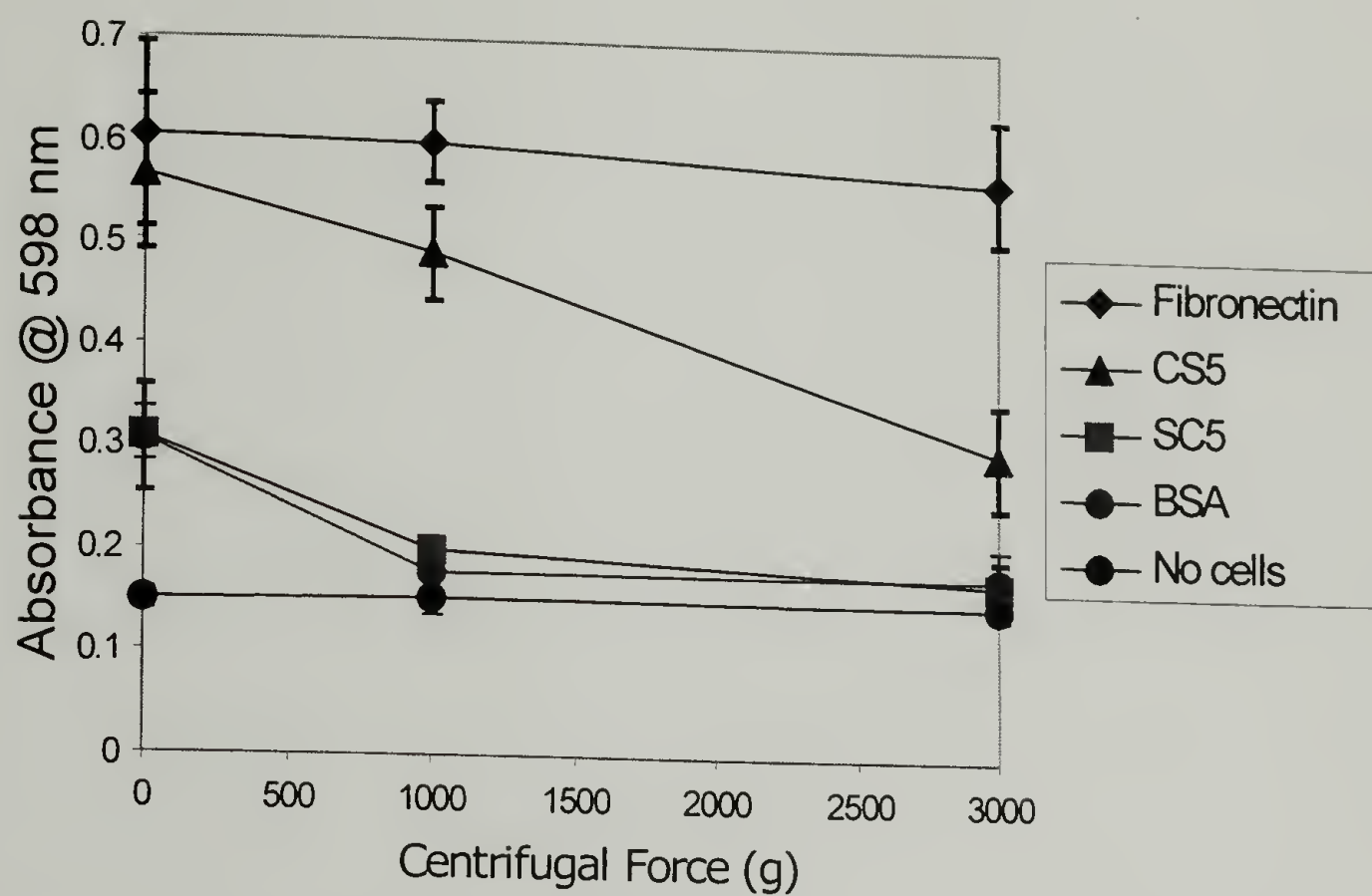


Figure 6.4 HUVEC adhesion, measured by crystal violet staining, to CS5 and SC5 relative to fibronectin and BSA.

6.4 References

1. Petka, W., et al., *Reversible hydrogels from self-assembling artificial proteins*. Science, 1998. **281**(5375): p. 389-392.
2. Mould, A.P. and M.J. Humphries, *Identification of a Novel Recognition Sequence for the Integrin $\alpha_4\beta_1$ in the COOH-terminal Heparin-Binding Domain of Fibronectin*. EMBO J., 1991. **10**(13): p. 4089-4095.
3. Mould, A.P., et al., *The CS5 Peptide is a Second Site in the IIICS Region of Fibronectin Recognized by the Integrin $\alpha_4\beta_1$: Inhibition of $\alpha_4\beta_1$ Function by RGD Peptide Homologues*. J. Biol. Chem., 1991. **266**(6): p. 3579-3585.
4. Massia, S.P. and J.P. Hubbell, *Vascular Endothelial Cell Adhesion and Spreading Promoted by the Peptide REDV of the IIICS Region of Plasma Fibronectin is Mediated by Integrin $\alpha_4\beta_1$* . J. Biol. Chem., 1992. **267**(20): p. 14019-14026.
5. Panitch, A., et al., *Design and Biosynthesis of Elastin-like Artificial Extracellular Matrix Proteins Containing Periodically Spaced Fibronectin CS5 Domains*. Macromolecules, 1999. **32**(5): p. 1701-1703.
6. Channavajjala, L., A. Eidsath, and W. Saxinger, *A Simple Method for Measurement of Cell-substrate Attachment Forces: Application to HIV-1 Tat*. Journal of Cell Science, 1997. **110**: p. 249-256.
7. Heilshorn, S., et al., *Endothelial Cell Adhesion to the Fibronectin CS5 Domain in Artificial Extracellular Matrix Proteins*. FASEB, 2002. **Submitted**.

CHAPTER 7

FUTURE RESEARCH DIRECTIONS

7.1 Mechanical and Biological Considerations

Sufficient tear resistance is an essential property for a vascular graft material. The material would generally need to be sutured into place and potentially need to resist failure if injured. The crosslinked artificial ECM (aECM) proteins described here have very low tear resistance. The materials are amorphous with nothing to inhibit crack propagation. The films crosslinked above the LCST show slightly better tear resistance as might be expected from an inhomogeneous sample but still much too low for suturability.

It is possible the protein could be crosslinked around a woven mesh or fabric that would serve to stop crack propagation. This could be used in the form of a complete graft or as a cuff. Increasing the crosslink density at the ends of the graft would toughen the material but also cause a compliance mismatch with the native vessel. The creation of suturing eyelets could circumvent this issue, but could be too tedious to be reasonable.

Fillers could improve the tear resistance. Such possibilities would include the hydrolysis of tetraethoxysilane (TEOS) to precipitate very small, well-dispersed particles into a crosslinked film [1].

Tear resistance is another major obstacle to overcome before these aECM protein materials can be used for testing as a vascular graft material.

Adhesion of HUVEC as well as other cell types such as smooth muscle cells, fibroblasts, platelets and leukocytes will need to be studied further to elucidate the interactions of these cells with the aECM protein. Alternative cell-binding domains have already been incorporated in similar aECM proteins and are being studied. In addition, growth factors and heparin-binding domains should be considered. It is possible that a combination of these different types of domains would serve as a better vascular graft.

7.2 References

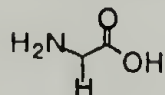
1. Mark, J. and B. Erman, *Filled Elastomers*, in *Rubberlike Elasticity: A Molecular Primer*. 1988, John Wiley and Sons: New York.

APPENDIX

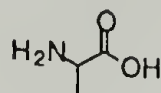
LIST OF AMINO ACIDS

ALIPHATIC

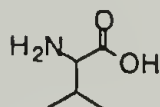
Glycine (Gly G)



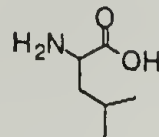
Alanine (Ala A)



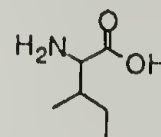
Valine (Val V)



Leucine (Leu L)

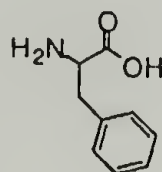


Isoleucine (Ile I)

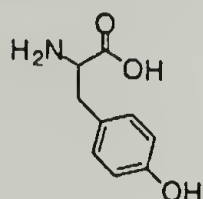


AROMATIC

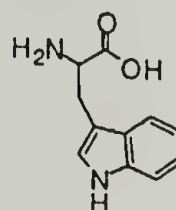
Phenylalanine (Phe F)



Tyrosine (Tyr Y)

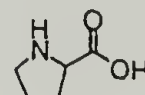


Tryptophan (Trp W)



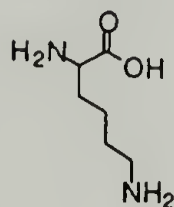
CYCLIC

Proline (Pro P)

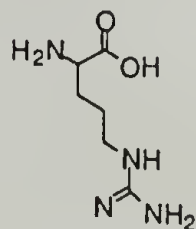


BASIC

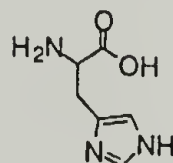
Lysine (Lys K)



Arginine (Arg R)

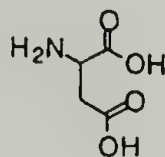


Histidine (His H)

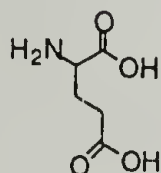


ACIDIC

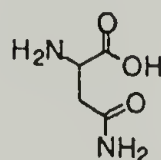
Aspartic Acid (Asp D)



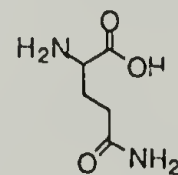
Glutamic Acid (Glu E)



Asparagine (Asn N)

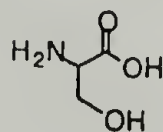


Glutamine (Gln Q)

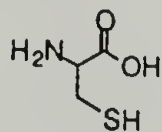


HYDROXYL OR SULFUR CONTAINING

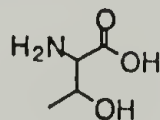
Serine (Ser S)



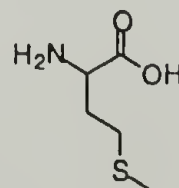
Cysteine (Cys C)



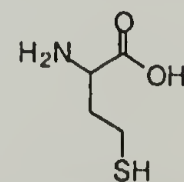
Threonine (Thr T)



Methionine (Met M)



Homocysteine (Hcy)



Precursor to
methionine

BIBLIOGRAPHY

1. SIGMA Chemical Co. Catalog. 1998. p. 708.
2. Abbott, W.M. and R.P. Cambria, Control of Physical Characteristics (Elasticity and Compliance) of Vascular Grafts, in *Biologic and Synthetic Vascular Prostheses*, ed. J.C. Stanley. 1982, New York: Gurne and Stratton. 189-220.
3. Abbott, W.M. and J.J. Vignati, Prosthetic Grafts: When are They a Reasonable Alternative? *Seminars in Vascular Surgery*, 1995. 8(3): p. 236-245.
4. Aklonis, J.J. and W.J. MacKnight, *Introduction to Polymer Viscoelasticity*. 1983: John Wiley & Sons.
5. Ayad, S., et al., *The Extracellular Matrix Factsbook*. FactsBook Series. 1994, San Diego: Academic Press Inc.
6. Bain, C.D., et al., Formation of monolayer films by the spontaneous assembly of organic thiols from solution onto gold. *J. Am. Chem. Soc.*, 1989. 111(1): p. 321-335.
7. Bergel, D., The Dynamic Elastic Properties of the Arterial Wall. *Journal of Physiol.*, 1961. 156: p. 458-469.
8. Bevilacqua, M.P., et al., Recombinant Tumor Necrosis Factor Induces Procoagulant Activity in Cultured Human Vascular Endothelium: Characterization and comparison with the Actions of Interleukin I. *Proc. Nat. Acad. Sci. USA*, 1986. 83: p. 4533.
9. Bos, G., et al., Small-diameter vascular graft prostheses: current status. *Archives of Physiology and Biochemistry*, 1998. 106(2): p. 100-115.
10. Carey, D.J., Control of Growth and Differentiation of Vascular Cells by Extracellular Matrix Proteins. *Ann. Rev. Physiol.*, 1991. 53: p. 161-177.
11. Chandran, K.B., *Cardiovascular Biomechanics*. New York University Biomedical Engineering Series, ed. W. Welkowitz. 1992, New York: University Press. 539.
12. Channavajjala, L., A. Eidsath, and W. Saxinger, A Simple Method for Measurement of Cell-substrate Attachment Forces: Application to HIV-1 Tat. *Journal of Cell Science*, 1997. 110. p. 249-256.
13. Charonis, A.S., et al., A Novel Synthetic Peptide from the B1 Chain of Laminin with Heparin-Binding and Cell Adhesion-promoting Activities. *J. Cell Biol.*, 1988. 107: p. 1253- 1260.

14. Cima, L.G., Polymer substrates for controlled biological Interactions. *J. Cell. Biochem.*, 1994. 56: p. 155-161.
15. Clowes, A.W., M.A. Reidy, and M.M. Clowes, Kinetics of Cellular Proliferation After Arterial Injury: Smooth Muscle Cell Growth in Absence of Endothelium. *Lab. Invest.*, 1983. 49(3): p. 327-333.
16. Clowes, A.W., R.D. Kirkman, and M.A. Reidy, Mechanism of Arterial Graft Healing: Rapid Transmural Capillary Ingrowth Provides a Source of Intimal Endothelium and Smooth Muscle in Porous PTFE Prostheses. *Am. J. Path.*, 1986. 123: p. 220-230.
17. Clowes, A.W. and M.A. Reidy, Prevention of Stenosis After Vascular Reconstruction: Pharmacological Control of Intimal Hyperplasia- A Review. *J. Vasc. Surg.*, 1991. 13(6): p. 885-891.
18. Colucci, M., G.I. Balcon, and R. Lorenzet, Cultured Human Endothelial Cells Generate Tissue Factor in Response to Endotoxin. *J. Clin. Invest.*, 1983. 71: p. 1893.
19. Conte, M.S., The Ideal Small Arterial Substitute: A Search for the Holy Grail? *FASEB J.*, 1998. 12: p. 43-45.
20. Cox, G.W., et al., Characterization of IL-2 receptor expression and function on murine macrophages. *Journal of Immunology*, 1990. 145: p. 1719-1726.
21. Dicoletto, P.E. and D. Bowen-Pope, Cultured Endothelial Cells Produce a Platelet-Derived Growth Factor-like Protein. *Proc. Nat. Acad. Sci. USA*, 1983. 80: p. 1919-1923.
22. Drury, J.K., et al., Experimental and Clinical Experience with a Gelatin Impregnated Dacron Prosthesis. *Ann. Vasc. Surg.*, 1987. 1: p. 542-547.
23. Duncan, R. and e. al., *Anal. Biochem.*, 1983. 132: p. 68-73.
24. Ferrari, F.A. and J. Capello, Protein-Based Materials, ed. K. McGrath and D. Kaplan. 1997, Boston, MA: Birkhauser. 37.
25. Fox, P.L. and P.E. DiCorleto, Regulation of Production of a Platelet-Derived Growth Factors-like Protein in Cultured Bovine Aortic Endothelial Cells. *J. Cell Physiol.*, 1984. 121: p. 298-308.
26. Freishlag, J.A. and W.S. Moore, Clinical Experience with a Collagen-Impregnated Knitted Dacron Vascular Graft. *Ann. Vasc. Surg.*, 1990. 4: p. 449-454.

27. Fuchs, S., F. Delorenzo, and C.B. Anfinsen, Studies on the Mechanism of the Enzymic Catalysis of Disulfide Interchange in Proteins. *J. Biol. Chem.*, 1967. 242: p. 398.
28. Fung, Y.C., *Biomechanics: Mechanical Properties of Living Tissues*. Second ed. 1993, New York, NY: Springer-Verlag New York, Inc.
29. Gosline, J., Hydrophobic Interaction and a Model for the Elasticity of Elastin. *Biopolymers*, 1976. 17: p. 677-695.
30. Gosline, J. and C. French, Dynamic Mechanical Properties of Elastin. *Biopolymers*, 1979. 18: p. 2019-2103.
31. Gosline, J.M. and J. Rosenbloom, Elastin, in *Extracellular Matrix Biochemistry*, K.A. Piez and A.H. Reddi, Editors. 1984, Elsevier Science Publishing Co.: New York, NY.
32. Gosselin, C., et al., ePTFE /coating with Fibrin Glue, FGF-1 and Heparin: Effect on Retention of Seeded Endothelial Cells. *J. Surg. Res.*, 1996. 60: p. 327-332.
33. Gray, L.J., et al., FGF-1 Affixation Stimulates ePTFE Endothelialization without Intimal Hyperplasia. *J. Surg. Res.*, 1994. 57: p. 596-612.
34. Greco, R.S., *Implantation Biology: The Host Response and Biomedical Devices*. 1994: CRC Press, Inc. 417.
35. Greisler, H.P., et al., Prostacyclin production by blood-contacting surfaces of endothelialized vascular prostheses. *J. Cardiovasc. Surg.*, 1990. 31: p. 640-645.
36. Greisler, H.P., *New Biologic and Synthetic Vascular Prostheses*. 1991, Austin, TX: R.G. Landes Company.
37. Greisler, H.P., et al., Spatial and Temporal Changes in Compliance Following Implantation of Bioresorbable Vascular Grafts. *J. Biomed. Mat. Res.*, 1992. 26: p. 1449-1461.
38. Greisler, H., Angiogenic Mechanisms in Healing of Synthetic Grafts, in *How to Build a Blood Vessel*, L.F.R.I.I.V.D. Conference, Editor. 1997: Bethesda, MD. p. 58-61.
39. Guar, R.K. and K.C. Gupta, A Spectrophotometric Method for the Estimation of Amino Groups on Polymer Supports. *Analytical Biochemistry*, 1989. 180: p. 253-258.

40. Habeeb, A.F.S.A., Reaction of Protein Sulfhydryl Groups with Ellman's Reagent. *Meth. Enzymol.*, 1972. 25: p. 457.
41. Heilshorn, S., et al., Endothelial Cell Adhesion to the Fibronectin CS5 Domain in Artificial Extracellular Matrix Proteins. *FASEB*, 2002. Submitted.
42. Herbert, C.B., A.M. Hernandez, and J.A. Hubbell, Platelet Adhesion to Polyurethane Blended with Polytetramethylene Oxide. *Biotech. Bioeng.*, 1996. 52: p. 81-88.
43. Hermanson, G.T., *Bioconjugate Techniques*. 1996, San Diego: Academic Press.
44. Hoeve, C., The Elastic Properties of Elastin. *Biopolymers*, 1974. 13: p. 677-686.
45. Huang, C., Physicochemical studies of collagen and collagen-mucopolysaccharide composite materials: model materials for skin, in *Mechanical Engineering*. 1974, MIT: Cambridge, MA. p. 376.
46. Hubbell, J.A., et al., Endothelial Cell-Selective Materials for Tissue Engineering in the Vascular Graft Via a New Receptor. *Biotechnology*, 1991. 9: p. 568-572.
47. Hubbell, J.A., S.P. Massia, and P.D. Drumheller, Surface-grafted Cell-binding Peptides in Tissue Engineering of the Vascular Graft. *Ann. N Y Acad. Sci.*, 1992: p. 253-258.
48. Humphries, J.J., et al., Identification of an Alternatively Spliced Site in Human Plasma Fibronectin that Mediates Cell Type-specific Adhesion. *J. Cell Biol.*, 1986. 103: p. 2637-2647.
49. Hynes, R.O., *Ann. Rev. Cell Biol.*, 1985. 1: p. 67.
50. Hynes, R.O., Integrins: Versatility, Modulation, and Signaling in Cell Adhesion. *Cell*, 1992. 69: p. 11.
51. Ingber, D., Prodding Cells to Make Proteins. *Science*, 1998. 279(27): p. 1308.
52. Jones, P.A., Construction of an Artificial Blood Vessel Wall from Cultured Endothelial and Smooth Muscle Cells. *Proc. Natl. Acad. Sci. USA*, 1979. 76(4): p. 1882-1886.
53. Kajiyama, T. and A. Takahara, Surface Properties and Platelet Reactivity of Segmented Poly(etherurethanes) and Poly(etherurethaneureas). *J. Biomat. Appl.*, 1991. 6: p. 42-71.

54. Kaplan, D., Spiderless spider webs. *Nature Biotechnology*, 2002. 20(3): p. 239-240.
55. Kinley, C.E. and A.E. Marble, Compliance: A Continuing Problem with Vascular Grafts. *J. Cardiovasc. Surg.*, 1980. 21: p. 163-170.
56. Kleinman, H.k., et al., *Vitamins and Hormones*, 1993. 47: p. 161.
57. Knoller, S., S. Shpungin, and E. Pick, The Membrane-Associated Component of the Amphiphile-Activated, Cytosol-Dependent Superoxide-Forming NADPH Oxidase of Macrophages is Identical to Cytochrome b559. *Journal of Biological Chemistry*, 1991. 266: p. 2785-2804.
58. Kohler, T.R., et al., Mechanisms of Long-Term Degradation of Arterialized Vein Grafts. *Am. J. Surg.*, 1990. 160: p. 257.
59. Komoriya, A., et al., The Minimal Essential Sequence for a Major Cell Type-Specific Adhesion Site (CS1) within the Alternatively Spliced Type III Connecting Segment Domain of Fibronectin is Leucine-Aspartic Acid-Valine. *J. Biol. Chem.*, 1991. 266: p. 150-175.
60. Konig, W. and R. Geiger, *Perspectives in Peptide Chemistry*, ed. A. Eberle, R. Geiger, and T. Weiland. 1981: S Karger. 31-44.
61. Kornblihtt, A.R., et al., Primary Structure of Human Fibronectin: Differential Splicing May Generate at least 10 Polypeptides from a Single Gene. *EMBO J.*, 1985. 4: p. 1755.
62. Kretchi, M., et al., Chemical sequence control of beta-sheet assembly in macromolecular crystals of periodic polypeptides. *Science*, 1994. 265(5177): p. 1427-1432.
63. L'Heureux, N., et al., A Completely Biological Tissue-Engineered Human Blood Vessel. *FASEB*, 1998. 12: p. 47-56.
64. Lang, H., C. Deutschl, and H. Vogel, A new class of thiolipids for attachment of lipid bilayers on gold surfaces. *Langmuir*, 1994. 10: p. 197-210.
65. Langer, R.W. and J. Vacanti, *Tissue Engineering*. *Science*, 1993. 260: p. 920-926.
66. Lee, J., C.W. Macosko, and D.W. Urry, Elastomeric Polypentapeptides Cross-linked into Matrices and Fibers. *Biomacromolecules*, 2001. 2: p. 170-179.
67. Lee, J., C.W. Macosko, and D.W. Urry, Swelling Behavior of γ -Irradiation Cross-Linked Elastomeric Polypentapeptide-Based Hydrogels. *Macromolecules*, 2001. 34: p. 4114-4123.

68. Lee, J., C.W. Macosko, and D.W. Urry, Mechanical Properties of Cross-Linked Synthetic Elastomeric Polypentapeptides. *Macromolecules*, 2001. 34: p. 5968-5974.
69. Lindner, V., et al., Inhibition of Smooth Muscle Cell Proliferation in Injured Rat Arteries: Interaction of Heparin with Basic Fibroblast Growth Factor. *J. Clin. Invest.*, 1992. 90(November): p. 2044-2049.
70. Lundblad, R.L., *Techniques in Protein Modification. Chemical Reagents for Protein Modification*. 1995, Boca Raton, Fl.: CRC Press.
71. Lusclnskas, F.W. and J. Lawler, Integrins as Dynamic Regulators of Vascular Function. *FASEB*, 1994. 8: p. 929-938.
72. Lustenberger, P., P. Formstecher, and M. Dautrevaux, Quantitative Determination of Alkylamino Side-Chains Coupled to Agarose Beads. *Journal of Chromatography*, 1980. 193: p. 451-457.
73. Mark, J. and B. Erman, Filled Elastomers, in *Rubberlike Elasticity: A Molecular Primer*. 1988, John Wiley and Sons: New York.
74. Massia, S.P. and J.P. Hubbell, Vascular Endothelial Cell Adhesion and Spreading Promoted by the Peptide REDV of the IIICS Region of Plasma Fibronectin is Mediated by Integrin $\alpha 4\beta 1$. *J. Biol. Chem.*, 1992. 267(20): p. 14019-14026.
75. McGrath, K.P. and D. Kaplan, *Protein-Based Materials. Bioengineering of Materials*, ed. D. Kaplan. 1996, Medford, MA: Birkhauser. 429.
76. McGrath, K., et al., Electrostatic interactions in leucine zippers: effects on stability and specificity of interaction. *Journal of Bioactive and Compatible Polymers*, 2000. 15(4): p. 334-356.
77. McMillan, R.A. and V.P. Conticello, Synthesis and Characterization of Elastin-Mimetic Protein Gels Derived from a Well-Defined Polypeptide Precursor. *Macromolecules*, 2000. 33(13): p. 4809-4821.
78. McPherson, J.M., S. Sawamura, and R. Armstrong, An examination of the biologic response to injectable, glutaraldehyde crosslinked collagen implants. *J. Biomed. Mater. Res.*, 1986. 20: p. 93-107.
79. Mecham, R., *Ann. Rev. Cell Biol.*, 1991. 7: p. 71.
80. Methods, A.S.A.T., *Standard Test Methods for Tensile Properties of Thin Plastic Sheet*ing.

81. Meyer, D. and A. Chilkoti, Purification of recombinant proteins by fusion with thermally-responsive polypeptides. *Nature Biotechnology*, 1999. 17(11): p. 1112-1115.
82. Meyer, D. and A. Chilkoti, Genetically encoded synthesis of protein-based polymers with precisely specified molecular weight and sequence by recursive directional ligation: examples from the elastin-like polypeptide system. *Biomacromolecules*, 2002. 3(2): p. 357-367.
83. Mould, A.P., et al., Affinity Chromatographic Isolation of the Melanoma Adhesion Receptor for the IIICS Region of Fibronectin and Its Identification as the Integrin $\alpha 4\beta 1$. *J. Biol. Chem.*, 1990. 265(7): p. 4020-4024.
84. Mould, A.P. and M.J. Humphries, Identification of a Novel Recognition Sequence for the Integrin $\alpha 4\beta 1$ in the COOH-terminal Heparin-Binding Domain of Fibronectin. *EMBO J.*, 1991. 10(13): p. 4089-4095.
85. Mould, A.P., et al., The CS5 Peptide is a Second Site in the IIICS Region of Fibronectin Recognized by the Integrin $\alpha 4\beta 1$: Inhibition of $\alpha 4\beta 1$ Function by RGD Peptide Homologues. *J. Biol. Chem.*, 1991. 266(6): p. 3579-3585.
86. Musella, R.A. and E.N. Willey, Evaluation of Patency of Synthetic and Autogenous Venous and Arterial Micrografts in Rats. *Microsurgery*, 1985. 6: p. 85-91.
87. National Heart, L.a.B.I., Morbidity and Mortality: 1998 Chartbook on Cardiovascular, Lung and Blood Diseases. 1998: National Institute of Health.
88. Nicholas, F.L. and C.H. Gagnieu, Denatured Thiolated Collagen: Crosslinking by Oxidation. *Biomaterials*, 1997. 18(11): p. 815-821.
89. Nicholas, F.L. and C.H. Gagnieu, Denatured Thiolated Collagen: Synthesis and Characterization. *Biomaterials*, 1997. 18(11): p. 807-813.
90. Nicol, A., D.C. Gowda, and D.W. Urry, Cell Adhesion and Growth on Synthetic Elastomeric Matrices Containing ARG-GLY-ASP-SER. *J. Biomed. Mat. Res.*, 1992. 26: p. 393.
91. Nicol, A., et al., Cell Adhesive Properties of Bioelastic Materials Containing Cell Attachment Sequences, ed. c. Carraher and c. Gebelein. 1994, New York: Plenum Press.
92. O'Brien, J., et al., Nylons from nature: synthetic analogs to spider silk. *Advanced Materials*, 1998. 10(15): p. 1185.

93. Panitch, A., Design, Synthesis, and Characterization of Artificial Extracellular Matrix Proteins for Tissue Engineering, in Polymer Science and Engineering. 1997, University of Massachusetts, Amherst: Amherst.
94. Panitch, A., et al., Design and Biosynthesis of Elastin-like Artificial Extracellular Matrix Proteins Containing Periodically Spaced Fibronectin CS5 Domains. *Macromolecules*, 1999. 32(5): p. 1701-1703.
95. Payne, A.R., ed. Reinforcement of Elastomers., ed. G. Kraus. 1965, Interscience: New York. Chapter 3.
96. Petka, W., et al., Reversible hydrogels from self-assembling artificial proteins. *Science*, 1998. 281(5375): p. 389-392.
97. Richardson, J.S., *Advanced Protein Chemistry*, 1981. 34: p. 167-339.
98. Roach, M. and A. Burton, The Reason for the Shape of the Distensibility Curves of Arteries. *Can. J. Biochem. Physiol.*, 1957. 35: p. 681-690.
99. Robbins, S., R. Cotran, and V. Kumar, *Pathologic Basis of Disease*. 3rd ed. 1984, Philadelphia, PA: W. B. Saunders Company. 1467.
100. Ross, R., E. Raines, and D. Bowen-Pope, Growth Factors from Platelets, Monocytes, and Endothelium: Their Role in Cell Proliferation. *Ann. NY. Acad. Sci.*, 1982. 397: p. 18-24.
101. Ross, M.H., L.J. Romrell, and G.I. Kaye, *Histology: A Text and Atlas*. Third ed. 1995, Baltimore, MD: Williams and Wilkins.
102. Rumisek, J.D., et al., Heat-denatured Albumin-Coated Dacron Vascular Grafts: Physical Characteristics and In-vivo Performance. *J. Vasc. Surg.*, 1986. 4: p. 136-143.
103. Sambrook, J., E.F. Frisch, and T. Maniatis, *Molecular Cloning*. 2nd ed. 1989, Plainview, NY: Cold Spring Harbor Laboratory Press.
104. Sarin, V.K., et al., Quantitative Monitoring of Solid-Phase Peptide Synthesis by the Ninhydrin Reaction. *Analytical Biochemistry*, 1981. 117: p. 147-157.
105. Scandola, M. and G. Pezzin, The Low-temperature Mechanical Relaxation of Elastin: The Solvated Protein. *Biopolymers*, 1978. 17: p. 213-223.
106. Szela, S., et al., Reduction-oxidation control of beta-sheet assembly in genetically engineered silk. *Biomacromolecules*, 2000. 1(4): p. 534-542.

107. Uhlich, T. and J.A. Hubbell. Hydrogel Formation by Photochemical Crosslinking of Proteins Using Eosin Y as Photosensitizer. in Society for Biomaterials. 1997. New Orleans, Louisiana.
108. Urry, D.W., et al., Synthetic, Cross-linked Polypentapeptide of Tropoelastin: an Anisotropic, Fibrillar Elastomer. *Biochemistry*, 1976. 15(18): p. 4083-4089.
109. Urry, D.W., et al., Biocompatibility of the Bioelastic Materials, poly (GVGVVP) and its γ -irradiation Cross-Linked Matrix: Summary of Generic Biological Test Results. *J. Bioact. Comp. Poly.*, 1991. 6: p. 263-282.
110. Urry, D.W., et al., Hydrophobicity Scale for Proteins Based on Inverse Temperature Transitions. *Biopolymers*, 1992. 32: p. 1243-1250.
111. Urry, D.W., et al., Properties, Preparations and Applications of Bioelastic Materials, in *Handbook of Biomaterials and Applications*. 1995, Marcel Dekker: New York.
112. Urry, D.W., et al., Protein Based Materials with a Profound Range of Properties and Applications: The Elastin DT Hydrophobic Paradigm, in *Protein-Based Materials*, K. McGrath and D. Kaplan, Editors. 1997, Birkhauser: Boston, MA.
113. Volpin, D., et al., Banded Fibers in High Temperature Coacervates of Elastin Peptides. *Journal of Biological Chemistry*, 1976. 251(21): p. 6871-6873.
114. Voorhees, A.B., A. Jaretzki, and A.H. Blakemore, The Use of Tubes Constructed from Vinyon N Cloth in Bridging Arterial Defects. *Ann. Surg.*, 1952. 135: p. 332.
115. Waluscheck, K.P., et al., *A. Eur. J. Endovasc. Surg*, 1996. 12: p. 321.
116. Welsh, E.R. and D.A. Tirrell, Engineering the Extracellular Matrix: A Novel Approach to Polymeric Biomaterials. I. Control of the Physical Properties of Artificial Protein Matrices Designed to Support Adhesion of Vascular Endothelial Cells. *Biomacromolecules*, 2000. 1(1): p. 23-30.
117. Williams, S.K., et al., Formation of a Functional Endothelium on Vascular Grafts. *Electron Microscopy Technique*, 1991. 19: p. 439-451.
118. Williams, S.T., D.C. Rose, and B.E. Jarrell, Microvascular Endothelial Cell Seeding of ePTFE Vascular Grafts: Improved Patency and Stability of the Cellular Lining. *J. Biomed. Mat. Res.*, 1994. 28: p. 203-212.
119. Williams, S.K., Endothelial Cell Transplantation. *Cell Transplantation*, 1995. 4: p. 401-410.

120. Winlove, C.P. and K.H. Parker, Physiochemical properties of vascular elastin, in *Connective Tissue Matrix : Part 2*, D.W.L. Hukins, Editor. 1990, The MacMillan Press Ltd.
121. Woods, A., et al., Adhesion and Cytoskeletal Organization of Fibroblasts in Response to Fibronectin Fragments. *EMBO J.*, 1986. 5(4): p. 665-670.
122. Xiao, Y. and A. Truskey, Effect of Receptor-Ligand Affinity on the Strength of Endothelial Cell Adhesion. *Biophys. J.*, 1996. 71: p. 2869-2884.
123. Yates, S.G., et al., The Preclotting of Porous Arterial Prostheses. *Ann. Surg.*, 1978. 188: p. 612-62 2.
124. Young, R.J. and P.A. Lovell, *Introduction to Polymers*. Second ed. 1991, London, UK: Chapman and Hall.
125. Yu, S., et al., Smectic ordering in solutions and films of a rod-like polymer owing to monodispersity of chain length. *Nature*, 1997. 389(6647): p. 167-170.
126. Ziegler, T. and R.M. Nerem, Tissue Engineering a Blood Vessel: Regulation of Vascular Biology by Mechanical Stresses. *J. Cell. Biochem.*, 1994. 56: p. 204-209.
127. Zilla, P., et al., Clinical In-vitro Endothelialization of Femoropopliteal Bypass Graft: An Actuarial Follow-up over Three Years. *J. Cardiovasc. Surg.*, 1994. 19: p. 540-548.
128. Zilla, P., et al., Long-term Effects of Clinical In-vitro Endothelialization on Grafts, in *How to Build a Blood Vessel*, L.F.R.I.i.V.D. Conference, Editor. 1997: Bethesda, MD.
129. Zwolak, R.M., M.C. Adams, and A.W. Clowes, Kinetics of Vein Graft Hyperplasia: Association with Tangential Stress. *J. Vasc. Surg.*, 1987. 5: p. 126-136.

